Pipeline and Hazardous Materials Safety Administration Phase 1 Final Report

In-Ditch Validation Methodology for Determination of Defect Sizing

Peter den Boer, Harvey Haines, Lars Hörchens,
Pushpendra Tomar, and Jeff Vinyard

August 23, 2016

Contract Number: DTPH56-13-T-000008

Intentionally blank

Final Report

on

IN-DITCH VALIDATION METHODOLOGY FOR DETERMINATION OF DEFECT SIZING

to

PHMSA

DTPH56-13-T-000008

August 23, 2016

Prepared by

**Peter den Boer, Harvey Haines, Lars Hörchens,
Pushpendra Tomar, and Jeff Vinyard**

**Applus RTD
11801 South Sam Houston Parkway West
Houston, TX 77031**

DISCLAIMER

This document presents findings and/or recommendations based on engineering services performed by employees of ApplusRTD USA, Inc. The work addressed herein has been performed according to the authors' knowledge, information, and belief in accordance with commonly accepted procedures consistent with applicable standards of practice, and is not a guaranty or warranty, either expressed or implied.

The analysis and conclusions provided in this report are for the sole use and benefit of the Client. No information or representations contained herein are for the use or benefit of any party other than the party contracting with ApplusRTD USA, Inc. The scope of use of the information presented herein is limited to the facts as presented and examined, as outlined within the body of this document. No additional representations are made as to matters not specifically addressed within this report. Any additional facts or circumstances in existence but not described or considered within this report may change the analysis, outcomes and representations made in this report.

TABLE OF CONTENTS

LIST OF FIGURES

LIST OF TABLES

Acknowledgements

In addition to the Pipeline and Hazardous Materials Administration the authors would like to thank Enbridge Pipeline and TransCanada Pipeline for directly cofounding this work. In addition we wish to thank the many pipeline companies and organizations that contributed samples for study including Enbridge, TransCanada, Marathon, Koch and others. The Pipeline Research Council International helped fund additional NDT service providers to scan some of the samples in the study. And last we would like to thank Lucinda Smart for helping to prepare this report.

In-Ditch Validation Methodology for Determination of Defect Sizing

Peter den Boer, Harvey Haines, Lars Hörchens, Pushpendra Tomar, and Jeff Vinyard

INTRODUCTION

Basic description of the IWEX measurement system

IWEX, being an acronym for "**I**nverse **W**ave field **EX**trapolation", is an ultrasonic inspection technology for acoustical imaging. For pipe weld inspection, it relies on the usage of array transducers, which are positioned on wedges to the left and right of the weld. Instead of generating ultrasonic beams as commonly done with Phased Arrays, IWEX uses each array element consecutively as a source, while receiving with all array elements. Signals are picked up by all array elements from reflected or diffracted waves from the material boundaries or flaws in or near the weld. The dataset obtained this way contains a large number of A-scans, each of which corresponds to a different source-receiver combination. This type of data acquisition is usually referred to as 'full matrix capture'.

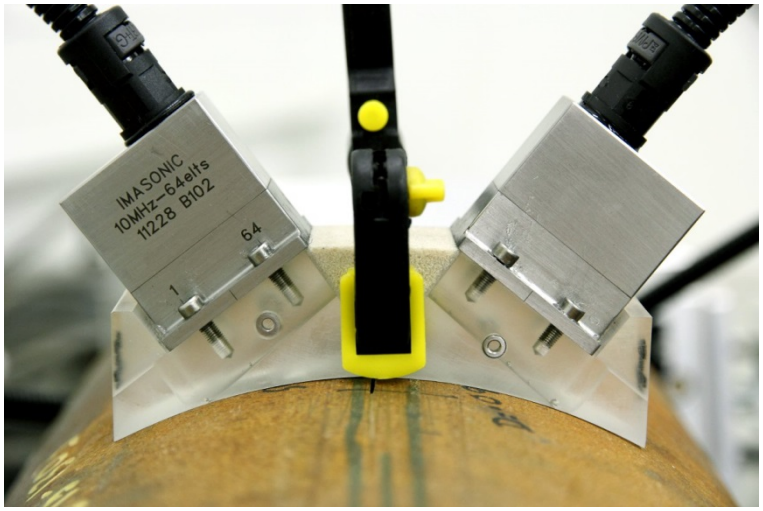

Figure 1. Laboratory test setup for IWEX on seam welds

In contrast to conventional ultrasonic approaches, the data is not used 'as is' in an A-scan representation, but processed to generate a two-dimensional image. This image corresponds to a virtual cross-section of the material representing the real dimensions of the object inspected. It provides an easily interpretable visual representation that resembles a metallographic section obtained from destructive testing.

The figure below shows an IWEX image of a 16-inch diameter ERW seam weld with a wall thickness of 6.35 mm (0.250-in) (left side) and the corresponding metallographic section (right side).

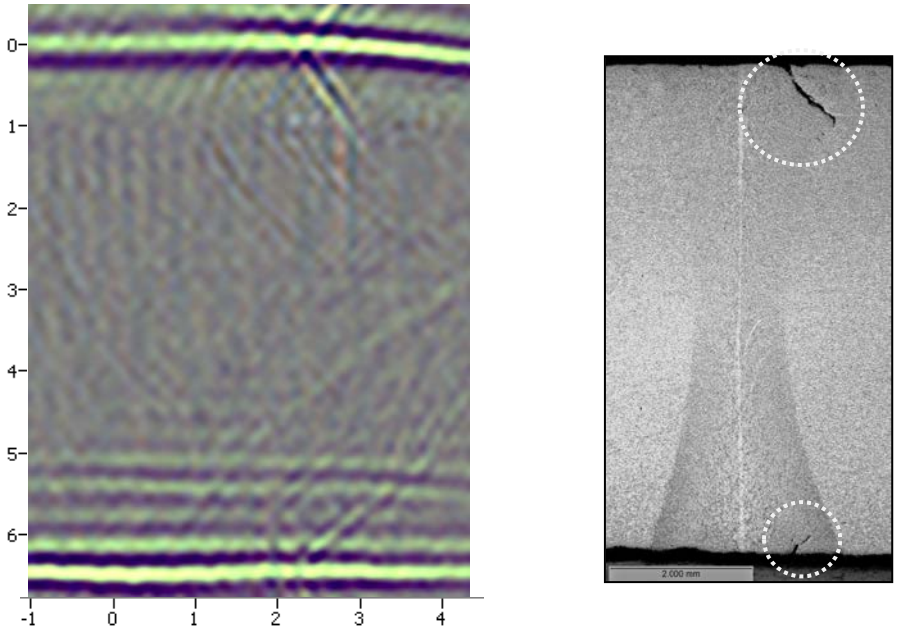

Figure 2. IWEX image (left) and corresponding macro photograph (right) of an ERW seam weld with a wall thickness of 6.35 mm (0.250 in)

Since 2010, a dedicated, hardware-based IWEX system for the inspection of girth welds has been developed. The adaptation for seam weld inspection started in 2012.

Generation of the IWEX image

The general approach of acoustical imaging has been used in the context of seismic exploration and medical acoustics for several decades. It is only within the last decade that the basic technology has been adopted and refined to be applicable for non-destructive inspection.

The figure below shows the three principal paths (blue) from an element at the center of the array to a point in the region of interest (green rectangle) for a seam weld setup.

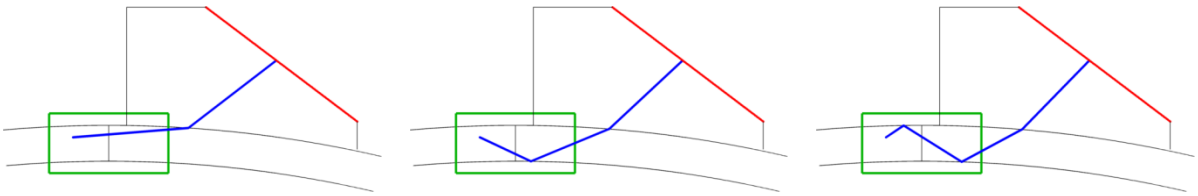

Figure 3. Principal paths from an array element to an image point that are taken into account in the image formation process with IWEX.

A numerical procedure was developed to calculate the ray path taken from a certain array element to a certain point in the area of interest and the respective travel time for each of these three cases. To this end, an iterative method is used to find the path with the shortest travel time.

In phased array applications, the different sound paths are generated physically by firing different array elements with appropriate delays to generate and steer ultrasonic beams thereby focusing at points in the region of interest. This approach is inherently limited by the time required for the sound to propagate through the sample. This means that sound waves can be focused only at a limited number of points within a given period of time.

For IWEX inspection, signals of all possible source-receiver combinations of the array elements are measured. It is only after the measurement that different delay laws are applied to focus at all points of a pixel grid in the defined region of interest. This focusing operation is carried out in hardware processing by a field-programmable gate array (FPGA), which generates the IWEX images before sending them to a computer for further processing and evaluation.

In order to form the images, the travel times from all array elements to all points in the image have to be calculated and made available to the hardware. During the inspection, this information is used to look up samples in the recorded A-scans and add their contribution to the respective points in the image.

Inclusion of skip paths

One of the major advantages of IWEX is the simultaneous usage of different acoustical paths for generating the image. By combining the three principal paths described above, several modes for interrogating the weld volume can be formed. The modes currently used in the IWEX system are shown in Figure 4. Note that the modes correspond to different directions of acoustical illumination and reception. In the measurement software, the images obtained by using the different paths are presented in a single overlay image. By combining these different directions for inspection, defects of arbitrary orientation can be detected. Thereby, the overall chance of missing a defect is minimized.

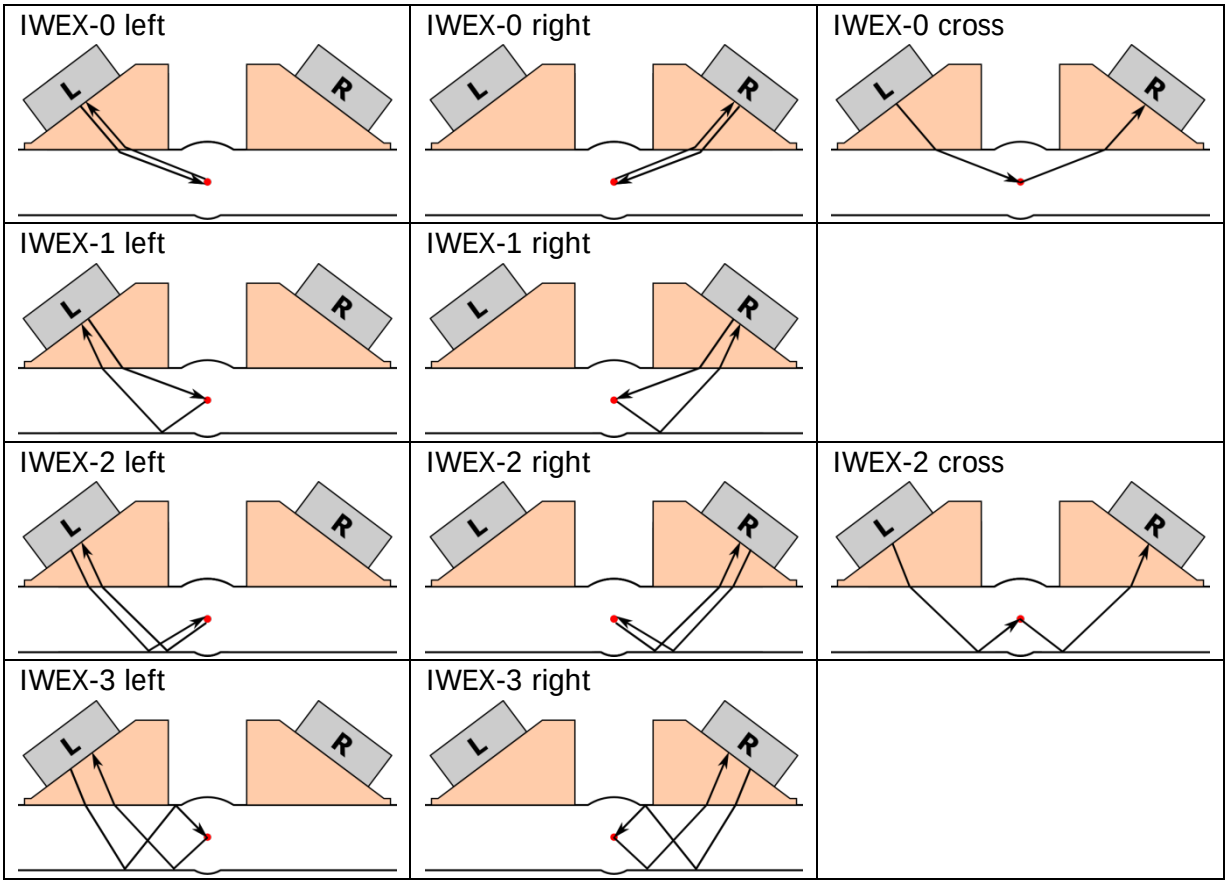

Figure 4. Different combined paths between two array elements that are taken into account in the image formation process with IWEX

SUMMARY AND CONCLUSION

After two rounds of testing and conclusions the IWEX system has developed to the point that field engineers can understand the system and gain images in the field for imaging axially oriented flaws in the ERW seam and pipe body. Field engineers who are exposed to and use the system are all believers that full matrix capture imaging using IWEX is an easier method for interpreting the types of flaws present in the pipe, especially in the ERW seam weld, where differentiating among the various types of flaws and defects is currently very difficult using existing technology such as single transducer shear wave UT or beam steering methods such as phase array UT.

A standard method of describing defects in an ERW seam is needed. The development team has started using nomenclature in API standard 5T1 to describe flaws and defects in the ERW seam. Experience gained from the project shows the industry could improve upon this standard to fully describe all of the potential flaw types in ERW seams. Current inspections using existing technology often describe flaws as cracks, crack-like, or possible cracks where differentiating

among cold welds, surface breaking hook cracks, non-surface breaking upturned fibers, fatigue cracks, and laminations would be much more informative to the operator in making integrity decisions. IWEX, with its ability to image features regardless of flaw orientation, has a key advantage over existing technology in this area. Although we found that IWEX UT imaging capability still had difficulty discriminating among defects for small defects <1 mm in height, we also concluded this was not critical as these small defects are almost always non-injurious. Our hope is this will continue to improve with ongoing developments in Phase 2 of the project.

Scanning trials show the best way to size defects is through tip diffraction signals that can be superimposed on top of signals showing the actual flaws. Initially amplitude attenuation of signals from the flaws was used for sizing, but this proved to provide insufficient accuracy of ±1 mm for flaw height. Tip diffraction signals are better at sizing with reliable sizing of ±0.5 mm in through-wall height with one case study where an accuracy of ±0.2 mm was obtained. Interestingly this higher accuracy was obtained using IWEX in studies predating this project where synthetic weld defects were studied. A better understanding of the variables used in obtaining images is needed to obtain this level on a routine basis. These variables include variability in the pipe such as wall thickness, pipe roundness, and trim issues and also include understanding variability in the measurement system such as precise measurements of wedge angle and material velocity, wedge standoff from the pipe, and other probe-wedge-pipe parameters. Ongoing studies in this area are part of the next phase of development sponsored by PHMSA and pipeline operators. Depth accuracy of ±0.2mm is needed to qualify ILI tools as the in-ditch method needs to be a more accurate method at measuring flaws than the ILI tools in order to determine the ILI tool accuracy.

The four most significant hardware and software improvements to the system during this phase of the research and development are:

- an improved set up software routine that requires significantly reduced manual adjustments to the system setup,
- a linear scanner capable of keeping the axial alignment of the system consistent and preventing the system from drifting circumferentially,
- a higher sampling rate capability that allows full matrix capture (FMC) processing at speeds that do not limit data acquisition rates because of data acquisition and processing, and
- an improved focusing technique for focusing the UT transverse to the linear array.

Although initially setting up the system proved difficult enough to prevent field engineers from obtaining images, by the end of the project field set-up and calibration could be performed automatically with adjustments required to improve the image for scanning and imaging flaws in the pipe.

A linear scanner was developed that was capable of tracking the seam precisely allowing the necessary axial straight images of the bond line which is helpful for interpreting flaws in the seam. This linear scanner proved to be better at scanning smaller diameter pipe (<16-in) than the initial testing using a modified tank scanner. In addition the linear scanner proved to be much better at tracking ERW seams than trying to steer a magnetic wheeled scanner down an ERW seam.

A higher sampling rate capability was developed by implementing efficiencies in processing of the FMC data acquired. The processing speed increased by a factor of 11-16 over previous processing speeds. The faster processing has effectively eliminated any limitation on the scanning speed for scanning the approximately inch wide area around an ERW seam using the current IWEX image processing.

Focusing in the plastic wedges between the UT transducers and pipe improved the resolution of the system transverse to the linear array. Although IWEX produces a very detailed image in the 2D imaging field from the inverse wave extrapolation technique, the resolution perpendicular to the array was limited to the width of the beam produced by the transducers. This resolution proved to be about 1 cm (0.4 in) until focusing was added to the wedges. This was longer than many of the cold welds observed in the bond line. The lens focusing in the wedged improved to resolution to a few millimeters.

1ST ROUND OF TESTING AND IMPROVEMENTS

Several improvements were carried out in the first round of testing. These included:

- Development of a higher sampling rate capability
- Design of wedges with lenses for optimal focusing in the axial direction

Development of higher sampling rate capability

As described in the section on the generation of IWEX images, the hardware has to research a number of time samples in the measured A-scans in order to calculate the value for a certain pixel of the image. For every image, this requires a huge look-up table to be read in order to determine where the relevant information for a certain pixel is located in the A-scans. For every pixel in the image, time indices for the A-scans of all channels (up to 256) must be read into memory. A typical IWEX image contains between 5,000 and 40,000 pixels, and ten different mode images are generated for every position scanned.

The main bottleneck of the original IWEX implementation was the bandwidth of the memory interface in the processing hardware, which is able to transfer about 1.6 gigabyte per second.

In addition to this, the system was designed in such a way that a full measurement of all A-scans was carried out before each of the mode images was generated.

To increase the processing speed, the following major modifications have been applied to the IWEX hardware system:

1. Whenever images can be calculated based on the same set of A-scan measurements, the A-scans are re-used. Because of the high IWEX processing speed, the A-Scan capture time forms a significant contribution to the time required for a complete measurement cycle. By reusing the A-scans captured during a previous sequence, the total time for a measurement cycle is reduced.
2. The travel time information is stored in the external memory in a compressed format. During IWEX processing, compressed matrix information is read from memory and decompressed on the fly in the FPGA, thereby reducing the required memory bandwidth.

The latter adaptation in particular enables a significant gain in processing speed. In the imaging matrices, the travel times are represented by sample indices in the A-scans and therefore related to the sampling rate of the system when digitizing the A-scans. These sample indices can be represented by integers which can be processed more quickly than floating point numbers.

The combination of the abovementioned modifications results in an acceleration by a factor of approximately 11 to 16, depending on the exact settings. Table 1 provides an overview of the scanning speed of the original implementation and the accelerated version. The figures are given for typical image sizes for seam welds, assuming that all ten IWEX modes are calculated.

The effect of the acceleration is more pronounced for bigger image sizes. This is because the modifications mainly affect the time for calculating the IWEX images, whereas the time required for the physical measurement of the A-scans forms the limiting factor for smaller image sizes.

Table 1. Sampling rate of the IWEX system before and after acceleration for typical image sizes required for application on axial seam welds. The acceleration factor achieved by the latest implementation is shown in the rightmost column.

Width [mm]	Height [mm]	Number of pixels	Original scanning speed [frames/s]	Accelerated speed [frames/s]	Acceleration factor
6	6	3721	2.81	32.1	11
8	6	4941	2.15	28.1	13
8	8	6561	1.65	22.9	14
10	10	10201	1.07	17.0	16

If required, an additional gain in speed can be obtained by the following adaptations:

- A coarser grid image could be used. This option has limited appeal, because the image grid spacing is already close to the limits required by the sampling criterion. Increasing the grid spacing any further might compromise the integrity of the image.
- Not all 10 IWEX modes might be relevant for all applications and samples. For example, it is possible that the IWEX-1 and IWEX-3 modes based on tandem paths contain similar information, rendering the calculation from one of the two modes unnecessary. This option requires extensive tests with different samples and different kinds of defects in order to determine the limitations and added value of using all 10 IWEX modes.
- In the current implementation, the image grid is equal in size in all 10 modes. However, there can be parts of the image that are not relevant or physically meaningful in some of the modes. For example, the area above the OD is not relevant when using a direct mode for imaging. By using individual image grid sizes per mode and only imaging the relevant part, a significant gain in scanning speed of up to 25% can be achieved. This comes at the cost of additional complexity in the measurement software. The different sub-images have to be aligned for visualization.

Design of wedges with lenses for optimal focusing in the axial direction

The wedges used for the arrays had to be adapted to seam welds in order to obtain optimal resolution and signal-to-noise ratio. Rexolite was chosen as the basic wedge material due to its low attenuation at higher frequencies.

It was decided to include a lens into the wedge in order to focus the beam and limit the beam spreading in the axial direction of the pipe (i.e., the scanning direction).

The inclusion of a lens has two advantages:

1. The length sizing of indications can be carried out more accurately because the beam is narrower in the scanning direction. The obtainable resolution is thereby increased.
2. The energy provided by the ultrasonic array is focused at a smaller region in the weld, resulting in improved signal-to-noise ratio for the detection and imaging of shorter axial flaws.

The lens was designed by including a conical interface in the wedge. The upper part of the wedge close to the array is made of Perspex. Due to the difference in sound velocity between Rexolite (2345 m/s) and Perspex (2730 m/s), diffraction occurs at the interface between the two materials.

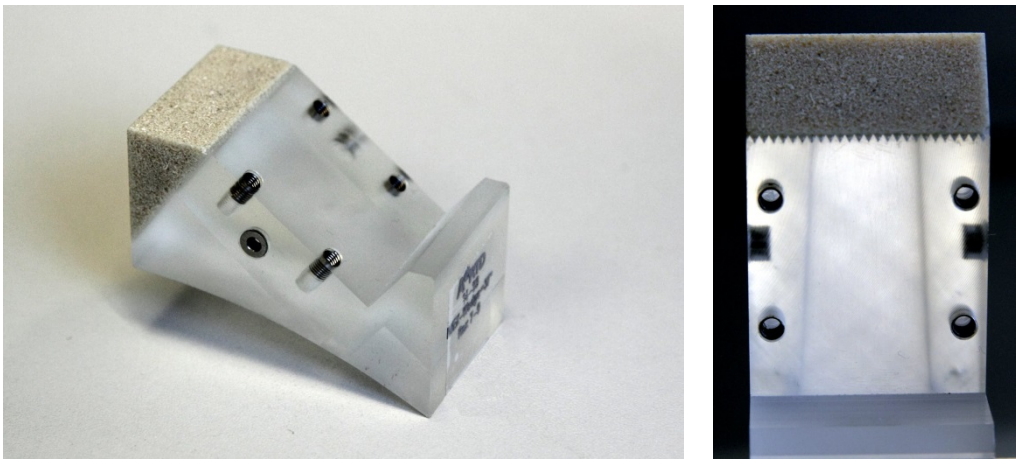

Figure 5. Wedges used for the seam weld inspection using IWEX: side view of a wedge designed for 8-in pipe showing the curvature of the wedge bottom (left), top view showing the shape of the conical lens included in the wedge (right).

Numerical simulations were carried out to determine the optimal lens diameter. Ray tracing was used in order to get an approximate value for the lens radius required. An example of a forward ray tracing simulation is shown in Figure 6.

Ray tracing does not include the influence of the frequency spectrum of the sources, nor does it include the directivity of the ultrasonic radiation pattern of the array elements. Therefore, additional, more advanced simulations have been carried out, taking the phase contributions of different parts of the array element to the sound field at the weld centerline into account.

The optimal lens for the seam weld application was determined to have a conical shape, with a radius of 7 mm at the top, and a radius of 9 mm at the bottom of the wedge. This configuration provided the best overall results for the various IWEX paths in the simulations. Wedges with the proposed lens were manufactured for different pipe diameters.

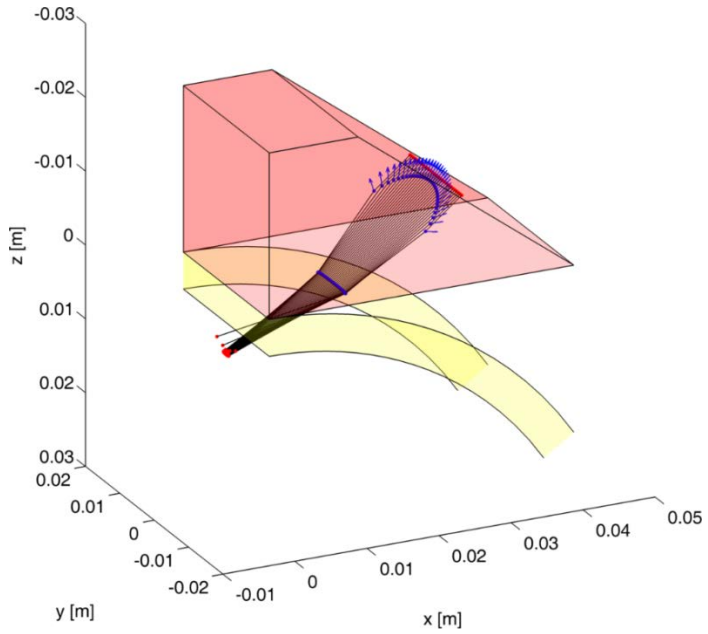

Figure 6. Ray tracing simulation carried out in order to determine the optimum radius of the lens included in the wedge. The wedge is drawn flat to indicate its position. The calculations for the paths are carried out using the curved interface of the pipe.

In addition to the simulations, measurements of the effect of including a lens in the wedge have been performed with a prototype wedge. A test block containing side-drilled cylindrical holes has been scanned to this end. Figure 7 shows the improvement in resolution obtained by including a lens in the wedge.

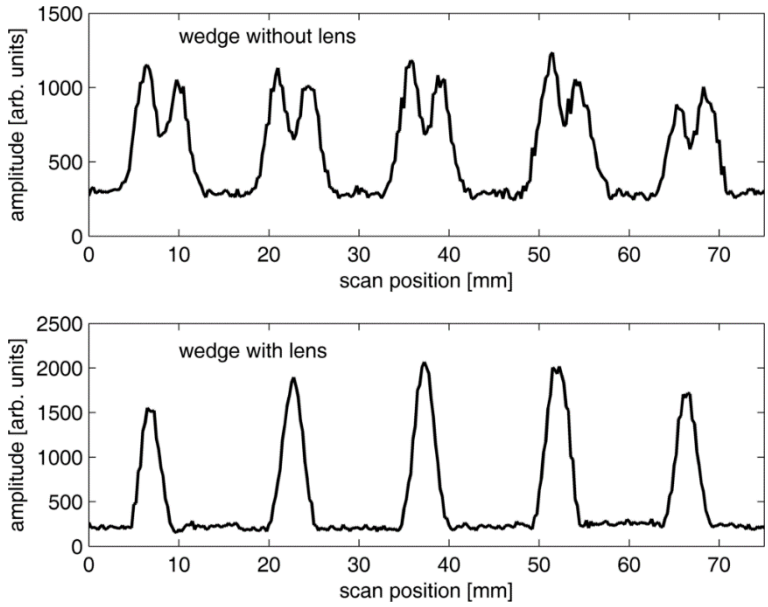

Figure 7. Scan of a reference block with cylindrical side-drilled holes. The inclusion of a lens improves both the amplitude response and the resolution in scan direction.

The reflection profile from a single side-drilled hole is shown in Figure 8. By introducing the lens, the length of the indication in the scan is reduced from 6.4 mm to 2.7 mm at -6 dB. This is equivalent to a reduction of about 40%. In addition to the decrease in scan direction, the profile exhibits only one clear peak unlike the unfocused beam.

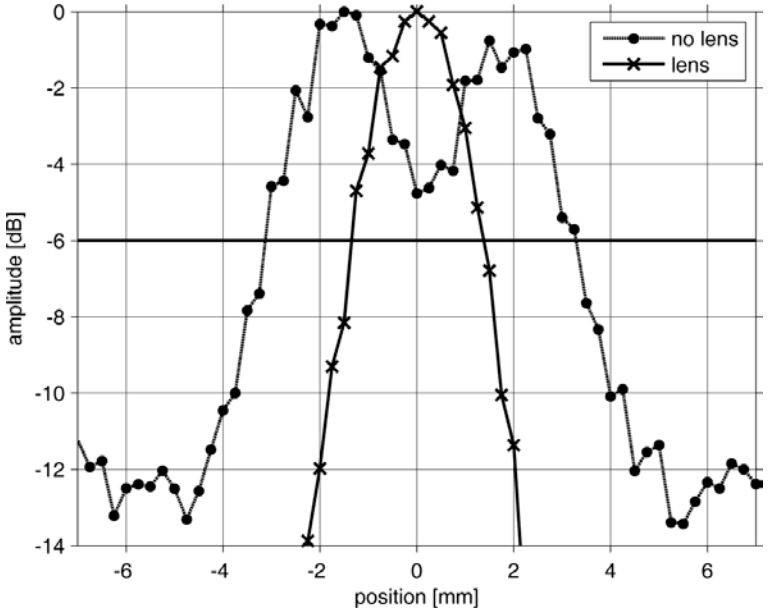

Figure 8. Reflection profile of a single cylindrical side-drilled hole.The inclusion of a lens improves the resolution in scan direction significantly.

Comparison of 7.5 MHz and 10 MHz IWEX array probes

IWEX imaging can be carried out with different array configurations. Two sets of array probes have been compared in order to assess the effect of frequency and element width on the image quality:

- 7.5 MHz, 128 elements, pitch 0.25 mm,
- 10 MHz, 64 elements, pitch 0.325 mm.

The 7.5 MHz are the probes which have been used for most seam weld scans presented so far. The 10 MHz probes are a newer design that has been developed to combine a higher frequency while lowering the number of active channels. These probes have been used for the imaging of stress corrosion cracking presented in the previous quarterly report. The elements of the 10 MHz probes are slightly bigger, which results in more energy per element being transmitted in to the sample, but also a slightly more pronounced directivity of each element.

The A-scans of the probes are compared for reflection at a free plate surface below the probe (see Figure 9). The time resolution of the 10 MHz probe is shown to be significantly better.

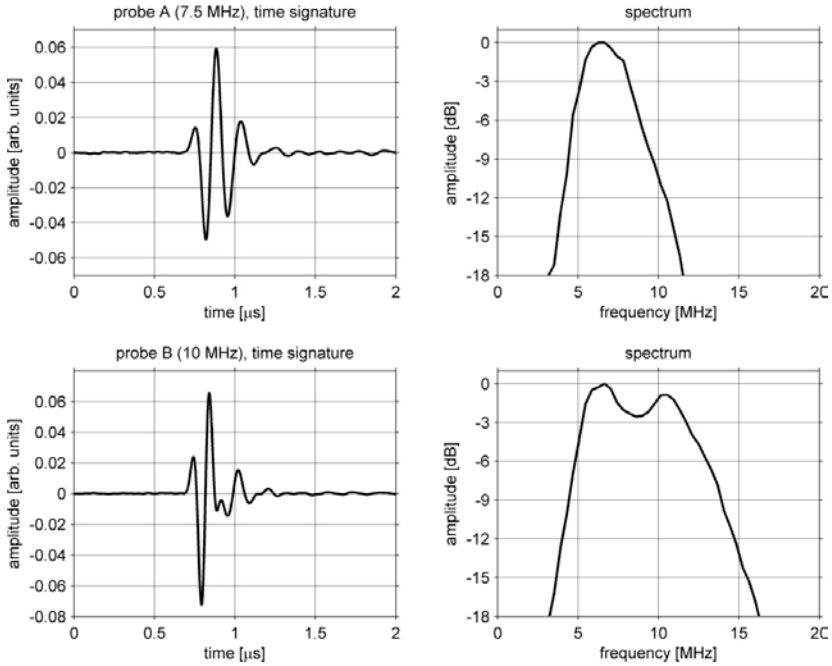

Figure 9. Time signals (left) and spectra (right) of 7.5 MHz (top) and 10 MHz (bottom) array probes used for IWEX.

Figure 10 presents IWEX images of a cylinder hole with a diameter of 0.5 mm, situated about 6 mm below the probe. It can be seen that the spatial resolution of the image taken at 10 MHz is clearly higher. In addition, the spatial spectrum shows the wider directivity and the broader range of angles for the 7.5 MHz probe.

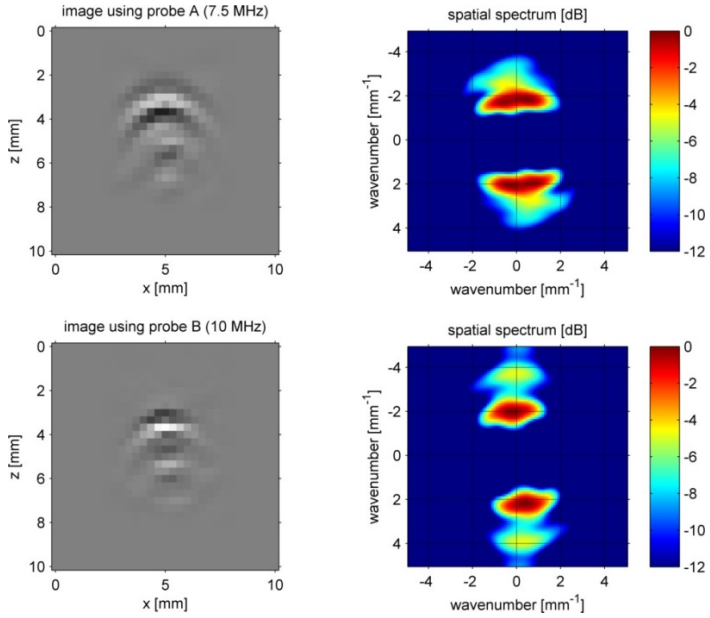

Figure 10. Images (left) of a cylinder hole of 0.5 mm diameter imaged with 7.5 MHz (top) and 10 MHz (bottom); associated spectra (right).

When looking at the resolution obtained in the IWEX images, the effective aperture of the array and the directivity of individual elements play a role as well. This is evident when using the array on a plastic wedge to generate images of the side face of a plate in tandem mode as shown in Figure 11. This experiment is intended to determine the difference in resolution for both probes when used to image vertically oriented flaws.

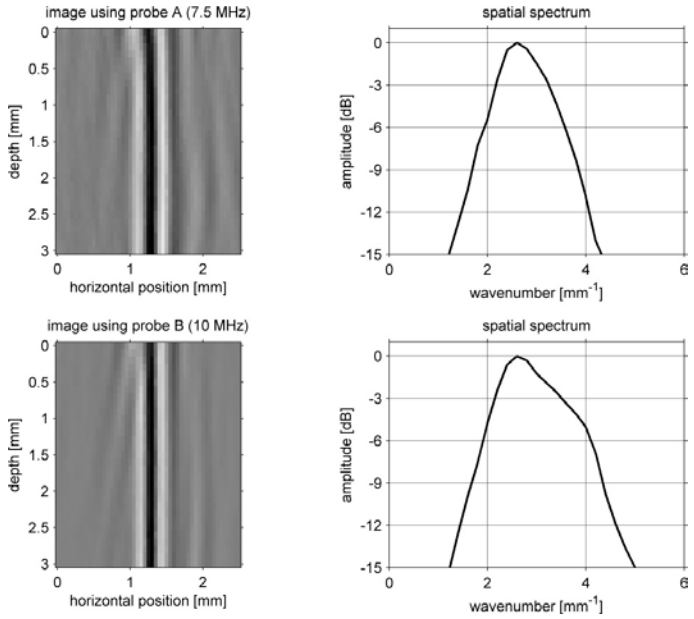

Figure 11. Images of the side face of a steel block in tandem mode at 7.5 MHz (top) and 10 MHz (bottom); associated spatial spectra in horizontal direction (right).

It can be seen that the difference in resolution between the 7.5 MHz and the 10 MHz probes is less pronounced in this case. Similar results are obtained for the images of a 2 mm notch with an angle of 30° presented in Figure 12. The images are obtained with the array mounted on a plastic wedge; the associated spatial spectra are shown in Figure 13.

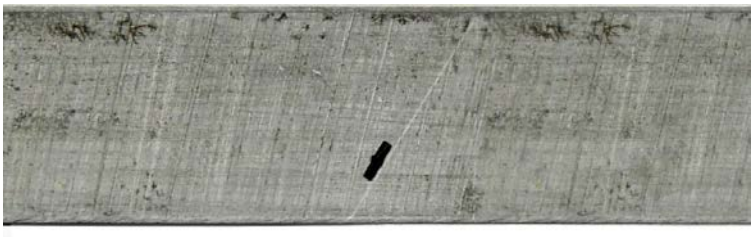

Figure 12. Test block with a 2 mm notch with an angle of 30° with respect to the vertical axis.

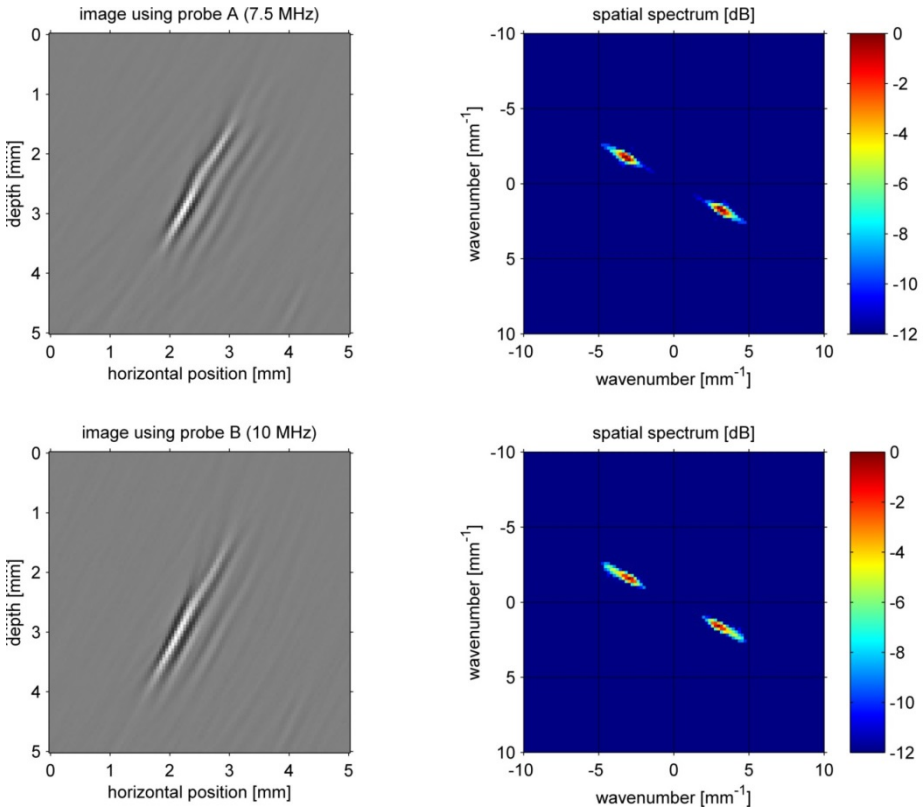

Figure 13. Images of a 2 mm notch tilted 30°taken at 7.5 MHz (top) and 10 MHz (bottom); associated spatial spectra (right).

The spectra along the main direction of imaging, i.e., normal to the notch, are shown in Figure 14 to simplify comparison. It can be seen that there is only a small difference in resolution. Nevertheless, the 10 MHz probe performs slightly better than the 7.5 MHz probe in terms of spatial bandwidth.

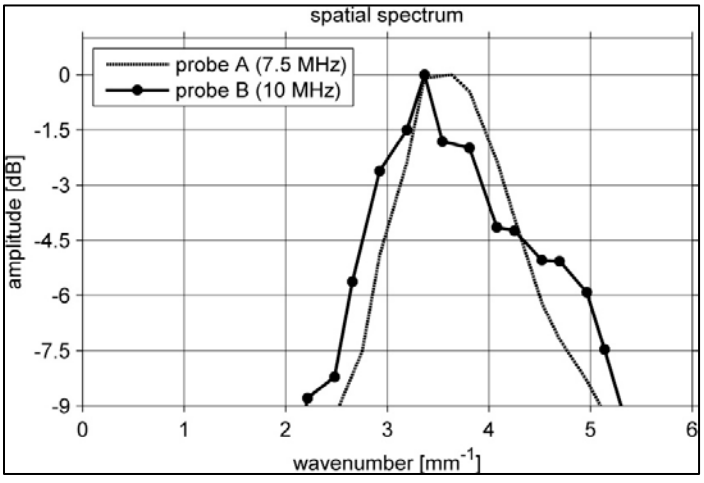

Figure 14. Comparison of spatial spectra for the images of the notch in main direction (normal to the notch)

The results of the comparison of the 7.5 MHz and 10 MHz array probes can be summarized as follows:

- As expected, the resolution of the time signals is better for the 10 MHz probe than for the 7.5 MHz probe.
- For imaging, parameters such as aperture, element directivity, and distance between array and defect play a role as well. Therefore, the increase in resolution when using a probe of higher frequency is less pronounced for images taken at typical working distance, which is in the order of the width of the array aperture. Nevertheless, the 10 MHz probe performs slightly better in all imaging tests.
- There are additional advantages when using the 10 MHz probe. It is designed for 64 elements whereas the 7.5 MHz probe has 128 elements. Therefore, the 10 MHz probe can be used with fewer active transmitters, thereby enabling higher scanning speeds. At the same time, the elements of the 10 MHz probe are slightly wider, which results in higher energy transfer per element into and from the sample.
- The more pronounced directivity of the 10 MHz probe turns out to have no negative effect on the image quality at typical distances between array and imaging area.

SAMPLES FROM THE FIRST ROUND OF TESTING

Samples needed to be obtained, organized, and prepared for initial testing. These samples were solicited through several avenues including failure analyses performed at Kiefner's metallurgical lab, cofounding partners TransCanada and Enbridge, and from PRCI member companies and the PRCI sample repository in Houston. The goal was to assimilate samples with varied characteristics such as different seam types, SCC, surface corrosion, selective seam corrosion, and minor deformations along the seam weld. Concurrently, the use of IWEX for various diameters and to allow higher resolutions, a 10 MHz probe, wedges for various diameters and a portable, encoded scanner platform also needed to be developed. High sampling rate development was also explored.

8-in x 0.188-in Samples

The initial set of samples was acquired because a set of destructive tests was scheduled to be performed at the Kiefner Metallurgical lab in Columbus, Ohio on 8-in 0.188-in wt ERW pipe samples. Defects were identified from a circumferential MFL ILI tool run and the operator wanted verification of sizing and severity for the defects identified from metallurgical sectioning and cryogenic fractography breaks.

Initially, no valid results were available from these tests. Two hypotheses for the poor results were discussed:

1. The wedges were manufactured at a machine shop near Houston rather than the ApplusRTD wedge manufacturing facility in Rotterdam. This caused the wedge material to be slightly different.
2. The pipe was the smallest diameter and thinnest wall pipe attempted to date at only 8.625-in diameter and 0.188-in wall thickness.

To determine the true cause of the problem, a short section of this pipe was sent to researchers at the Technology Center in Rotterdam for testing.

Test measurements with the IWEX system were taken in Rotterdam on 8.625-in pipe with a wall thickness of 4.775 mm containing an ERW seam weld. Notches were manufactured in the pipe to have controlled reflectors. An image of the test setup is shown in Figure 15.

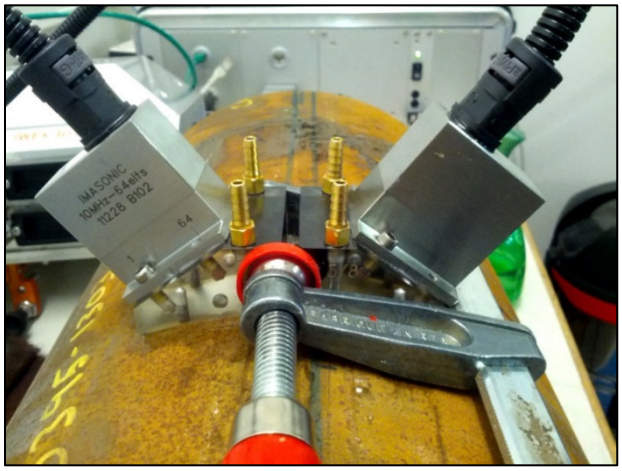

Figure 15. Basic IWEX test setup with wedges on both sides of the weld

A schematic drawing of the setup is shown in Figure 16. This is the basic view presented by the software, showing the imaging region at the weld centerline and the indications found.

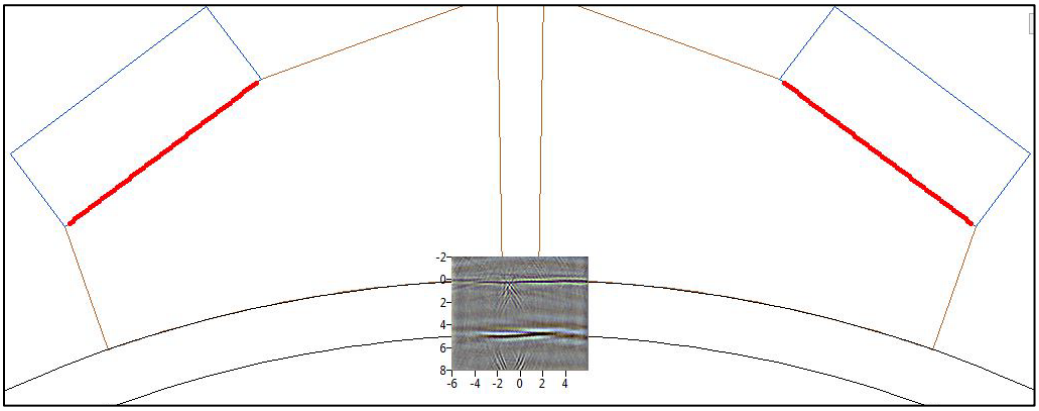

Figure 16. Basic IWEX test setup as shown in the software with an overlay image of the region of interest around the weld

A typical IWEX image of a piece of pipe without defects present is shown in Figure 17. The position of the inner pipe interface (ID) is shown by the bluish horizontal indication from the IWEX-0 mode. The green indication at the top of the image from the IWEX-2 mode represents the outer interface (OD).

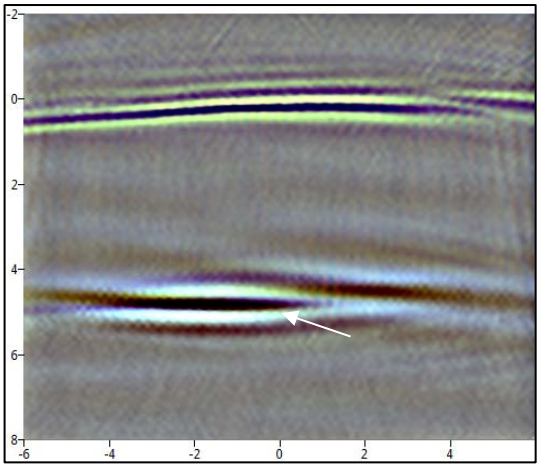

Figure 17. IWEX image of a clean piece of pipe

Whenever there is a defect present in the pipe, additional indications appear in the IWEX image. In general, a single flaw can lead to several different indications in the image picked up by the different IWEX modes. Figure 18 shows the IWEX image of a notch extending 20% into the pipe from the OD surface. In addition to vertical indications in the IWEX-3 mode and a tip diffraction picked up by the IWEX-2 cross mode (horizontal indication used for height sizing), the other two IWEX-2 modes from the right and left show corner effects at the top of the notch, leading to diagonal indications in the image.

In the current implementation, the operator can choose to look at the different IWEX modes separately. However, there is no tool available that links associated indications automatically. Therefore, the current output of the measurement software requires a skilled operator in order to correctly interpret the combination of indications present in the image.

During the tests, it became evident the IWEX system is susceptible to small changes in the setup geometry. Variations can be caused by movement of the wedges, leading to changes in their distance. Other variations can be caused by the pipe geometry.

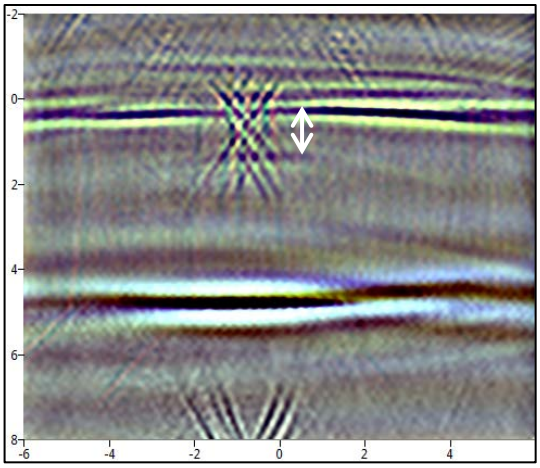

Figure 18. IWEX image of a 20% top notch, vertical extent indicated by the arrow. Indications are present in several modes, which are superimposed on each other. A mirror image of the defect is visible below the inner pipe interface.

Any deviation of the actual geometry from the assumed setup affects the image quality. In general, a shift of the different modes is the most prominent result. In addition, slight defocusing can occur.

These effects can be caused by changes in the pipe wall thickness, too. Figure 19 presents an example of this case. The actual wall thickness deviates from the geometrical model, leading to double indications of the inner pipe wall in the left half of the image. The bluish IWEX-0 mode shows that the pipe is actually thicker to the left side of the weld. The greenish IWEX-2 mode is a mirrored version of the same indication, based on the assumed nominal position of the inner pipe wall as a mirroring plane.

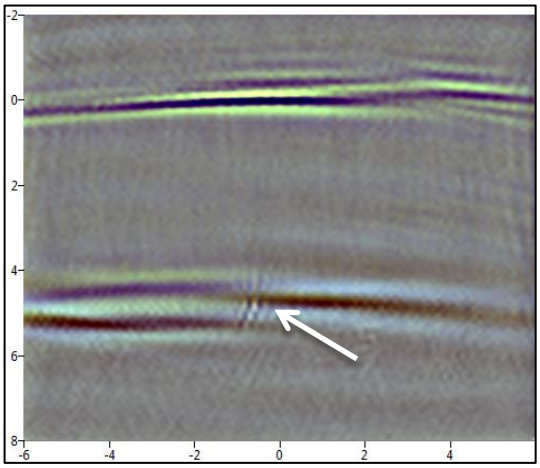

Figure 19. IWEX image with an example of poor trim. The difference in wall thickness between the left and right side is indicated by the arrow. The bluish IWEX-0 image shows the actual wall thickness. Another indication mirrored at the nominal position of the inner interface is visible in the greenish IWEX-2 mode just above the inner interface on the left side.

Two notches were manufactured into the 8-in pipe so that known reference defects would be present. The results yielded expected results; images of both the 20% and 50% through wall notch were obtained. The wedges used were the same ones used in Columbus during the 8-in pipe testing conducted there. This indicated there was a problem with the procedures, likely in the setup. These samples were not examined again in part because the IWEX testing was an opportunity, not a specific task of the client.

As a result of these tests it was determined the next North American tests would be performed on more familiar pipe of larger diameter and greater wall thickness. Samples would need to be made available that were specifically for IWEX testing.

24-in DSAW samples

The next available samples used for testing were 24-inch double submerged arc-welded (DSAW) pipe located in Canada. Wedges were manufactured for the tests from the Applus RTD shop in Rotterdam for testing performed at the Applus RTD facility in Edmonton, Alberta.

Initial testing by the Applications Center specialist in Edmonton failed to produce any images. This was the same situation that occurred on the previous 8-inch diameter tests. Images of the ID and OD were obtained away from the weld in the parent material, but could not be obtained in the weld zone after repeated tries. It was not immediately clear why these tests were unsuccessful and it was decided to send the equipment back to the Applications Center in Houston for troubleshooting and testing.

After multiple attempts at testing in Houston, it was decided to cutout a small section of the weld itself to send back to Rotterdam for additional testing. Ultimately the difficulty appears to be the large amount of weld metal in the root and cap that protrudes above and below the nominal wall thickness of the adjoining pipe body. Although the IWEX system was initially developed for girth welds that have ID and OD weld caps, the DSAW weld caps are larger and were thought to be creating difficulties.

As a result of gathering this information, improvements in the setup enabled the 24-in DSAW samples to be scanned in Edmonton. Only very shallow flaws were found, so only four anomalies were selected for sectioning. Two coupons with two anomalies each were sent to Ohio for sectioning. Although many more anomalies were discovered in the samples, none were very deep and none were significant enough to threaten the integrity of the pipe. Results were initially not conclusive because of sample marking procedures entailed using a punch to mark the location of the defects. Additional sanding removed sufficient material to reveal the tiny (<< 1mm deep) flaws. Although these flaws were real and causing ultrasonic anomalies they were not an integrity threat. The small size of these flaws made accurate sizing by IWEX difficult.

Although it appears that accurate sizing for these very small flaws may not be needed as long as they can be shown to be small and insignificant.

16-in ERW Samples

A short piece of 16-in pipe was sent to Houston in anticipation of the planned tests in Columbus. The Houston Application Center (AC) was to perform testing and debugging in order to develop a working procedure before returning to Columbus for testing on three different wall thicknesses of 16-in diameter pipe. However, a video session between Rotterdam and Houston revealed the problem to be incorrect input of a parameter describing left and right transducer separation. The NDE technicians in North America were making measurements next to the pipe, whereas the Rotterdam physicists had designed the software to make a more accessible measurement to be taken at the top of the wedges. After debugging this problem, successful images were obtained on the 16-in samples. This also allowed for measurements to be successful on the previous 24-in SAW sample of pipe. This was similar to the cause of problems scanning the 8.625-in pipe.

Below are images obtained from the Houston AC testing. The image on the left shows a seam weld with no defect although there is some trim variability, whereas the image on the right shows a lack of fusion (cold weld) anomaly in the seam. The right image also shows poor trim on the ID with an offset in the ID surface. The cross pattern on the OD is an artifact of a corner reflection at the base of the lack of fusion. In this case the IWEX-2 modes from the left and right produce 45-degree lines where the vertical crack-like anomaly meets the surface. These corner reflections are similar to what PA produces from the corner when identifying surface breaking cracks-like anomalies, only PA will not image the vertical flaw itself and must be inferred. IWEX images the vertical anomaly with a tandem mode such as IWEX-1 or IWEX-3 which requires an odd number of skips off the OD and ID surfaces.

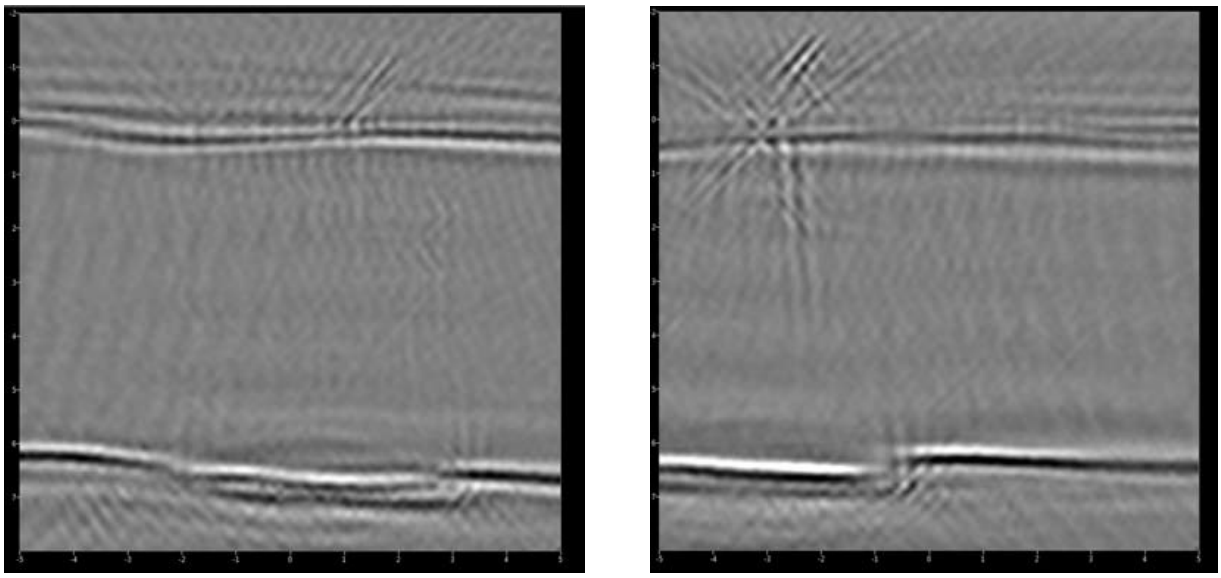

(a) (b)

Figure 20. 16-inch ERW samples inspected at Houston AC (a) no seam weld defect with trim variability, (b) lack of fusion anomaly

Testing proceeded in Columbus. The scanner was set up to take IWEX, PA and TOFD data simultaneously with each measurement sitting side by side and just a few inches apart. A sample of the data gathered is included in the table below. As can be seen from the table, the three techniques often produce similar results, but not always. Scan images are shown in Figure 21, Figure 22, and Figure 23.

Sample ID		Detection			OD Surface Breaking Flaw Depth (mm)			ID Surface Breaking Flaw Depth (mm)			Mid-Wall Flaw (mm) IWEX/PA/TOFD	
	Defect #	IWEX	PA	TOFD	IWEX	PA	TOFD	IWEX	PA	TOFD	Bottom	Height
A2	13	X	X	X	.3	.6	.4					
	14	X	X		.6	.6	NA					
	16	X	X	X	.8	1.3	1.0					
B2	4	X	X		.5	.4	NA					
	12	X	X	X	.5	.6	.5					
	14	X	X	X	.3	.4	.2					
E2	1	X	X	X	6.2	6.2	6.2					
	5	X	X					.6	.5	NA		

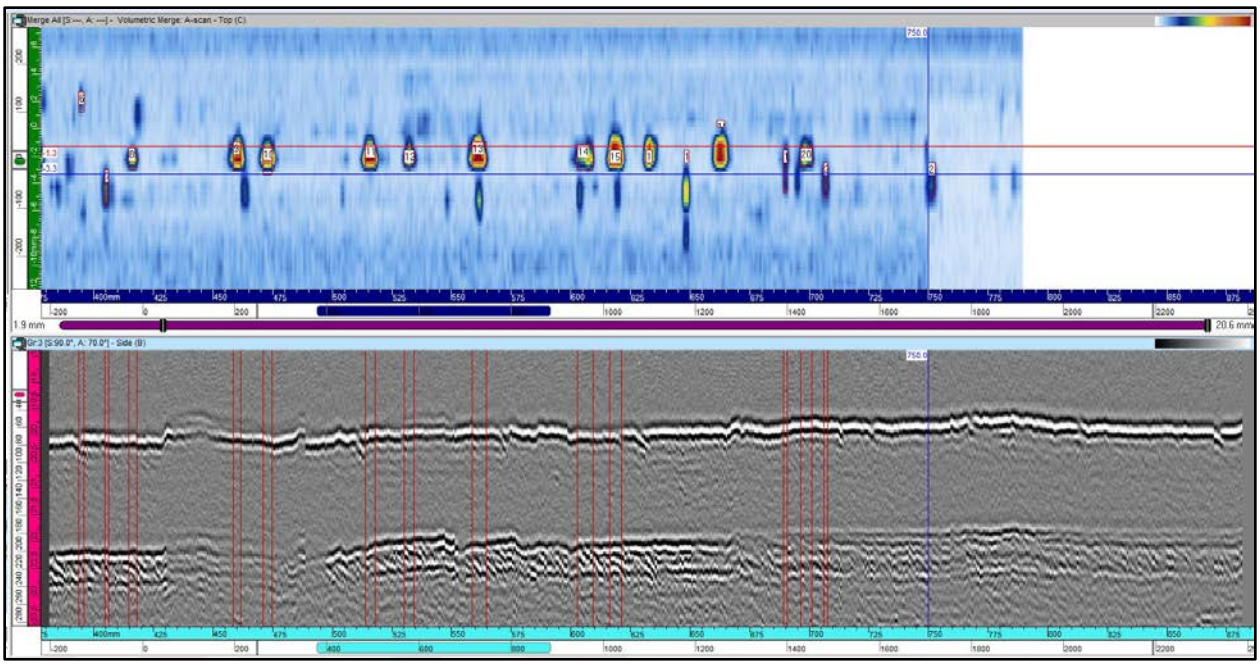

(a)

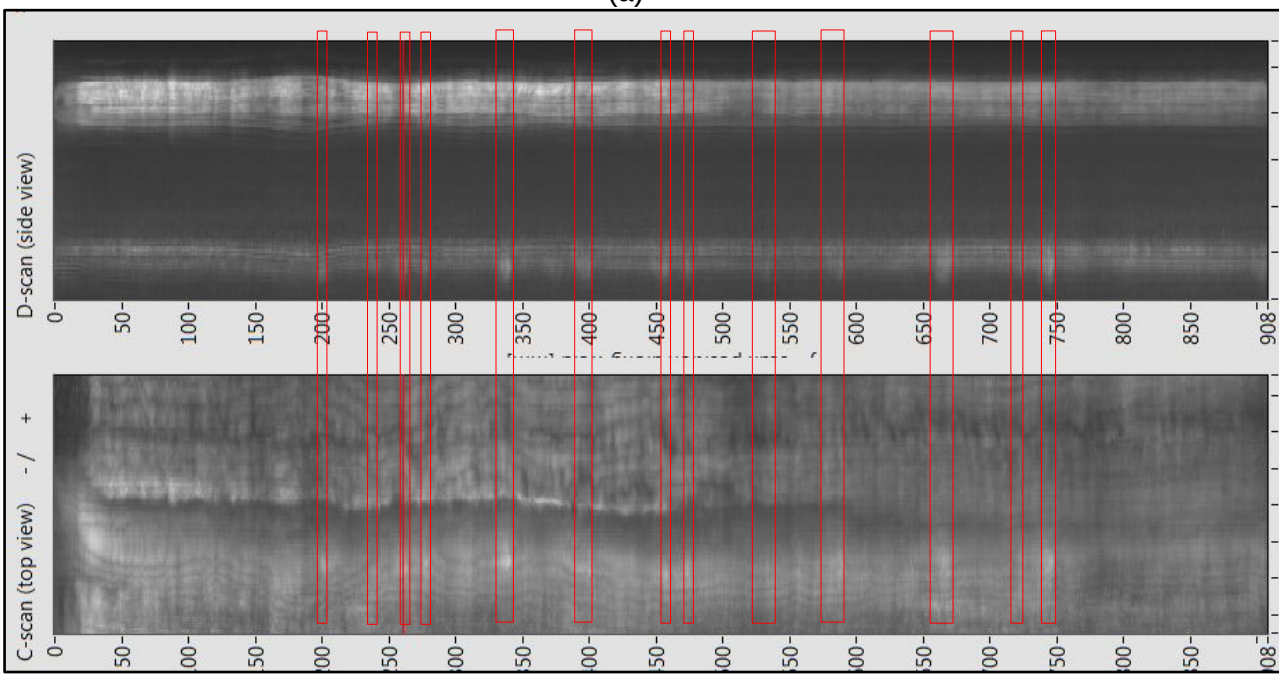

(b)

Figure 21. Phased Array scan on 16-inch diameter x 0.250-inch (6.2mm) Sample A2, (a) C-scan, TOFD, (b) IWEX C-scan and D-scan

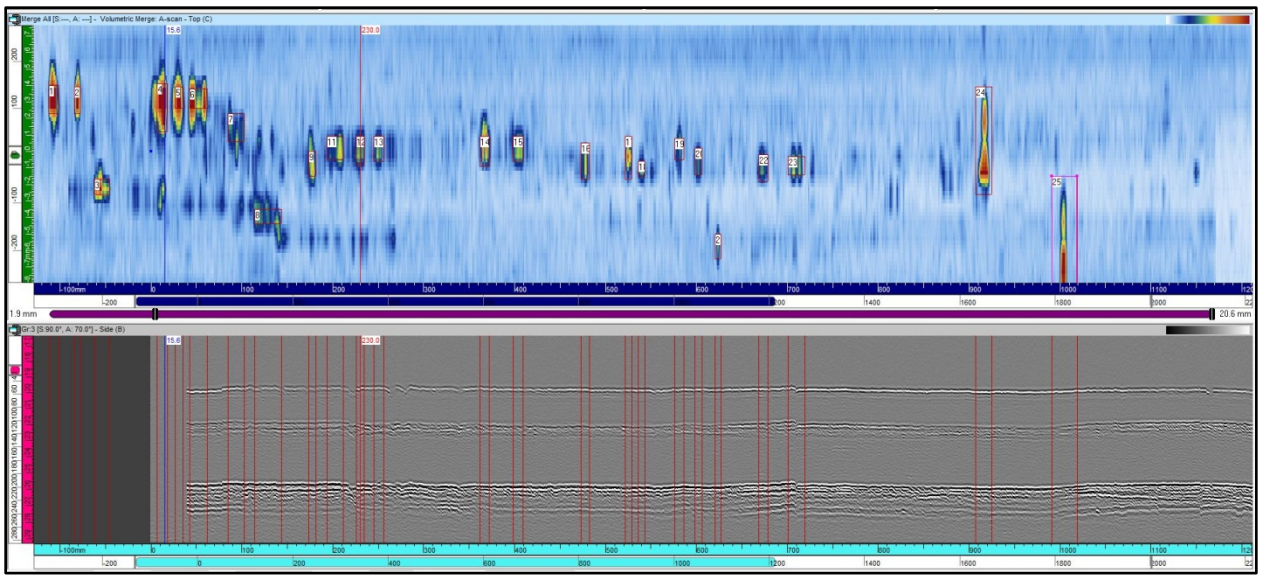

(a)

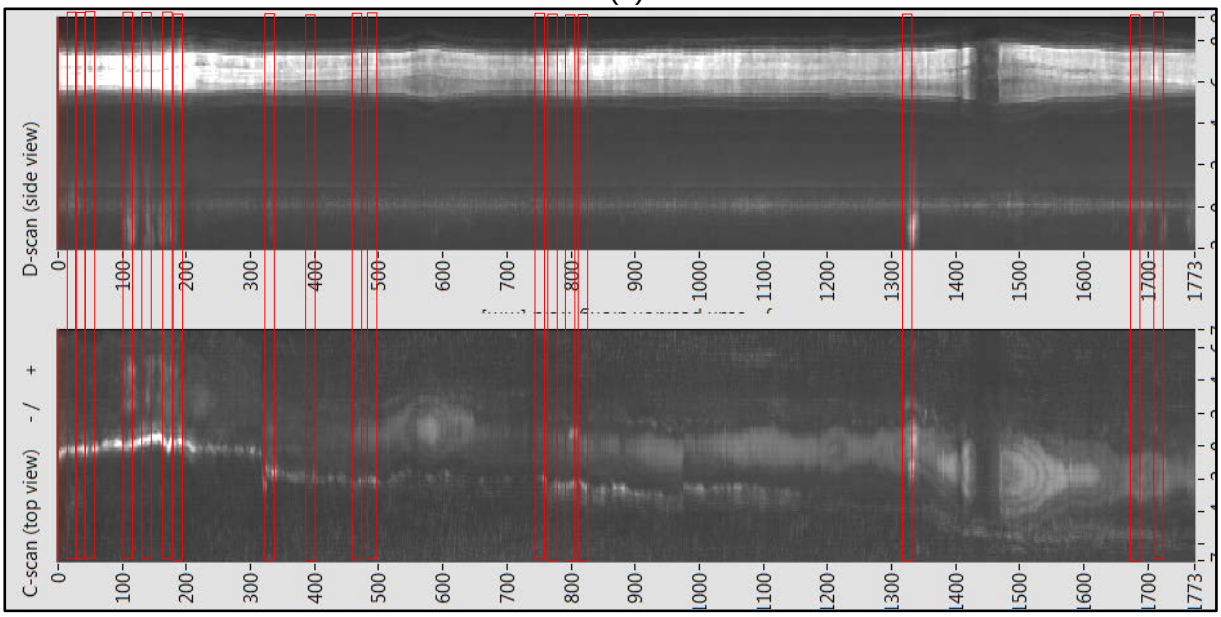

(b)

Figure 22. Phased Array scan on 16-inch diameter x 0.250-inch (6.2mm) Sample B2, (a) C-scan, TOFD, (b) IWEX C-scan and D-scan

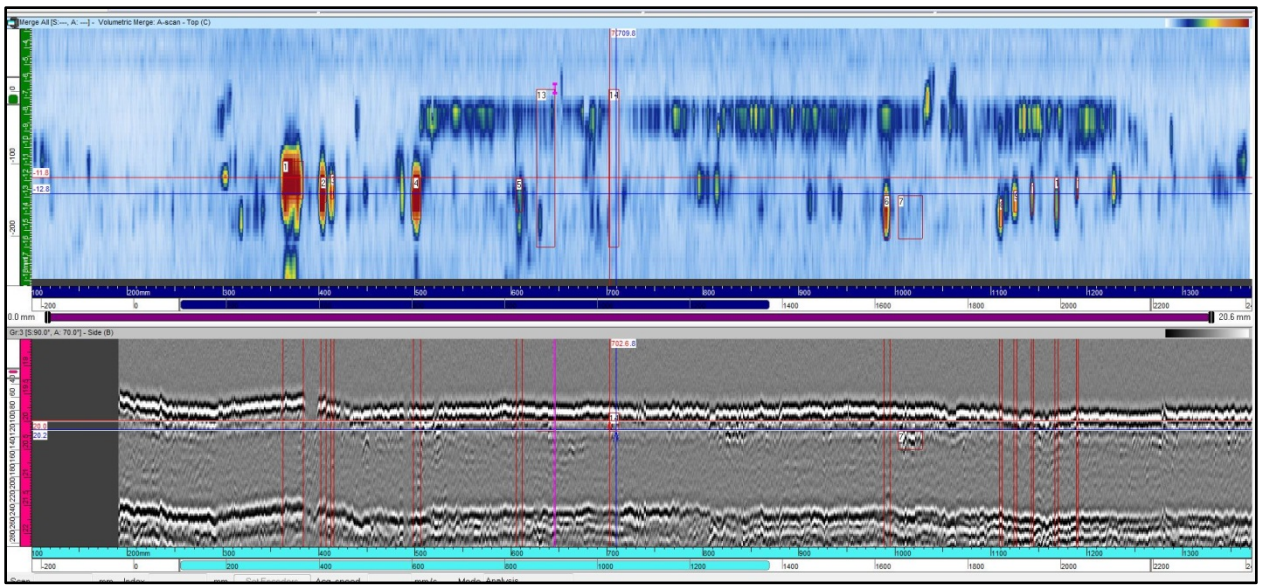

(a)

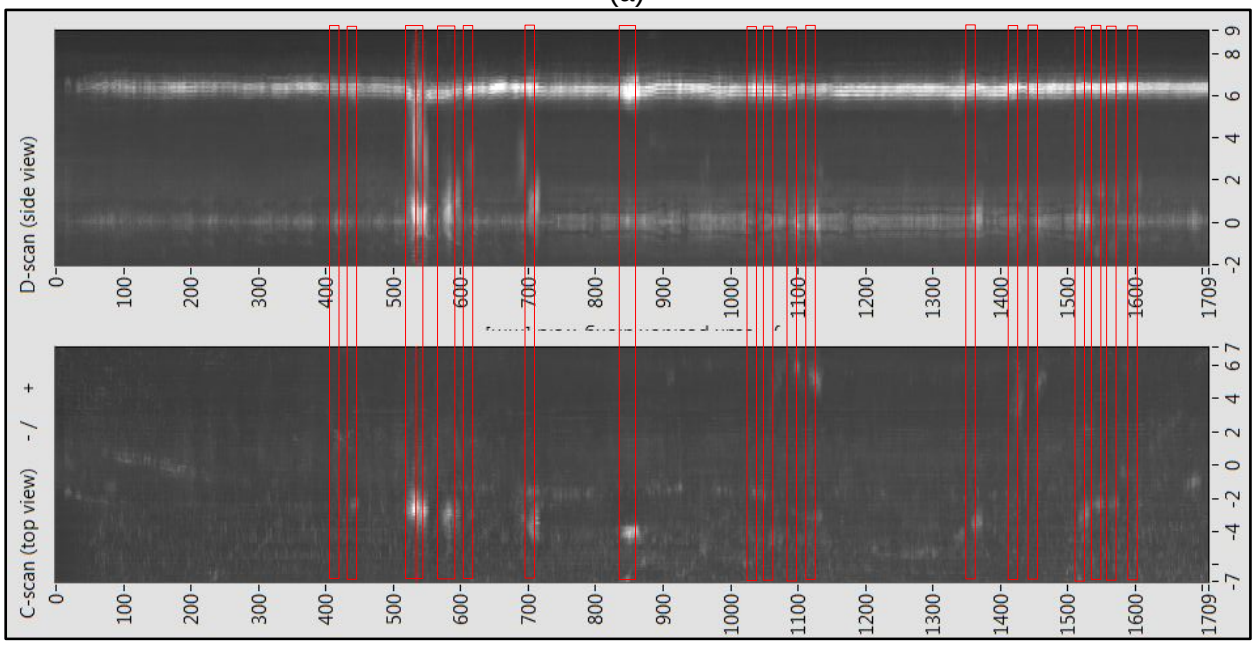

(b)

Figure 23. Phased Array scan on 16-inch diameter x 0.250-inch (6.2mm) Sample E2, (a) C-scan, TOFD, (b) IWEX C-scan and D-scan

The 16-in ERW samples were inspected twice. After the first set of inspections, good signals were obtained including multiple indications of lack of fusion (cold weld) anomalies. Upon breaking samples open for comparison, defects were not found in the inspected locations. It was determined that there were problems in the software associated with the odometer encoder causing samples to be broken open in the wrong locations. Software bugs were corrected and 16-in inspections were repeated on the remaining 16-in ERW samples. Defects were broken open in the Kiefner metallurgical lab and comparisons were made with sizing

obtained from the IWEX equipment. Although discrimination of various types of defects continues to impress the R&D team and others who have seen the data, sizing accuracy was not as good as expected considering previously published ±0.2mm data by the Rotterdam development team on synthetic defects placed in a simulated girth weld.

The poor accuracy is not fully understood and may have to do with the short length of the defects and the lack of focusing of the transducers, but this needs to be further examined. The 16-in wedges were made in 2012 before the start of this project. These were the earliest wedges made by the Rotterdam wedge manufacturing facility for inspection of axially oriented defects and did not contain focusing in the design. Following below are several tables and charts analyzing the sizing data obtained.

A table of defects analyzed for height and length of incomplete fusion flaws is shown below.

IWEX Defect No.	Vertical Location from Start (0) mm	Type of Defect	IWEX Length (mm)	IWEX Depth (mm)	IWEX Height (mm)	Lab Length (mm)	Lab Height (mm)	Lab Depth (%)
1	96	Incomplete Fusion (IF)	5	0	0.8			
2	105	Incomplete Fusion (IF)	5	0	0.8			
3	184	Incomplete Fusion (IF)	7	0	1.8	4.318	3.0	44%
4	286	Incomplete Fusion (IF)	8	0	0.5	3.048	1.3	18%
5	312	Incomplete Fusion (IF)	11	0	0.8	3.302	2.3	32%
6	373	Incomplete Fusion (IF)	7	0	1.2	3.556	2.5	37%
7	471	Incomplete Fusion (IF)	9	0	1.4			
8	489	Incomplete Fusion (IF)	9	0	0.7	5.842	3.0	44%
9	514	Incomplete Fusion (IF)	10	0	2.1			
10	545	Incomplete Fusion (IF)	23	0	4.2	2.794	4.1	59%
11	575	Incomplete Fusion (IF)	18	0	1.3	16.51	6.4	89%
12	657	Incomplete Fusion (IF)	7	0	0.6	3.81	2.3	32%
13	680	Incomplete Fusion (IF)	6	0	0.7	7.366	4.3	63%
14	698	Incomplete Fusion (IF)	5	0	1	9.144	2.0	30%
15	1025	Incomplete Fusion (IF)	11	0	1.7	5.08	2.0	30%

Unity plots of the height and length measurements from both the IWEX system and metallographic breaks along the seam are shown in Figure 24. Units are presented in mm, the customary units used for ultrasonic measurements. The IWEX heights are sometimes very close to the metallographic heights; however, on average, the IWEX system is under-sizing height for these lack-of-fusion defects. The lack-of-fusion defect length tends to be over-sized, which is expected since the transducers are unfocused.

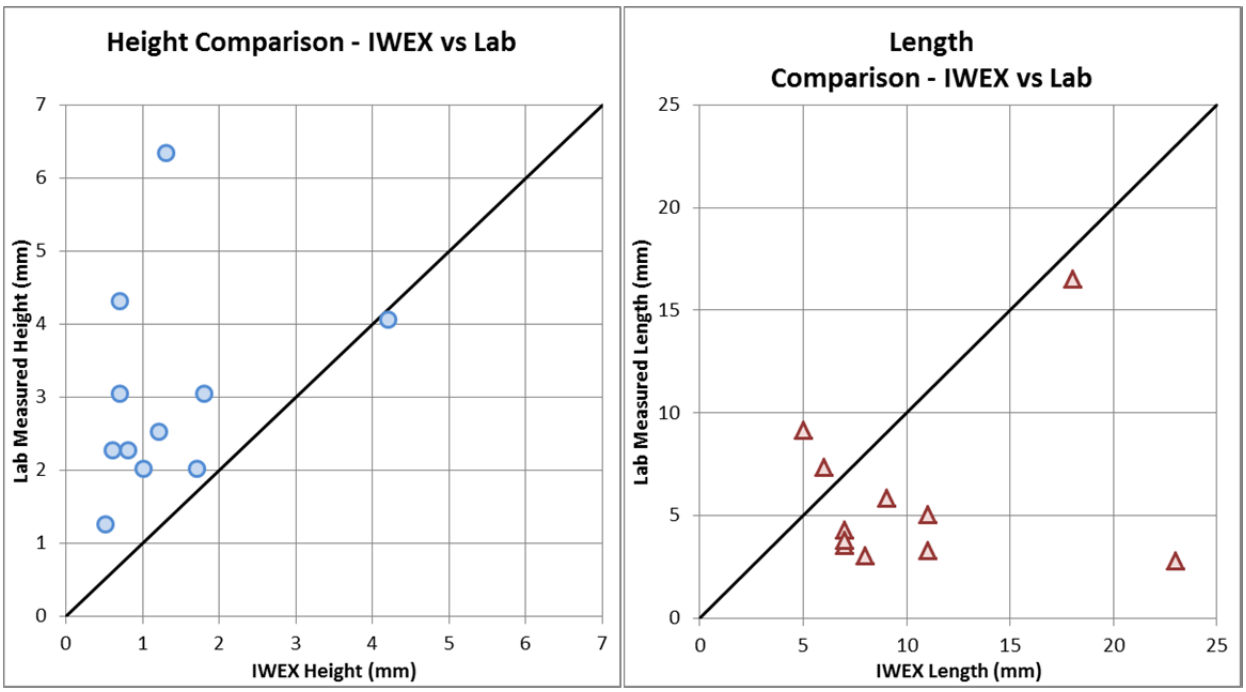

Figure 24. Unity plots of the measurement error for the 16-in ERW samples

Cumulative distribution plots of the measurement error are shown in Figure 25. Although the median height error for the samples is under-sizing of 1.3 mm, three samples have much larger errors of -2.3, -3.6, and -5.1 mm. The median length error is 3 mm, with one sample standing out with an anomalously large error over-sizing the length by 20 mm. Neither of these distributions appears to behave like a normal distribution, unlike a typical error distribution observed when measuring corrosion depth by ILI or in-ditch NDE.

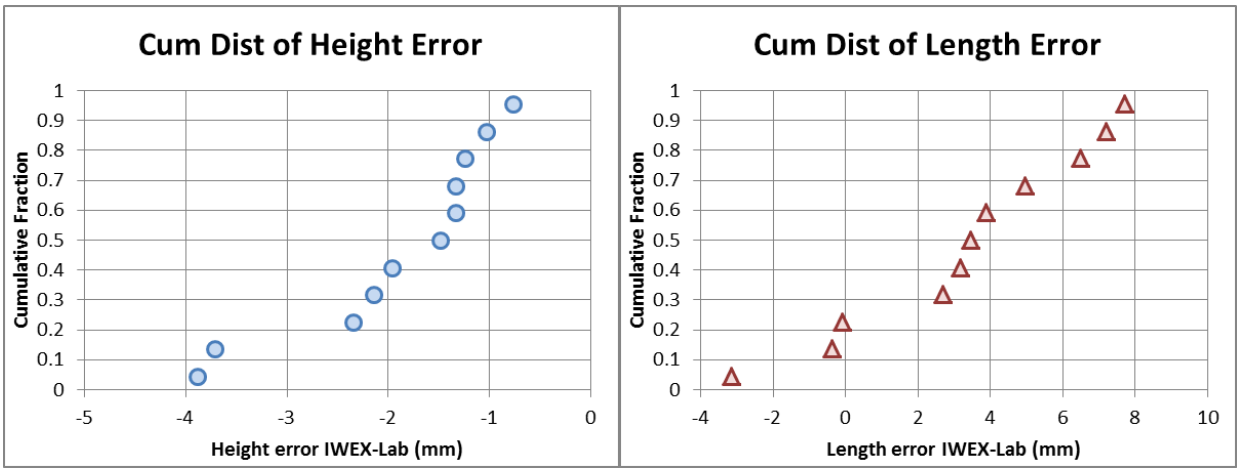

Figure 25. Cumulative distribution plots of the measurement error for 16-in ERW samples

A table of the defect size error in inches with pictures of the metallographic breaks is shown below for most of the defects. Units are in inches, typical of metallographic photographs taken

in the Kiefner failure analysis lab. Defects are also sorted from most negative (and worst) height error to the most positive height error to determine if there are any discernable trends in the photographs that could be related to the quantified measurement error. At first glance it appears the only distinctive feature for the worst two depth errors is the deepest part of the lack-of-fusion is at the end of the defect. It is not clear why this would lead to larger depth errors, but if it is related then better focusing should improve depth sizing by IWEX. Interestingly the 16-inch wedges are the only wedges that do not have focusing built into them. It is entirely coincidental that they were used on the first sizing trials. Additional images comparing the metallographic breaks to IWEX images are shown in Table 2.

Table 2. Metallographic IWEX and lab comparison data

		IWEX Measured		Lab Measured				Height Error	
IWEX Defect Number	Start Location mm	Length (in)	Height (in)	Length (in)	Height (in)	Seam WT (in)	Depth (%)	IWEX-Lab (mm)	Cumulative Fraction
16	1025	0.433	0.067	0.28	0.22	0.27	81%	-0.153	0.042
13	657	0.276	0.024	0.29	0.17	0.27	63%	-0.146	0.125
8	489	0.354	0.028	0.23	0.12	0.27	44%	-0.092	0.208
11	545	0.906	0.165	0.65	0.25	0.28	89%	-0.085	0.292
10	514	0.394	0.083	0.11	0.16	0.27	59%	-0.077	0.375
5	312	0.433	0.031	0.13	0.09	0.28	32%	-0.059	0.458
6	373	0.276	0.047	0.14	0.1	0.27	37%	-0.053	0.542
14	680	0.236	0.028	0.36	0.08	0.27	30%	-0.052	0.625
3	184	0.276	0.071	0.17	0.12	0.27	44%	-0.049	0.708
15	698	0.197	0.039	0.2	0.08	0.27	30%	-0.041	0.792
12	575	0.709	0.051	0.15	0.09	0.28	32%	-0.039	0.875
4	286	0.315	0.020	0.12	0.05	0.28	18%	-0.030	0.958

(a)

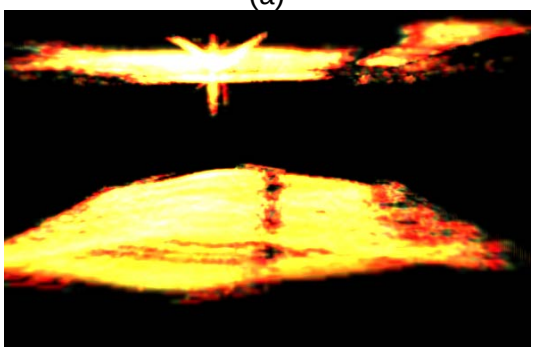

(b)

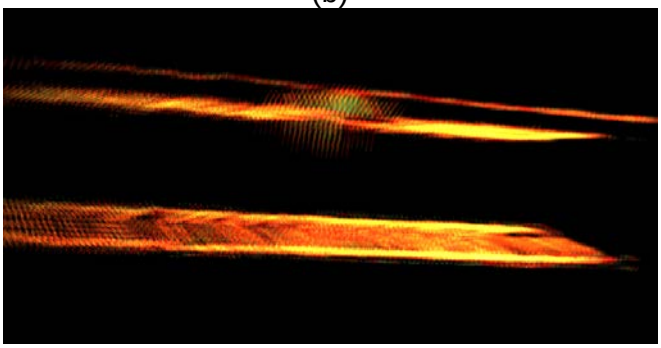

(c)

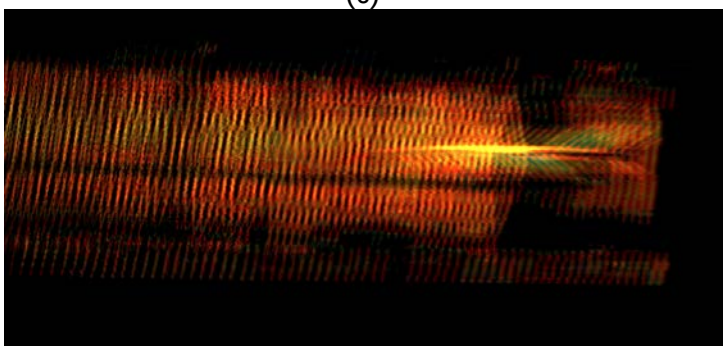

(d)

Figure 26. Reported flaw #16 (a) metallographic cross-section (b) IWEX 3D end view (c) IWEX 3D side view (d) IWEX 3D top view

(a)

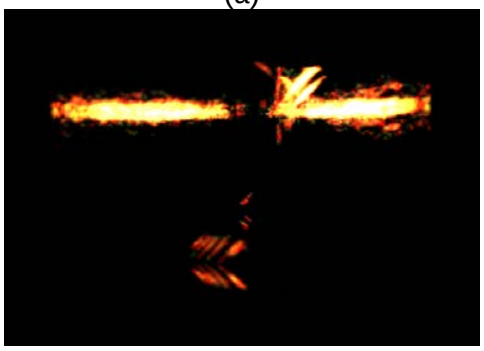

(b)

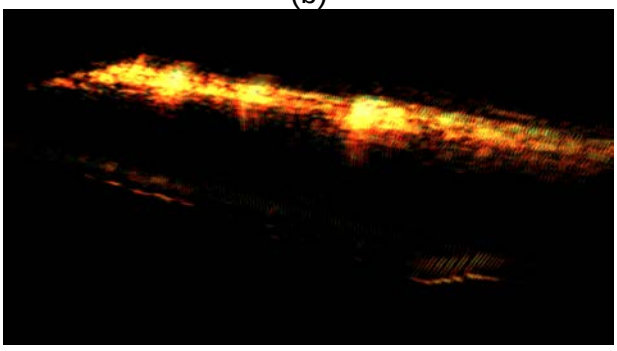

(c)

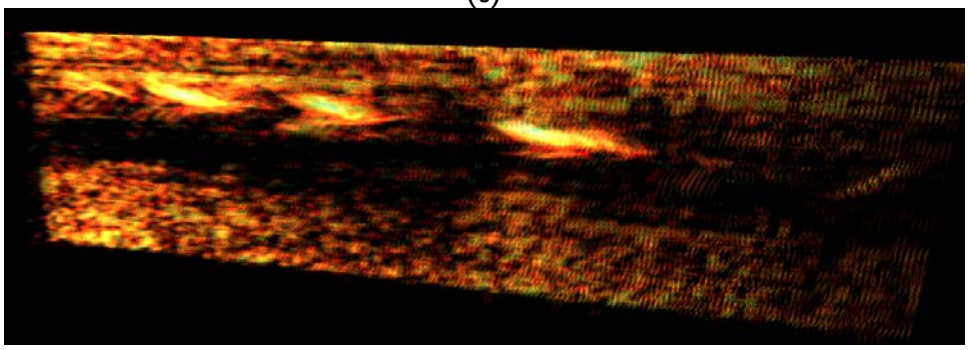

(d)

Figure 27. Reported flaw #13, #14, and #15 (a) metallographic cross-section (b) IWEX 3D end view (c) IWEX 3D side view (d) IWEX 3D top view

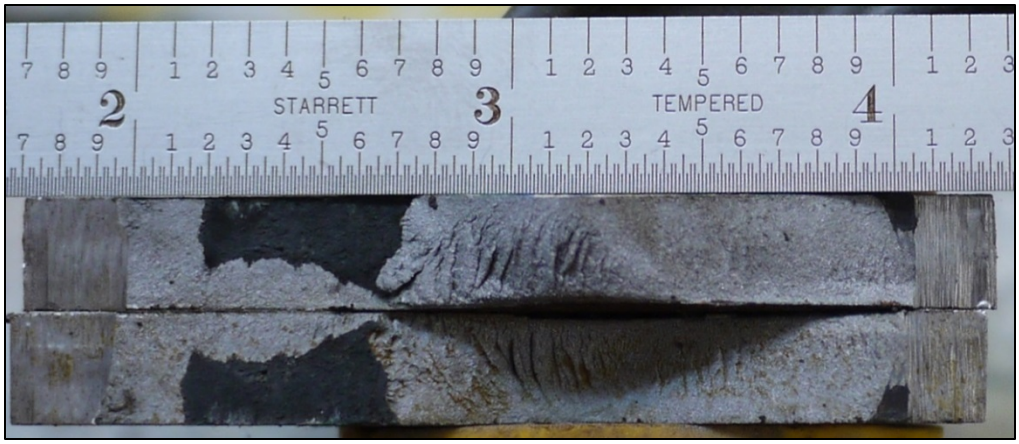

(a)

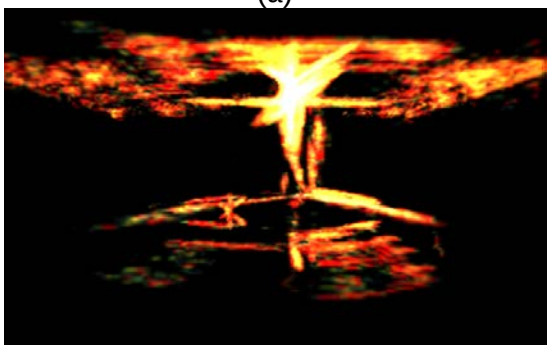

(b)

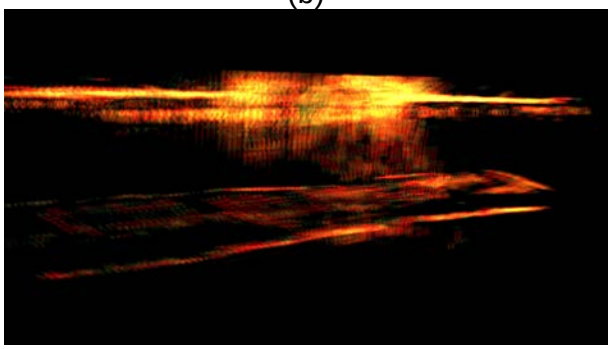

(c)

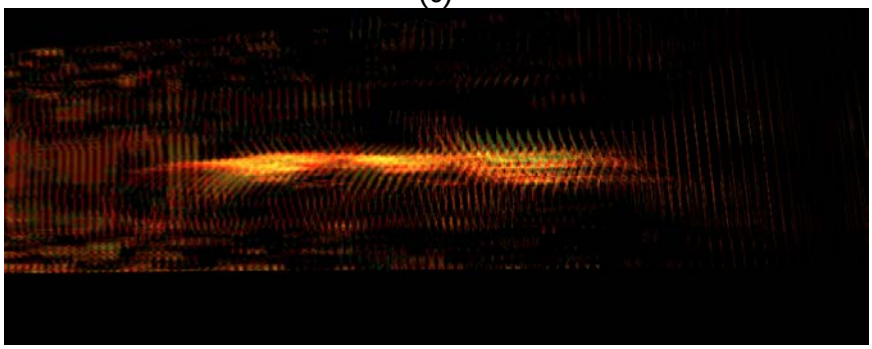

(d)

Figure 28. Reported flaw #11 (a) metallographic cross-section (b) IWEX 3D end view (c) IWEX 3D side view (d) IWEX 3D top view

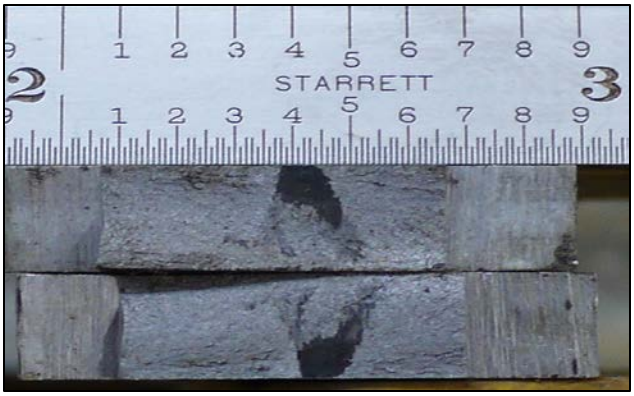

(a)

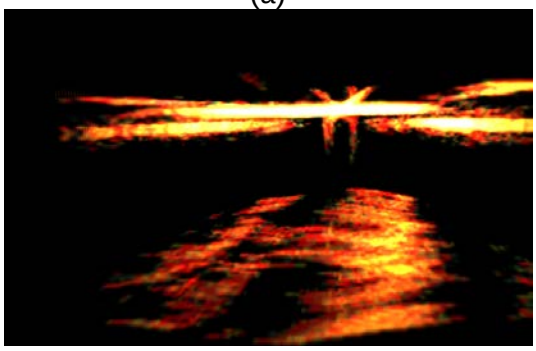

(b)

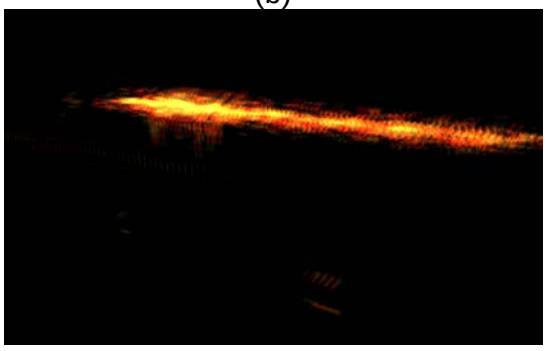

(c)

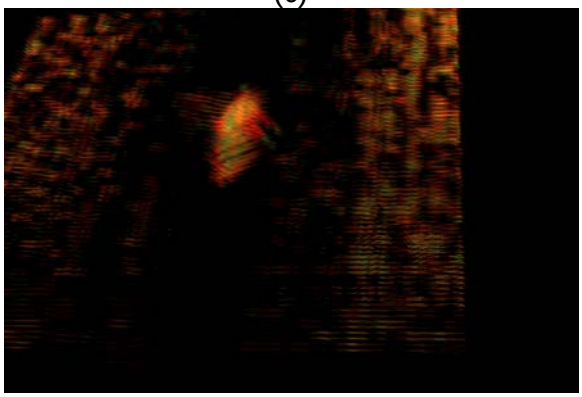

(d)

Figure 29. Reported flaw #10 (a) metallographic cross-section (b) IWEX 3D end view (c) IWEX 3D side view (d) IWEX 3D top view

(a)

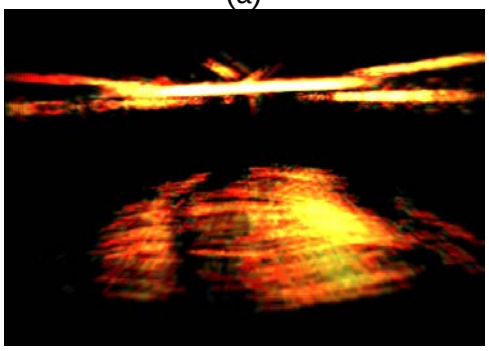

(b)

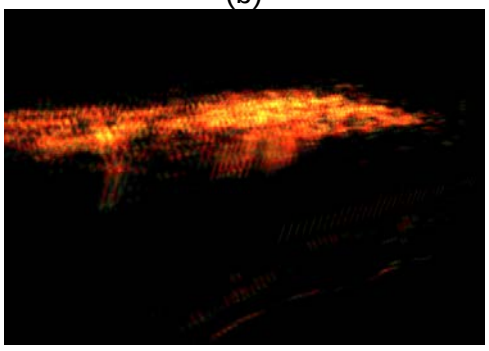

(c)

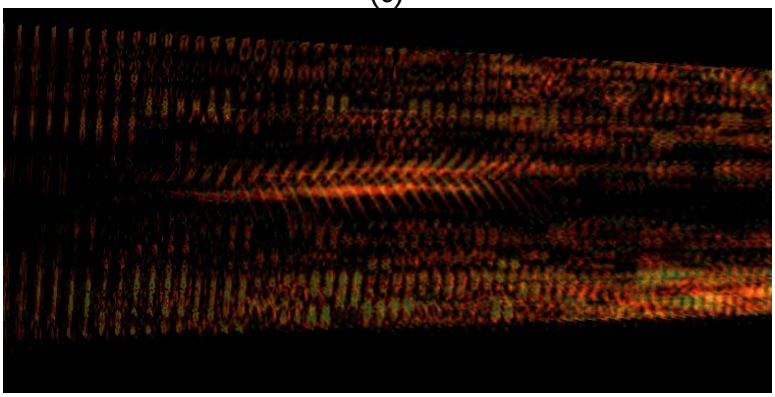

(d)

Figure 30. Reported flaw #10 (a) metallographic cross-section (b) IWEX 3D end view (c) IWEX 3D side view (d) IWEX 3D top view

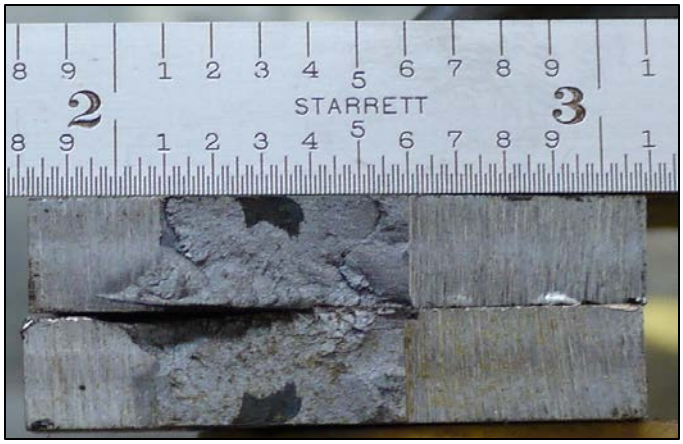

(a)

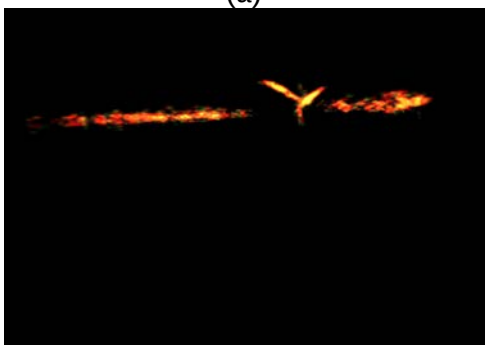

(b)

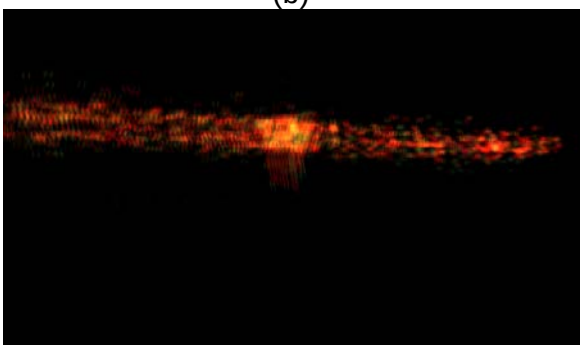

(c)

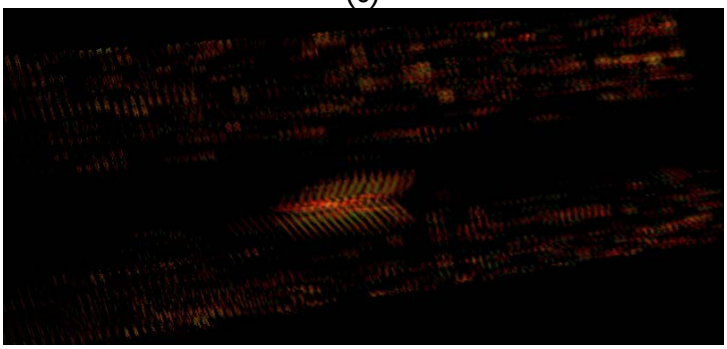

(d)

Figure 31. Reported flaw #6 (a) metallographic cross-section (b) IWEX 3D end view (c) IWEX 3D side view (d) IWEX 3D top view

(a)

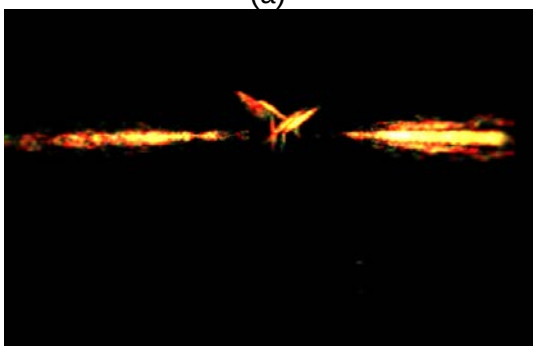

(b)

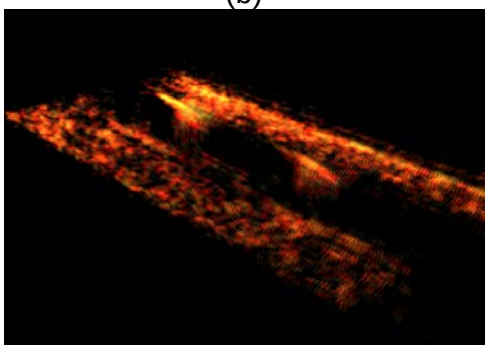

(c)

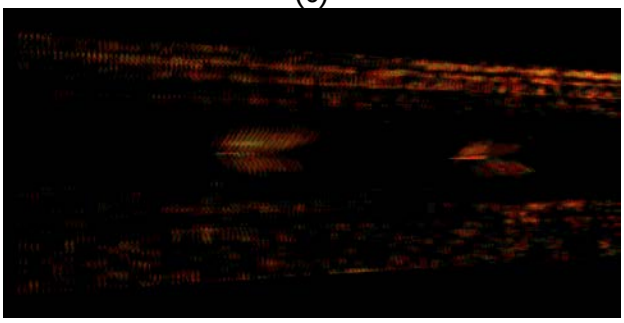

(d)

Figure 32. Reported flaws #4 and #5 (a) metallographic cross-section (b) IWEX 3D end view (c) IWEX 3D side view (d) IWEX 3D top view

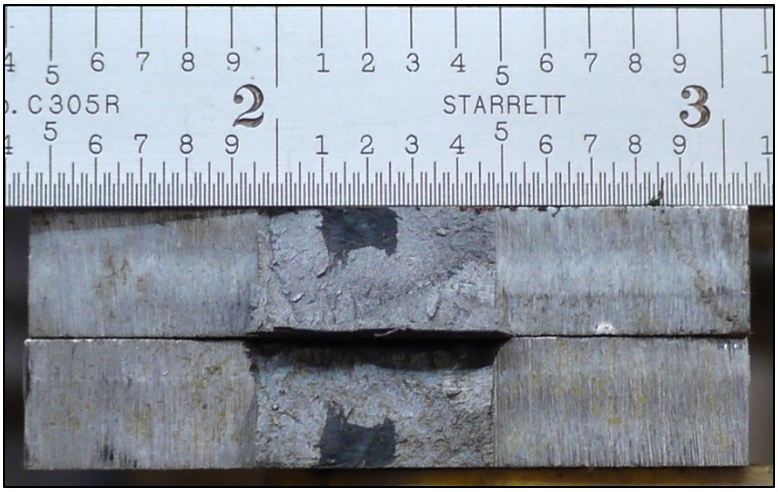

(a)

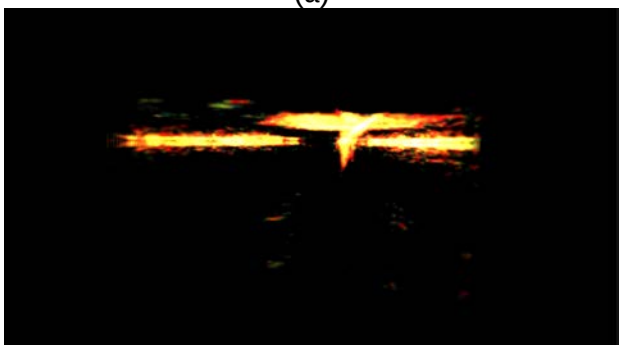

(b)

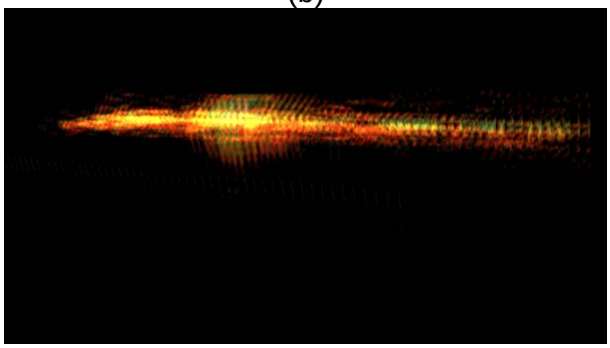

(c)

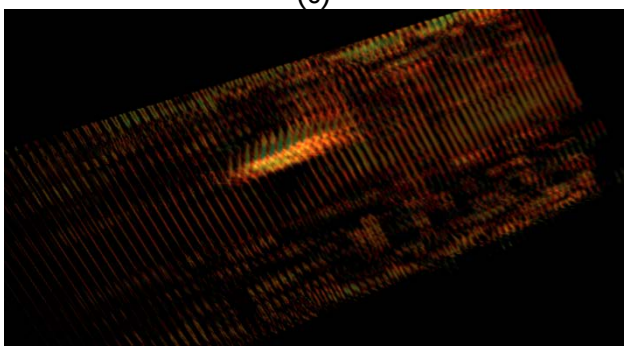

(d)

Figure 33. Reported flaw #3 (a) metallographic cross-section (b) IWEX 3D end view (c) IWEX 3D side view (d) IWEX 3D top view

The 16-in ERW samples were inspected a third time, this time using focused wedges. The first set of inspections produced good signals on the five samples but had problems with the software associated with the encoder. The second set of trials on the remaining four samples were inspected using the original unfocused wedges used for the initial 2012 seam weld inspections which predated this PHMSA R&D project. Although good signals were obtained and lack of fusion anomalies were easily identified the sizing was less than optimal. The beam width on the original wedges was approximately 10 mm, which is wider than all but one or two of the lack of fusion anomalies detected in the set of anomalies broken open in the trial. The third trial was performed on the remaining three samples using the focused wedges. The focused wedges have a beam width of about 3 mm and it appears from the initial results that sizing has improved. Results are presented in Table 3 with an IWEX screenshot image in Figure 34.

Table 3. Comparison between IWEX analysis and fracture surface results

Pipe ID	Axial Length (IWEX)	Axial Length (Fracture Surface)	Depth from OD (IWEX)	Depth from OD (Fracture Surface)	Height (IWEX)	Height (Fracture Surface)	Description
D-A	5	5.46	0.6	0	4.9	5.01	Incomplete Fusion Due to Cold Lap (IFD)
D-A	13	13.82	0.3	0	6	6.54	Incomplete Fusion Due to Cold Lap (IFD)
D-A	5	5.94	0.1	0	3.5	3.75 (4.61*)	Incomplete Fusion Due to Cold Lap (IFD)
D-A	6	8.04	0.1	0	3	3.6	Incomplete Fusion Due to Cold Lap (IFD)
B-B	4	6.3	0	0	3.1	3.37	Incomplete Fusion Due to Cold Lap (IFD)

(*for a length less than 0.5 millimeters, Defect 5 (PIPE ID: D-A) changes height from 3.75 to 4.61)

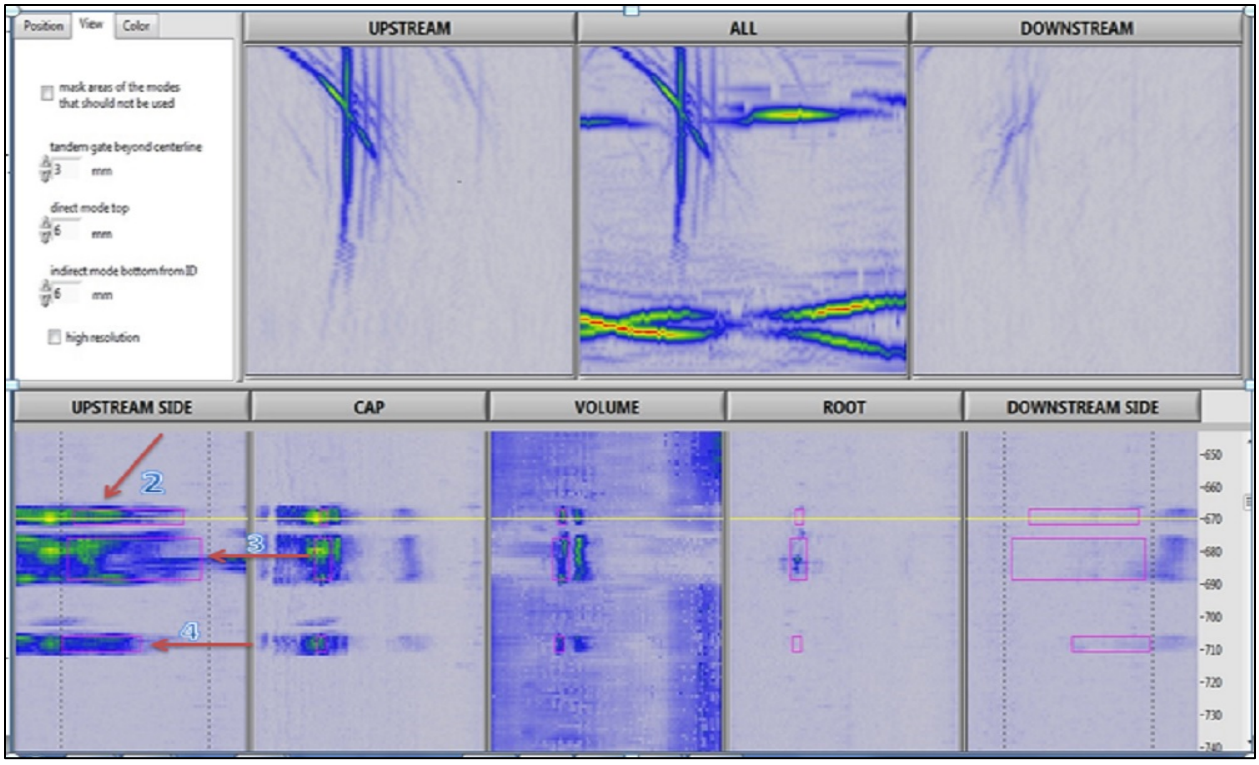

Figure 34. Pipe (ID: D-A) IWEX Image of Defects 2, 3 and 4

24-in SCC coupon

In order to test the applicability of IWEX to samples exhibiting stress corrosion cracking, experiments have been conducted with a sample containing high-pH SCC. This type of SCC is usually not associated with general corrosion of the pipe body. Therefore, the measurements are not complicated by coupling problems due to external corrosion. The sample is shown in Figure 35; it contains several visible cracks, some of which are through-wall.

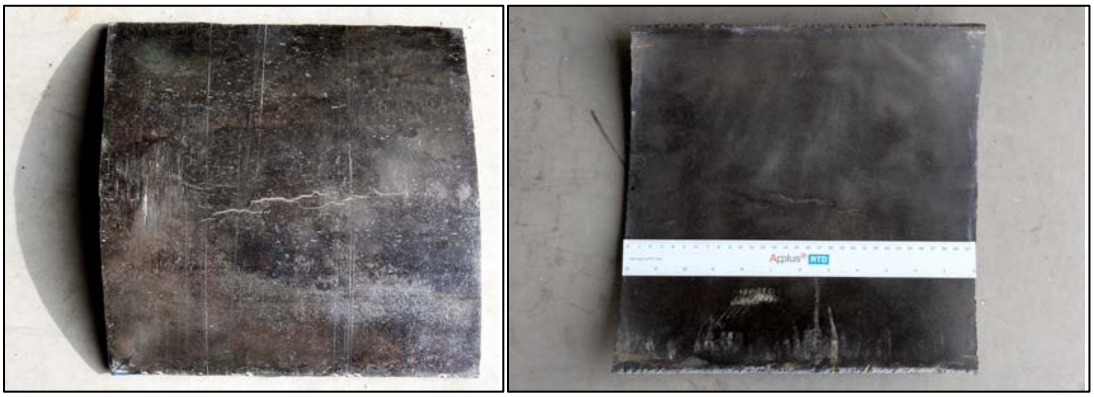

Figure 35. Pipe coupon containing SCC of about 12" length, 24" diameter, wall thickness 0.33" (8.5 mm)

The experiments were carried out using a water tank and a manipulator to move the probes.

The sample was submerged in water to simplify coupling of the wedges to the pipe coupon as shown in Figure 36.

Figure 36. Measurement setup with the pipe coupon being submerged in water (left); position of the two array probes on wedges with respect to the area of interest (right).

The IWEX measurement system was set up on a part of the sample which did not contain any cracks. The typical image is shown in Figure 37.

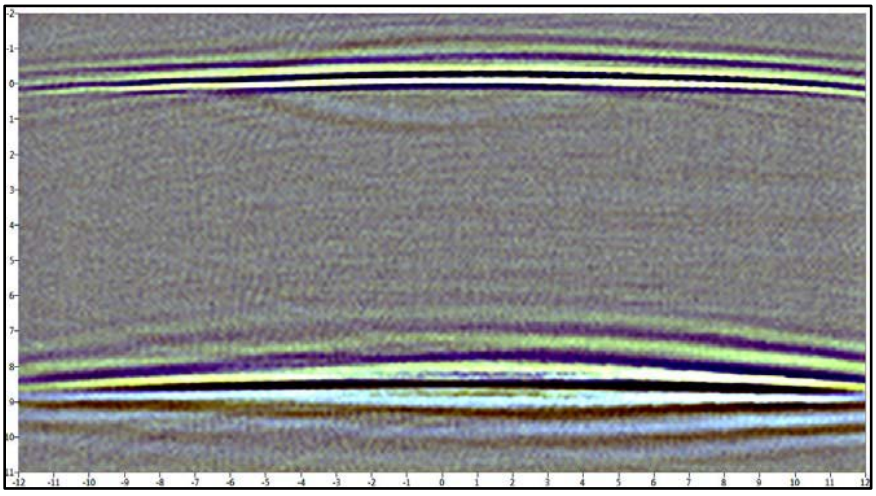

Figure 37. IWEX image of a clean part of the sample: only the interfaces are visible (all dimensions in millimeters).

An IWEX scan is carried out for a width of approximately 1 inch (24 mm). This is the maximum image width provided by the current IWEX system for the desired resolution of the image of 0.1 mm. In the scan direction, the resolution is chosen to be 0.5 mm. The IWEX images obtained during the scan show the presence and extent of the different cracks in the sample. Most cracks are surface-breaking at the outside of the pipe coupon. The corresponding indications in the image are mainly shown by the IWEX-3 mode, which is a tandem mode with an extra reflection at the outer surface. These indications are shown in red in Figure 38(a). In addition, there are corner effects due to specular reflections between the cracks and the outer surface. These

artifacts are green, diagonal indications crossing the outer surface, marked by arrows in Figure 38(a).

The outer pipe surface itself is not present or is weakly present in the image. This is caused by the cracks blocking acoustical energy from reaching the outer surface. In spite of the cracks creating an acoustical shadow zone, the detection of several cracks of similar height remains feasible for the example shown. This is due to the combination of direct, tandem, and skip imaging, which seems to be unhindered if the cracks are not extending further than half the wall thickness.

At the lower end of the cracks, tip diffractions are picked up by the IWEX-2 (skip) mode. The presence of these weaker indications is seen better when the IWEX-3 mode is switched off as shown in Figure 38(b). The height of the cracks can be determined roughly by the extent of the red IWEX-3 indications, but more accurately using the lower tip diffractions picked up by the IWEX-2 skip mode.

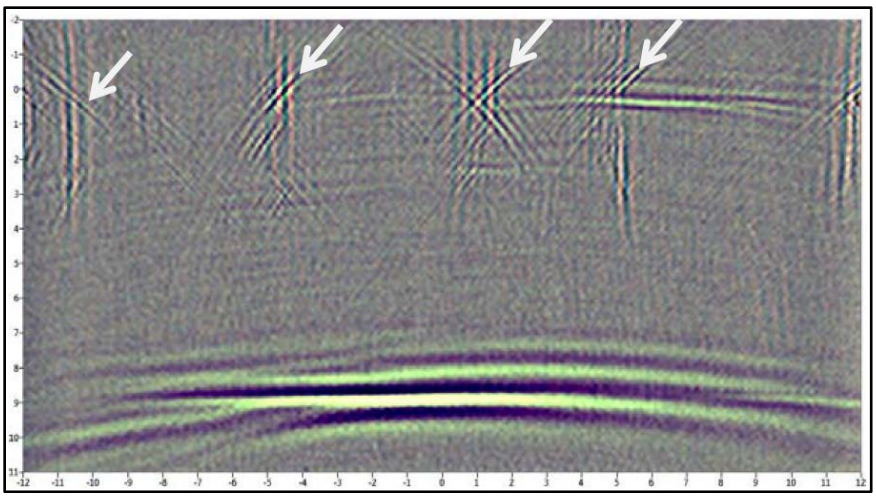

(a)

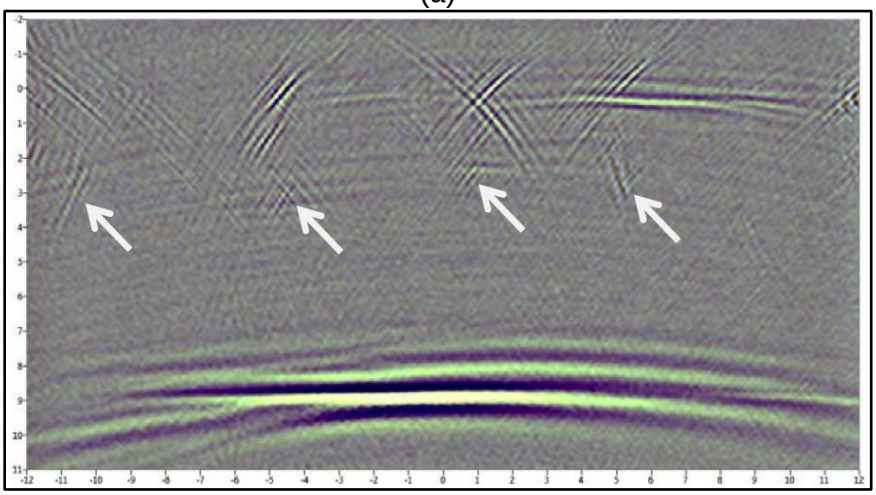

(b)

Figure 38. IWEX image of several cracks; Aside from the vertical indications, corner effects indicated by arrows occur (a). The height of the cracks can be determined accurately using tip diffraction, indicated by arrows (b); in this image, the red IWEX-3 made has been removed (all dimensions in millimeters).

An example of a through-wall crack is shown in Figure 39. In this particular case, the different IWEX modes represented by different colors contribute to different parts of the crack in the image. Only the combination of all modes shows the entire crack. If a through-wall crack is present, the inner and outer pipe surface disappear from the image altogether because no cross mode from one array probe to the other can no longer be measured. Obviously, if there are several through-wall cracks present at the same scan position, the region in between cannot be reached acoustically and, therefore, cannot be inspected.

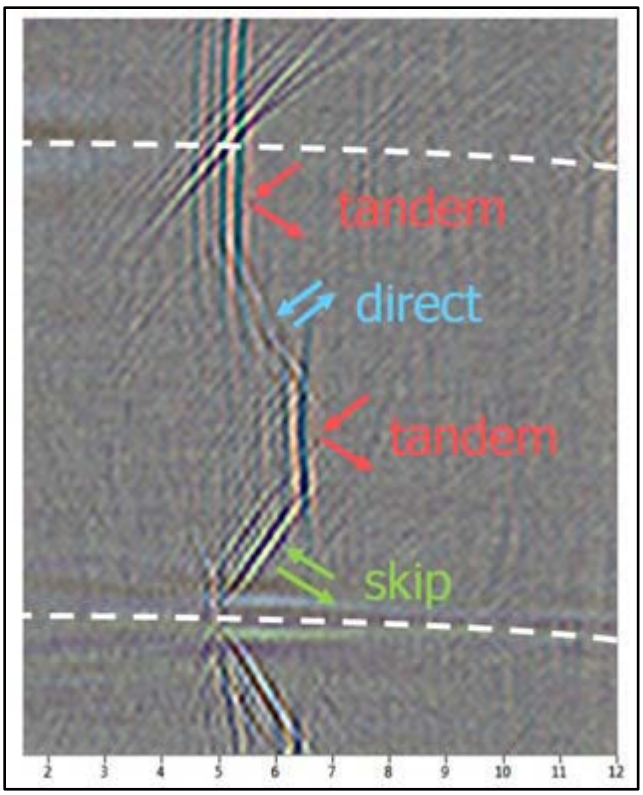

Figure 39. IWEX image of a through-wall crack. Note that the different modes image different parts of the crack dependent on the orientation. The modes contributing to the different parts are labeled (all dimensions in millimeter).

Figure 40 and Figure 41 show IWEX images of cracks exhibiting branches. In Figure 40, the different branches of the crack are captured from different sides. In Figure 41, the bifurcation of the crack at the right side is clearly visible, with the left part extending all the way through the sample, although weakly imaged.

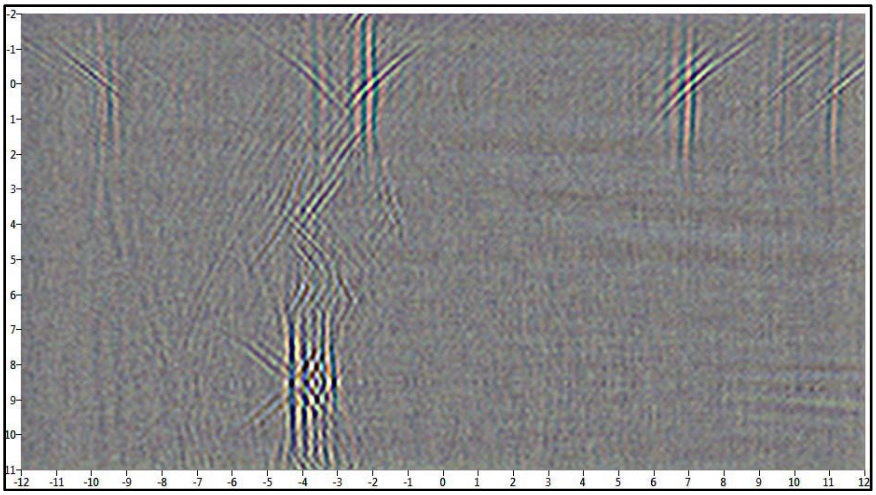

Figure 40. IWEX image of a crack exhibiting different branches. Note that the different modes image different parts of the crack dependent on the orientation (all dimensions in millimeters).

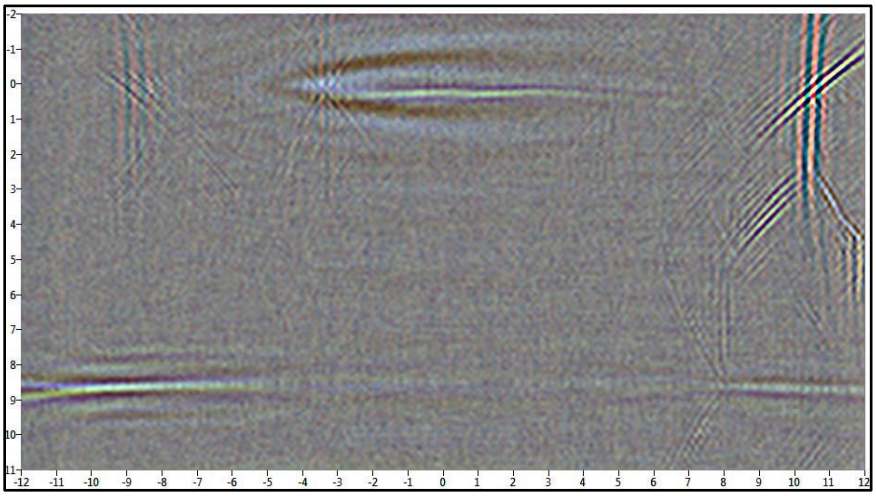

Figure 41. IWEX image of a crack exhibiting different branches. Note that the different modes image different parts of the crack dependent on the orientation (all dimensions in millimeters).

For the inspection of SCC colonies, it is clear that the width of 1 inch of the stroke scanned for this example forms a limitation. This limitation is imposed not only by the hardware supporting scans of widths of up to 1 inch for the desired resolution, but also by the acoustical coverage of the array probes, which enable insonification and measurement of a region of at most 1.2 inch in width. Therefore, scanning of several parallel strokes would be required for the inspection of a wider area of interest.

In order to facilitate the interpretation of the scans, it is expected that it would be helpful to investigate options for stitching these scanned strokes together. In this context, the achievable

mechanical alignment has to be determined, and options to register corresponding indications in several scans and ways of suppressing double indications have to be investigated.

Nevertheless, the current single-stroke example provides an idea of the capabilities of this inspection technique. Figure 42 presents a photograph of the region scanned with a three-dimensional visualization of the IWEX scan result superimposed. In this case, a fixed amplitude threshold has been chosen to determine the visibility of the indications in the three-dimensional visualization. The contributions of different IWEX modes are once more represented by different colors: blue for the direct mode, green for the skip mode, and red for the tandem mode.

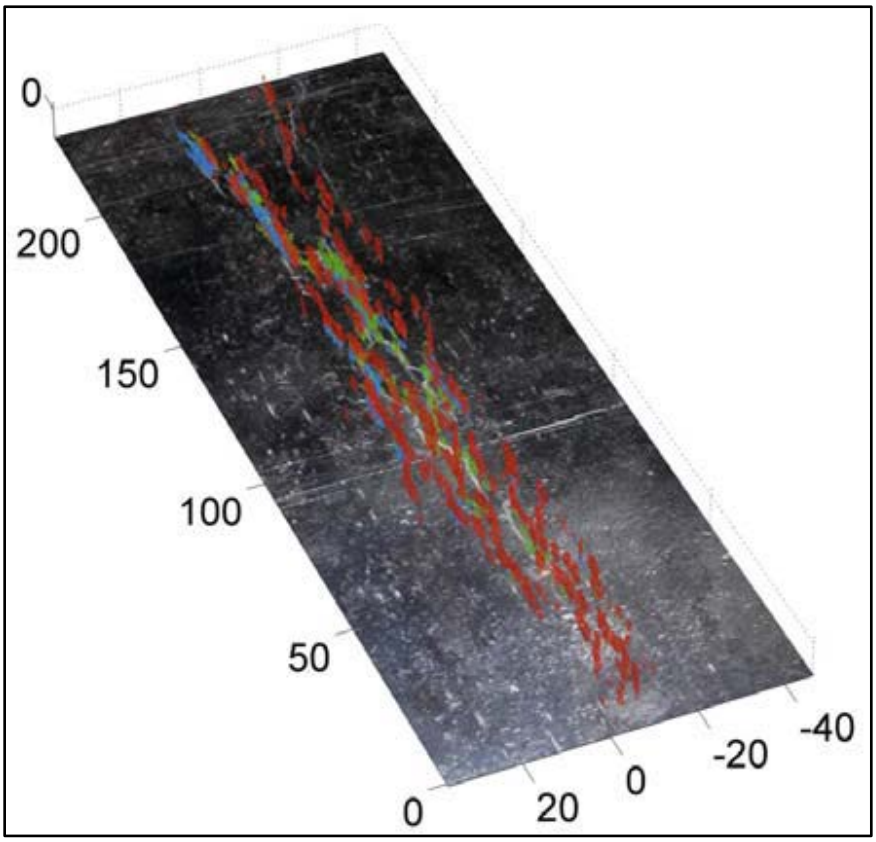

Figure 42. Three-dimensional visualization of the IWEX scan superimposed on a photograph of the sample (all dimensions in millimeters)

In Figure 43(b), a top view of the same visualization is shown. By comparison to the photograph of the sample depicted in Figure 43(a), the difference between visual inspection and the information provided by IWEX is demonstrated.

For the determination of the remaining strength of a material sample, the accurate sizing of the deepest crack in the colony is of interest. In an additional processing step, the scanned region is analyzed to find the deepest crack for every scan position and determine its depth. In a test implementation, the tip diffractions are combined with the tandem indications for reasons of

simplicity. The indication of greater depth is chosen to be leading, which can result in slight oversizing due to the vertical blurring of the tandem indications (compare Figure 43(a)).

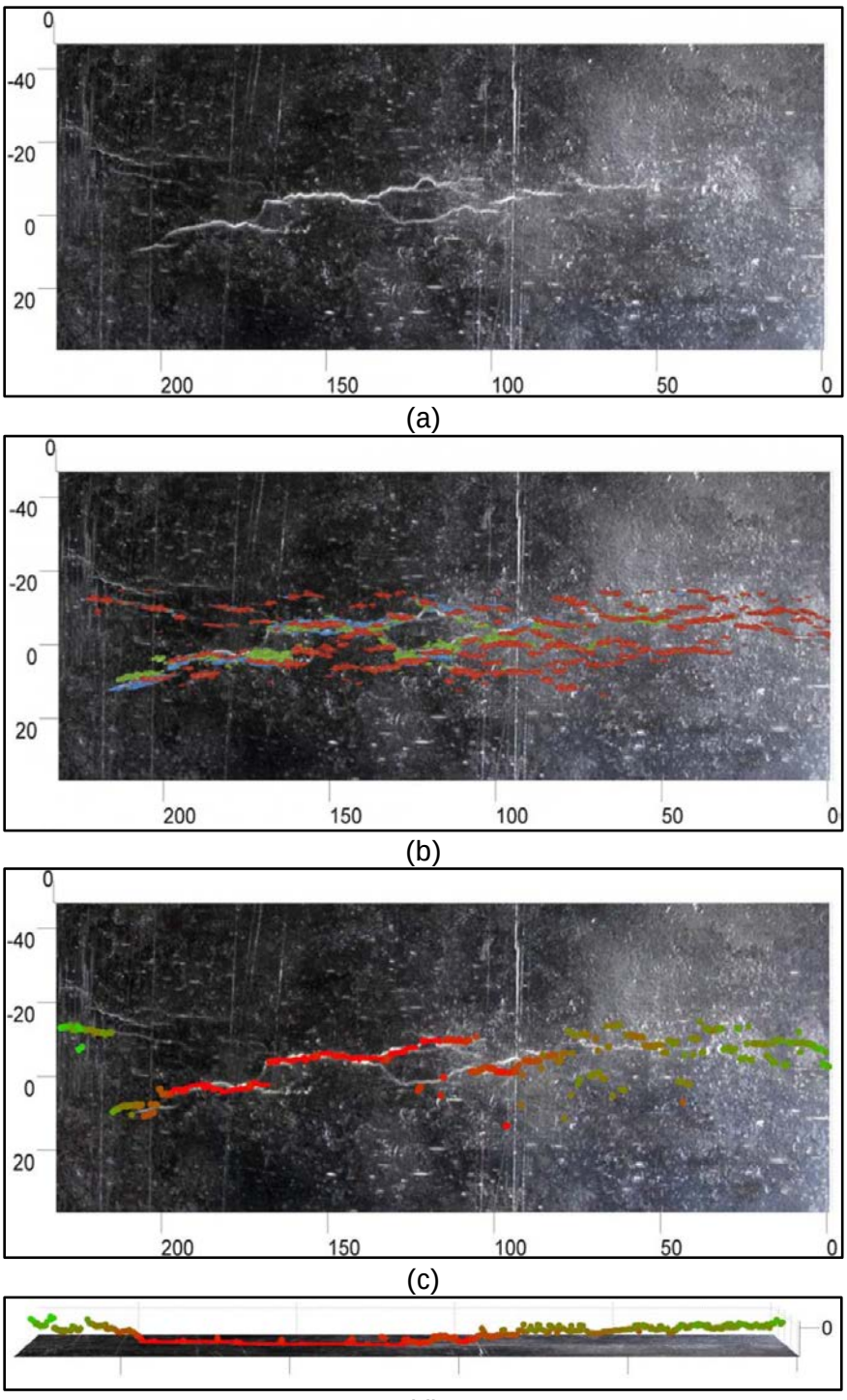

Figure 43. Photograph of the sample surface (a); IWEX scan superimposed with blue representing indications picked up by the direct mode (b); superposition of the deepest crack found per scan position with green indicating a shallow crack and red indicating a through-wall crack (c); side-view of (c) showing the depth of the deepest crack per scan position (d). All dimensions are shown in millimeters.

As shown in Figure 37(c) and Figure 37(d), the determination of the position of the deepest crack corresponds to the visual impression of the sample and provides additional insight in the structure of the SCC colony.

Summarizing the results, IWEX enabled the detection and sizing of the individual cracks of a colony of high-pH SCC. Ideally, the sizing of the cracks is carried out using tip diffractions. The different IWEX modes were shown to provide complimentary information, which is especially helpful in imaging cracks of varying orientation. Based on the IWEX scan of a stroke, it was possible to identify and size the deepest crack in the colony.

22-in ERW Samples

Five 22-in ERW joints were inspected in College Station, Texas. This test was considered a pre-trial of the scanner system before going to the field. The scan results were reported to the participating operator. Although the suction cup scanning system appears to work well for large diameter ERW pipe i.e. 20-in and above, the suction cups are not holding for smaller diameter pipes. Recent trials on 12-in and 8-in ERW have been rigged with straps to make the scanners work. As a result new scanner designs are being investigated. Although we still are interested in going to the field with the current system for some trials, a newer improved system with some sort of seam tracking system will be needed for future bell hole inspections of pipe.

Part No.	116050	Diameter: 22"				Length:	(4960 mm)	Measured Thickness:	.288" (7.3mm)		Year placed in service:		Date Examined:	25-Jun-14	
IWEX Defect Number	Vertical Location from Start (0) mm	Type of Defect	Length (mm)	Depth (mm)	Height (mm)	Vertical Location from Start (0) mm	Type of Defect	Length (mm)	Depth (mm)	Height (mm)	Vertical Location from Start (0) mm	Type of Defect	Length (mm)	Depth (mm)	Height (mm)
1	170	LOF/ OD Surface	88	0.8	0.8	170	LOF	106	1.5	1.5	170	LOF	88		
2	1019	LOF/ OD Surface	35	1.1	1.1	1019	LOF	53	1.8	1.8		LOF	22	0.7	0.7
3	1221	LOF	9	2.7	1.5	1221	LOF	16	3.3	1.8	NA	NA	NA	NA	NA
4	3150	LOF/ OD Surface	77	1.1	1.1	3150	LOF	113	1.5	1.5	3150	LOF	78		

Figure 44. A photo of the 22-in pipe inspected with the IWEX system

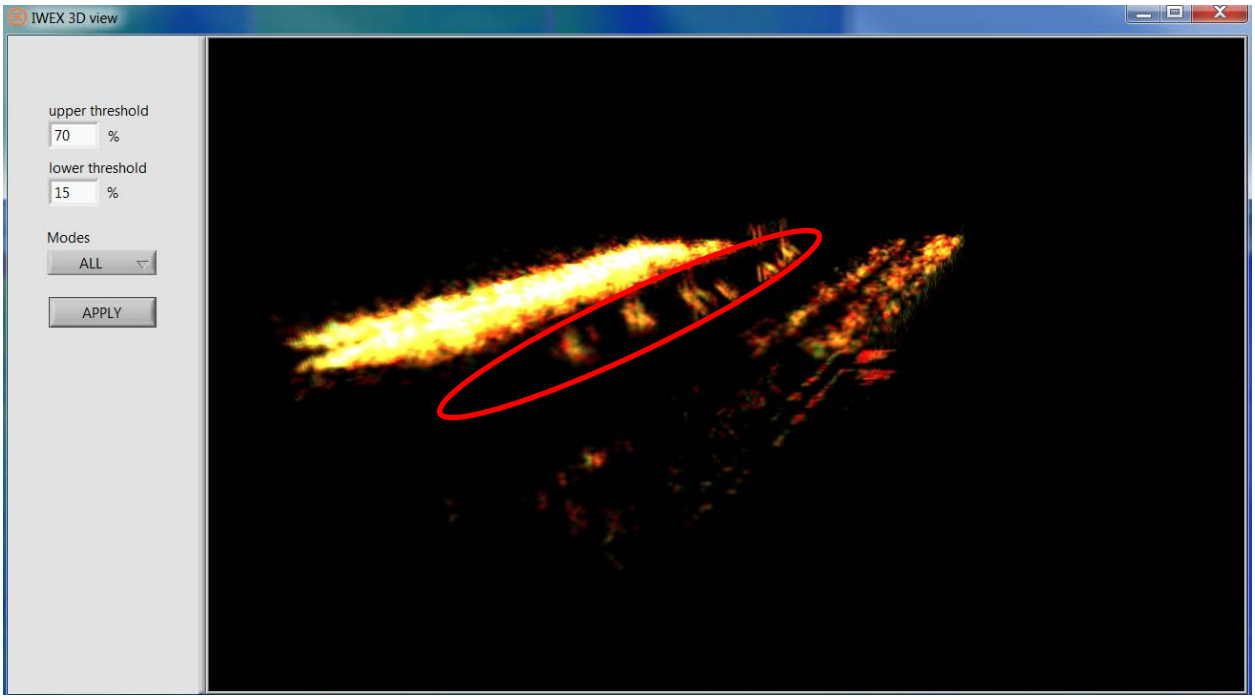

Figure 45. Part 116050, 45 + 88 mm, D 0.0 – 0.8, H 0.8mm, DS 90° Side with flow LOF OD surface

Figure 46. Part 116050, 894 + 35mm, D 0.0 – 1.1, H 1.1mm, US 270 Side with flow LOF OD surface

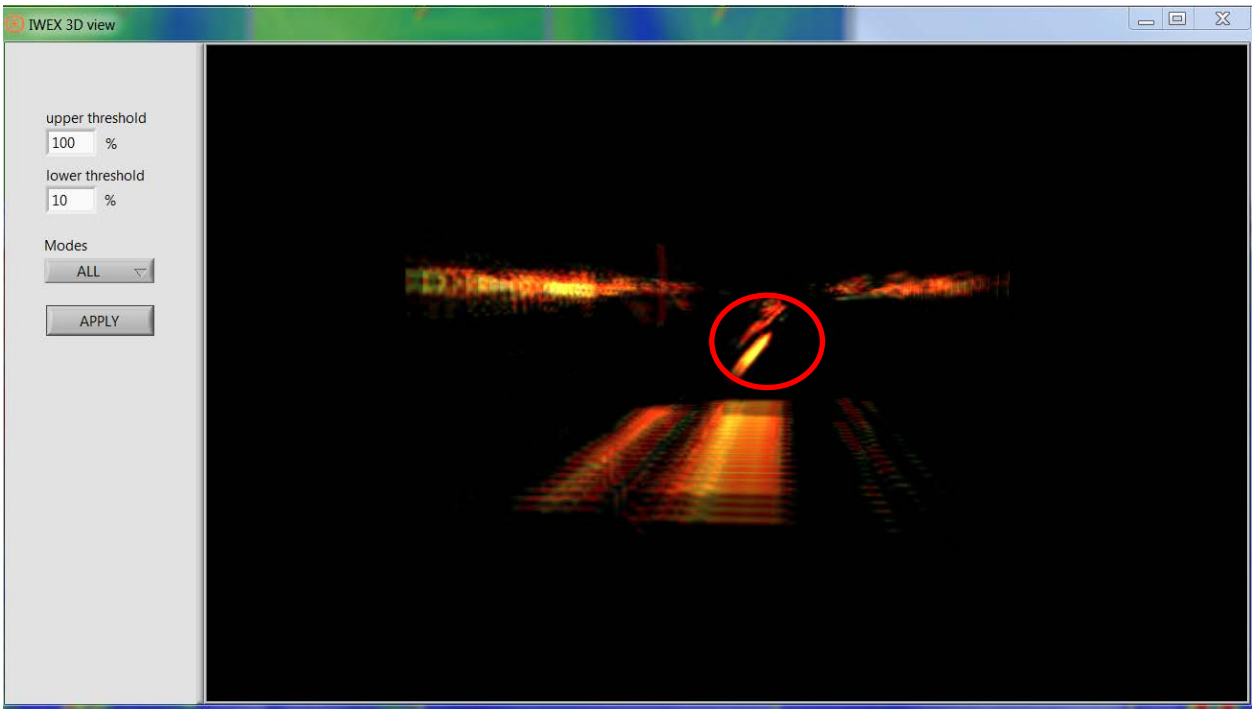

Figure 47. Part 116050, 1096 + 9 mm, D1.2- 2.7, H 1.5mm, DS 90° Side with flow Sub surface LOF

Figure 48. Part 116050, 3025 + 77mm, D 0.0 – 1.1, H 1.1mm, US 270 Side with flow OD surface LOF

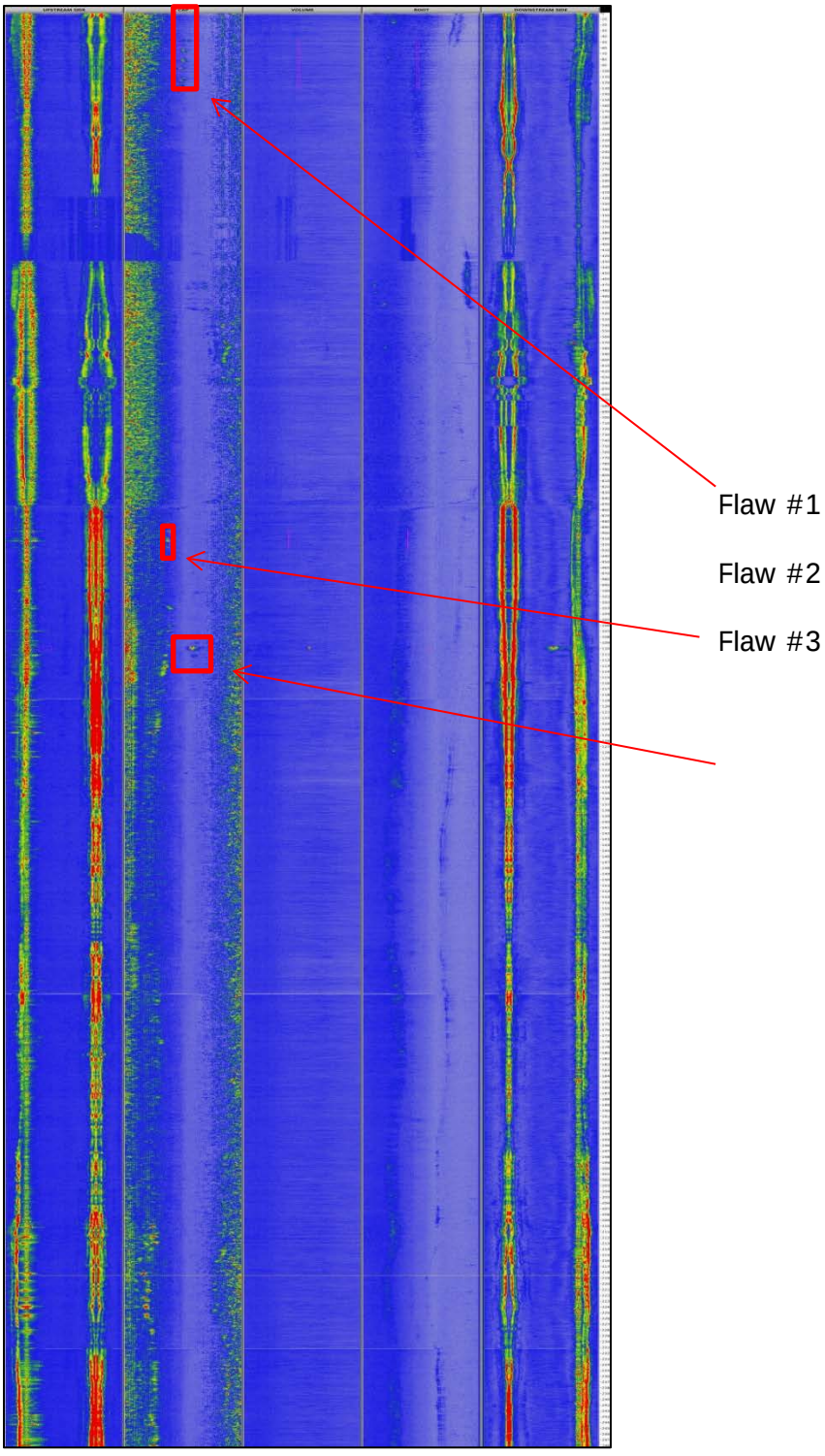

Figure 49. Pipe Sample 116050, 22in, Avg Wall Thickness .299in/ 7.6mm, Scan direction with Flow Distance 3 meters

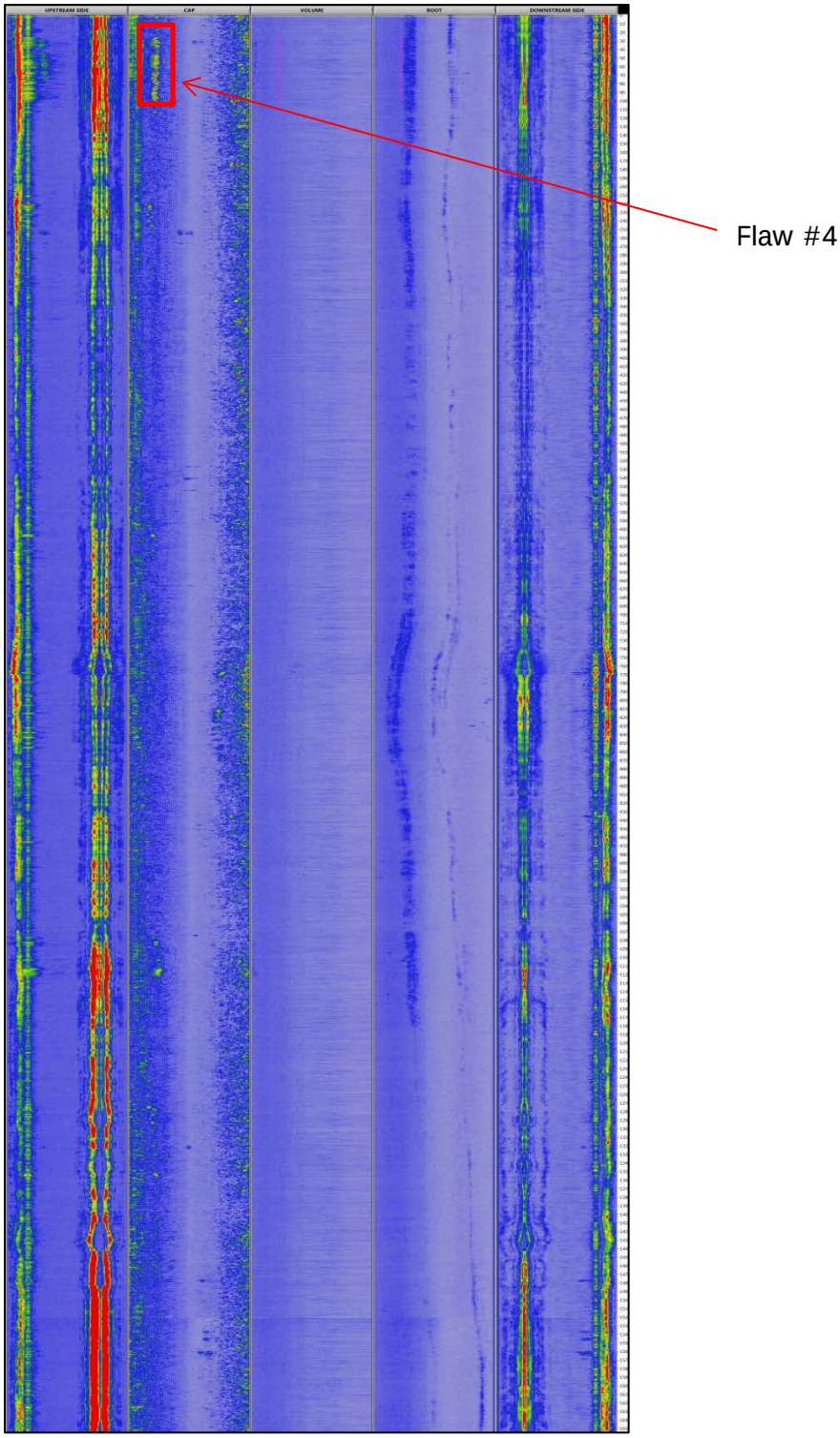

Figure 50. Pipe Sample 116050 Starting at 3 meters, total length of scan 1916mm

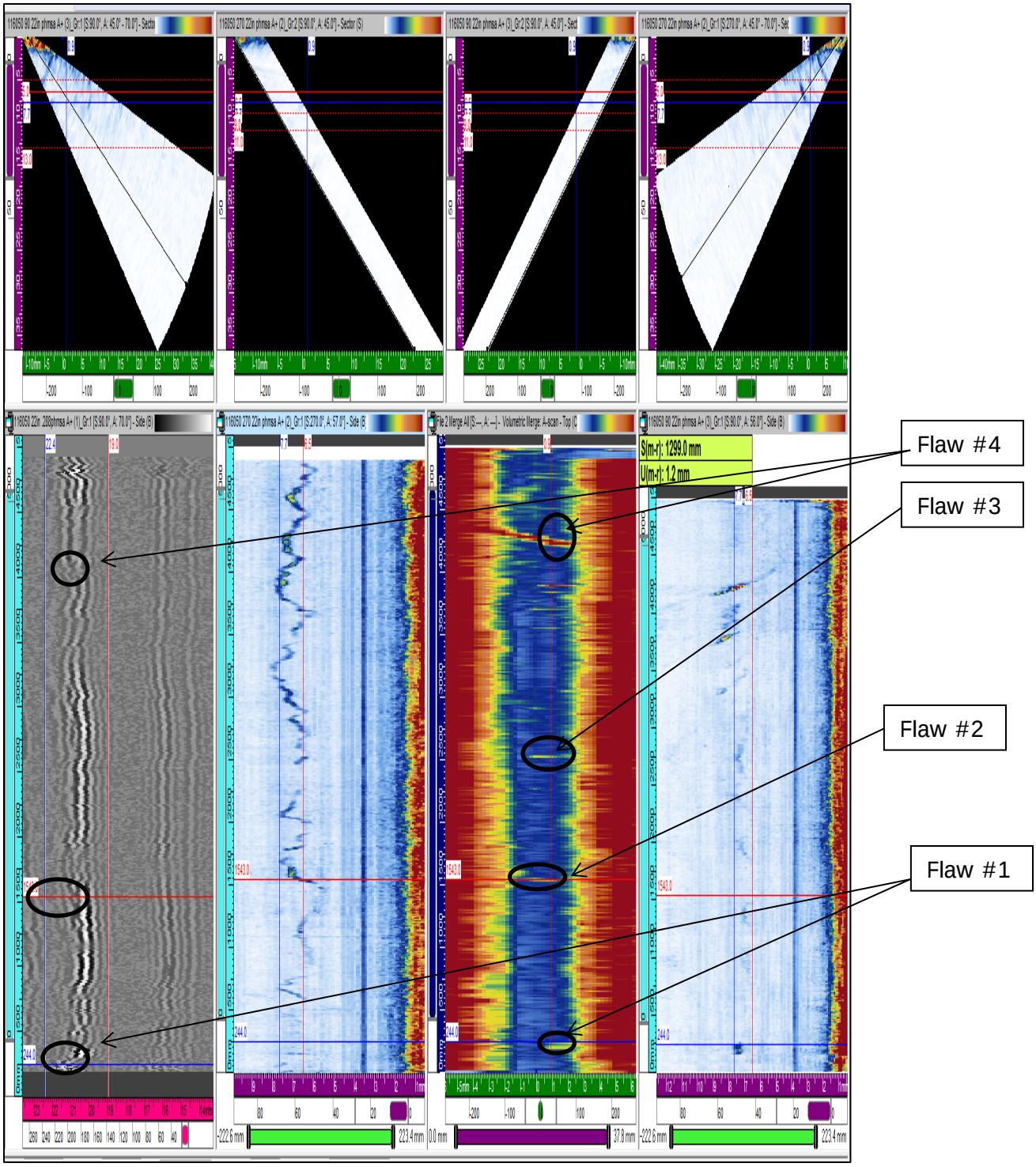

Figure 51. Pipe sample 116050, PAUT and TOFD Scan

Part No.	149890	Diameter: 22"				Length :	(4470m m)	Measured Thickness:			.288" (7.3mm)	Date Examined :	June 25,2014		
IWEX Defect Number	Vertical Location from Start (0) mm	Type of Defect	Length (mm)	Depth (mm)	Height (mm)	Vertical Location from Start (0) mm	Type of Defect	Length (mm)	Depth (mm)	Height (mm)	Vertical Location from Start (0) mm	Type of Defect	Length (mm)	Depth (mm)	Height (mm)
1	1071	LOF/ OD Surface	9	1.6	1.6	1	1074	LOF	16	1.1	1.1	1	1059	LOF	6
2	1246	LOF/ ID Surface	157	7.1	1.4	2	1246	LOF	157	7	1.3	2	1205	LOF	83

Figure 52. A photograph of the second 22-in ERW pipe inspected

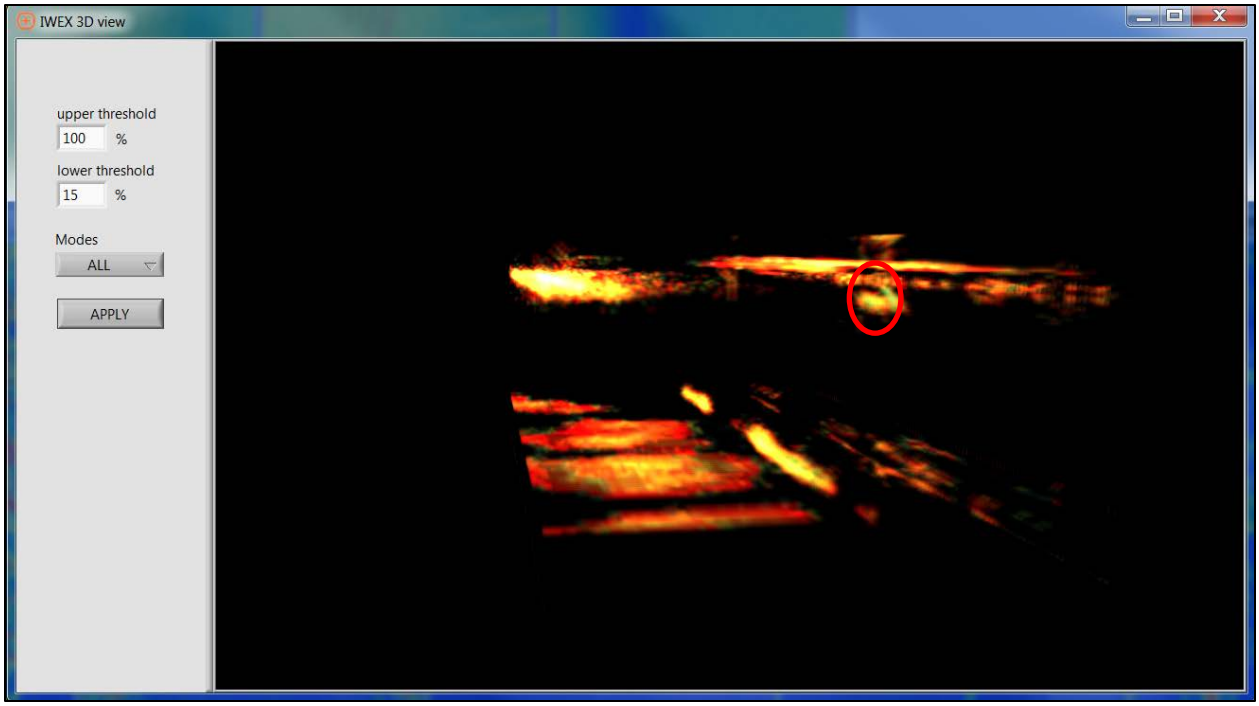

Figure 53. Pipe sample 149890, 871 + 9.0mm, D 0.0 – 1.6mm, H 1.6mm, DS 90 side with flow OD surface LOF

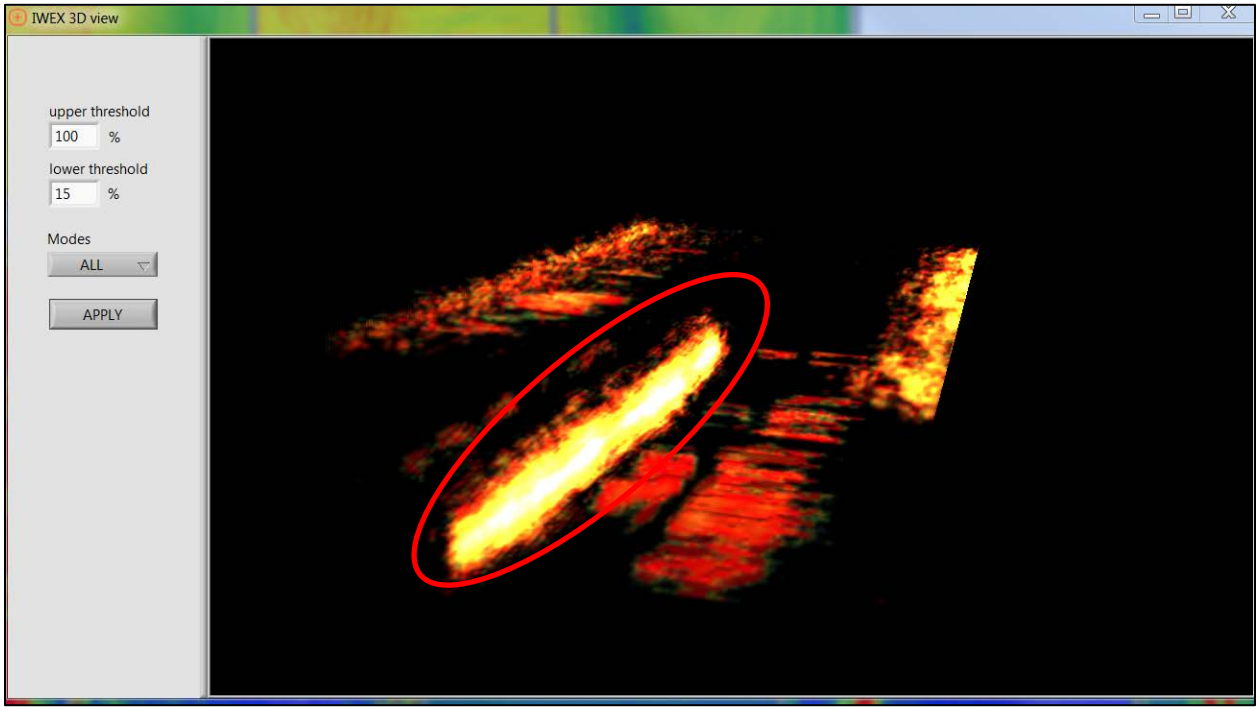

Figure 54. Pipe sample 149890, 1846 + 157mm, D5.7 – 7.1, H 1.4, US 270 side LOF ID surface

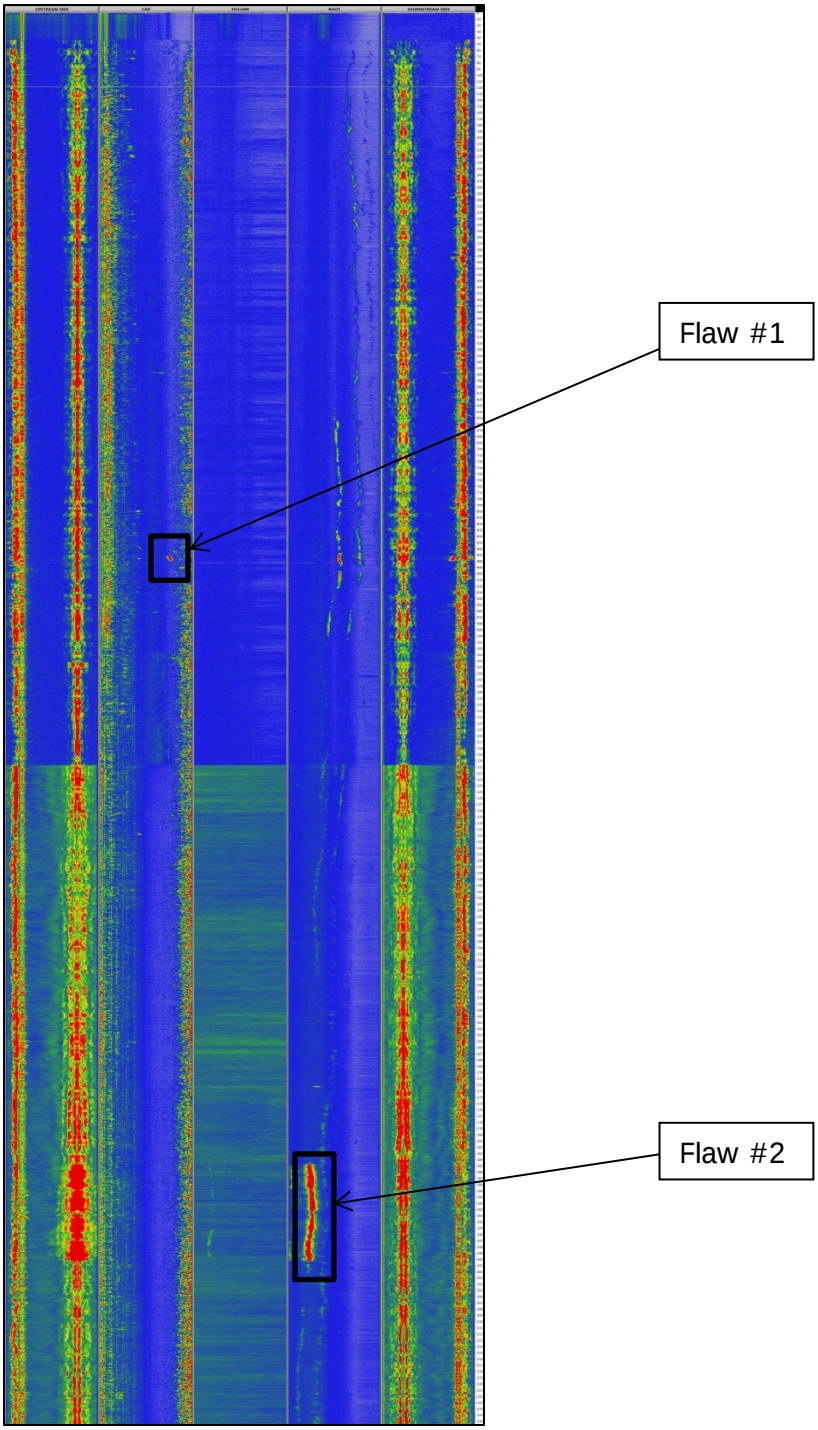

Figure 55. Pipe Sample 149890 22in AVG Wall Thickness .299in/ 7.6mm Scan direction with Flow Distance 2.2 meters

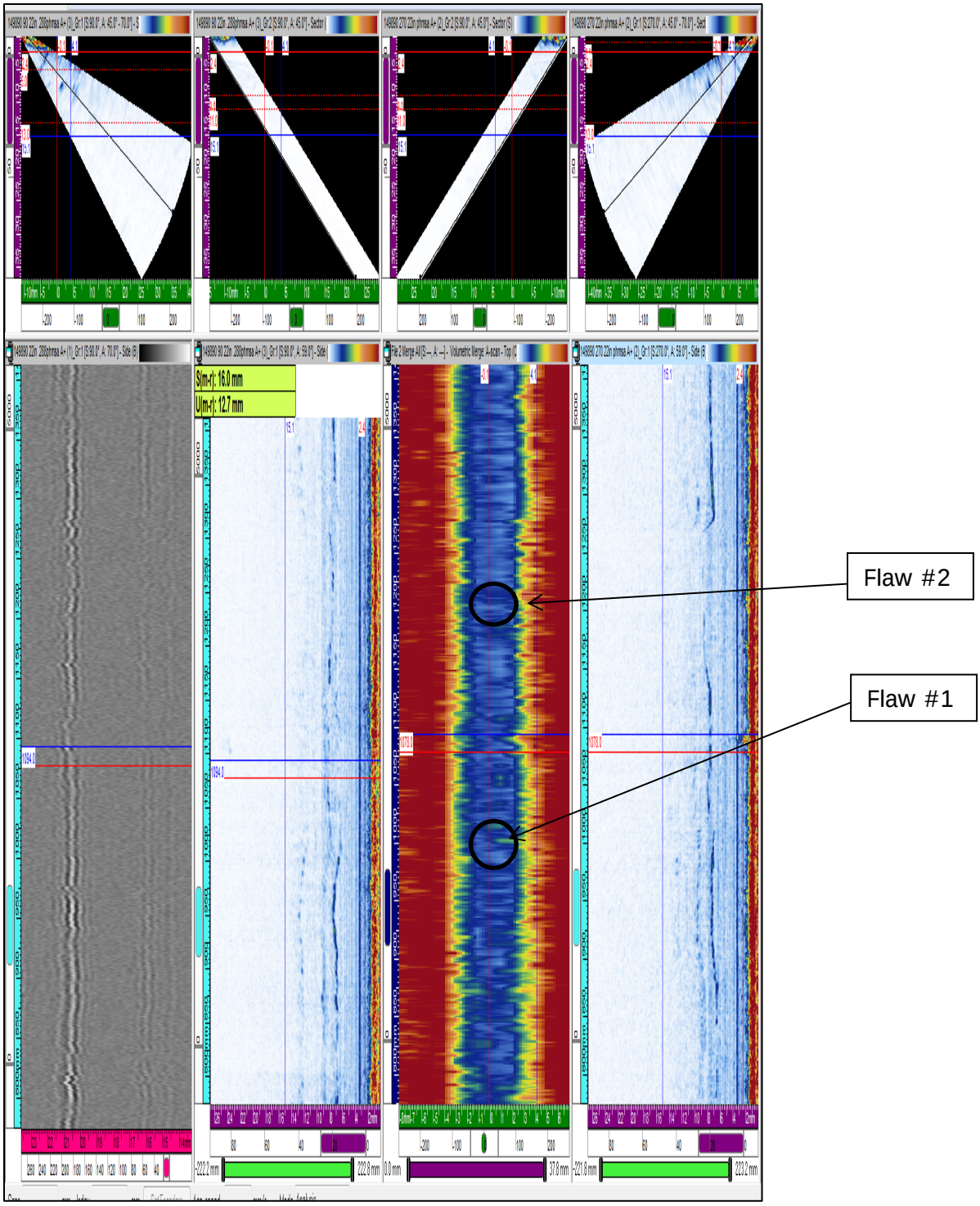

Figure 56. Pipe sample 149890 PAUT and TOFD Scan

Part No. 156320	Diameter: 22"					Length : (4960mm)		Measured Thickness : .288" (7.2mm)			Date Examined : June 25 2014				
IWEX Defect Number	Vertical Location from Start (0) mm	Type of Defect	Length (mm)	Depth (mm)	Height (mm)	Vertical Location from Start (0) mm	Type of Defect	Length (mm)	Depth (mm)	Height (mm)	Vertical Location from Start (0) mm	Type of Defect	Length (mm)	Depth (mm)	Height (mm)
1	1258	LOF/OD Surface	5	0.7	0.7	1250	LOF/OD Surface	9	1	1		NA			
2	1258	LOF	5	2.9	0.5	1251	LOF	3	4	1	1258	LOF	5	3	0.7
3	2989	LOF/OD Surface	51	1.3	1.3	2989	LOF/OD Surface	62	1.5	1.5		NA			
4	4337	Trim Tool Defect/ID Surface	45	7.3	1	4333	Trim Tool Defect/ID Surface	55	7.3	0	4338	Trim Tool Defect/ID Surface	43	7.33	0.9

Figure 57. A picture of the third joint inspected of the 22-in pipe.

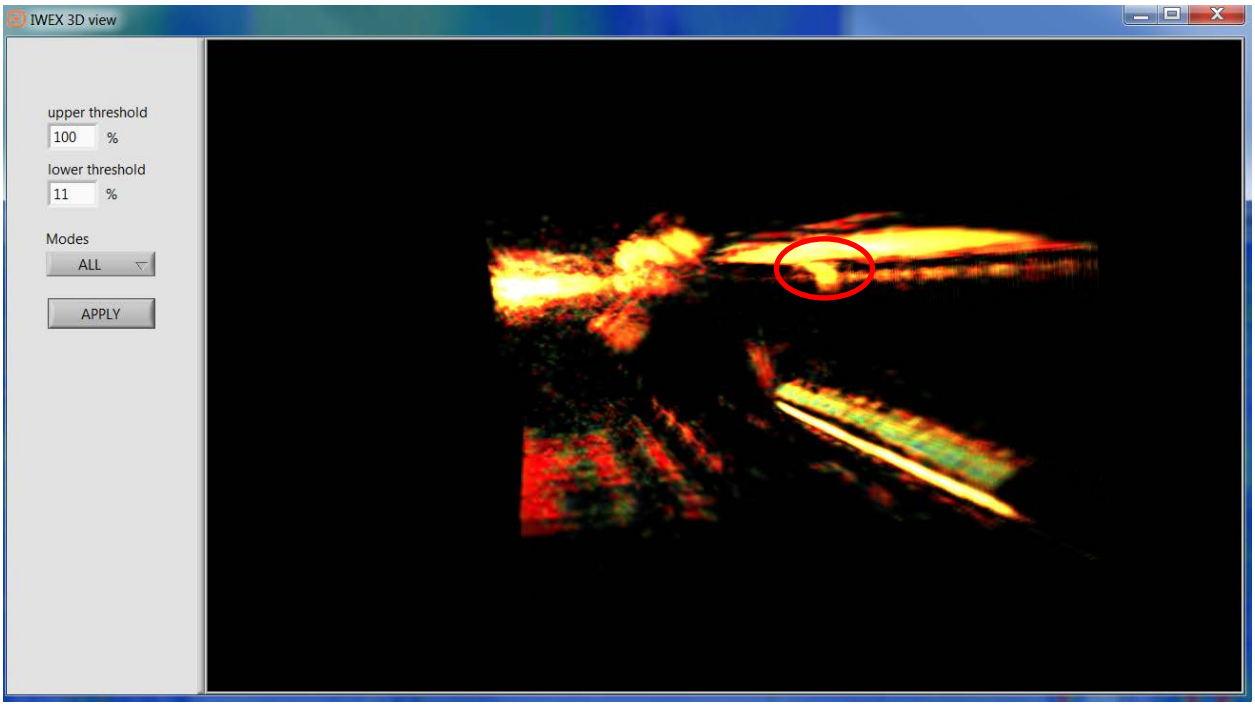

Figure 58. Pipe Sample 159070, 1258 + 5mm, D 0.0 – 0.7mm, H 0.7mm, DS 90 side with flow OD Surface

Figure 59. Pipe Sample 159070, 1258 + 5mm, D 1.6 – 2.9mm, H 0.5mm, DS 90 side with flow LOF

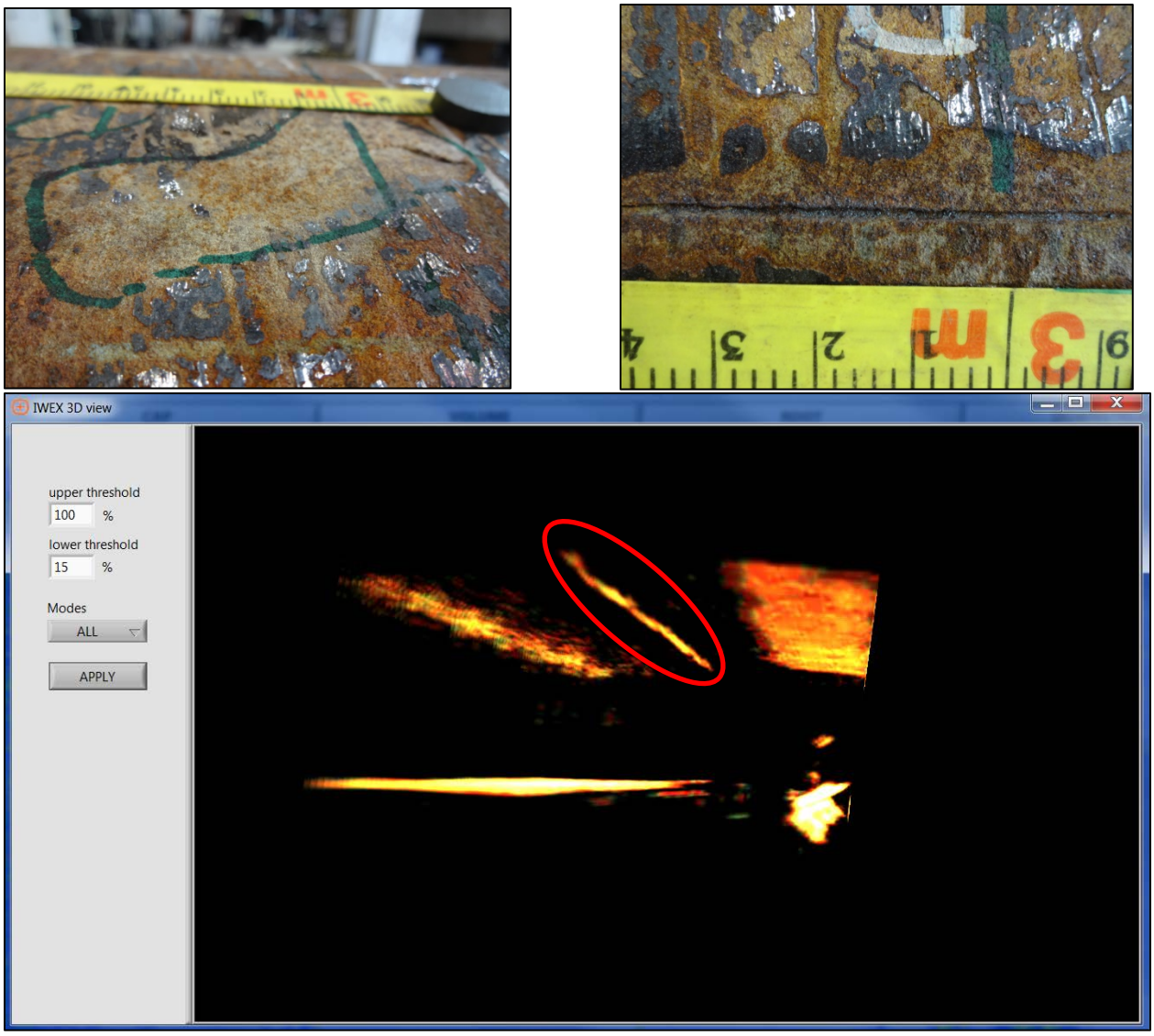

Figure 60. Pipe Sample 159070, 2989 + 51mm, D 0.0 – 1.3mm, H 1.3mm, DS 90 side with Flow LOF - Due to surface conditions only one probe could image this flaw.

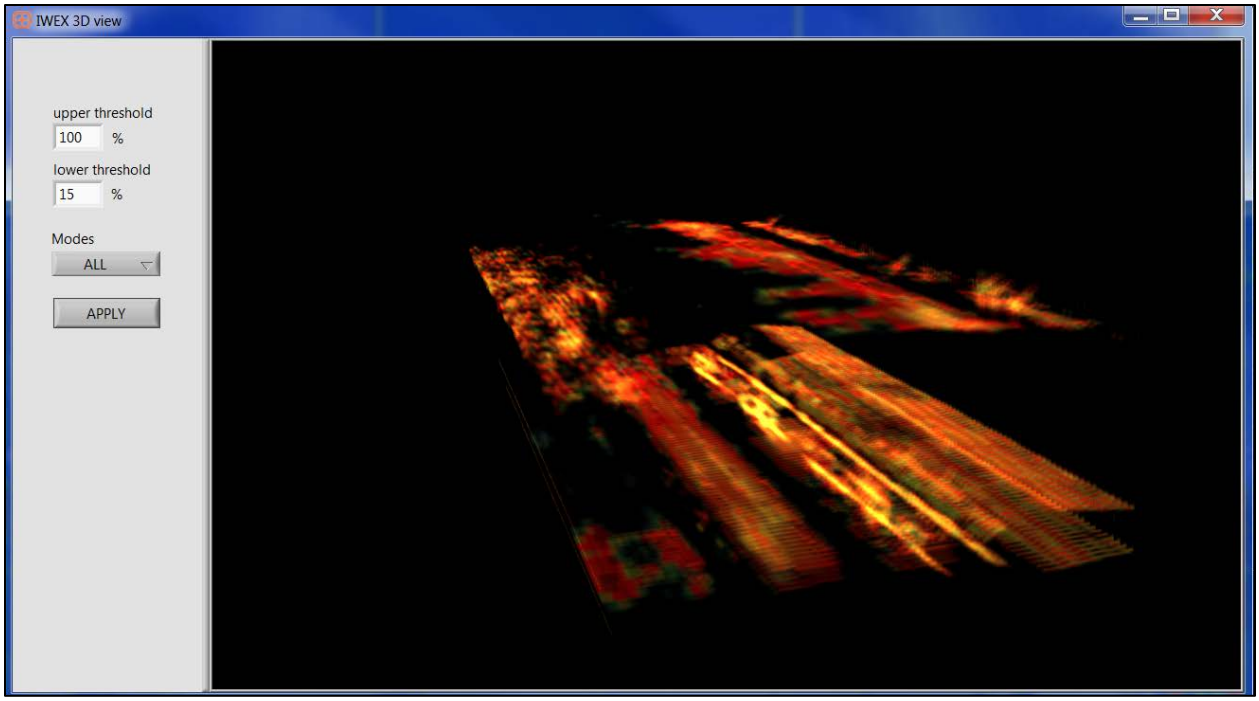

Figure 61. Pipe Sample 159070, 4337 + 45.0mm, D 6.3 – 7.3mm, H 1.0mm, Center Edge

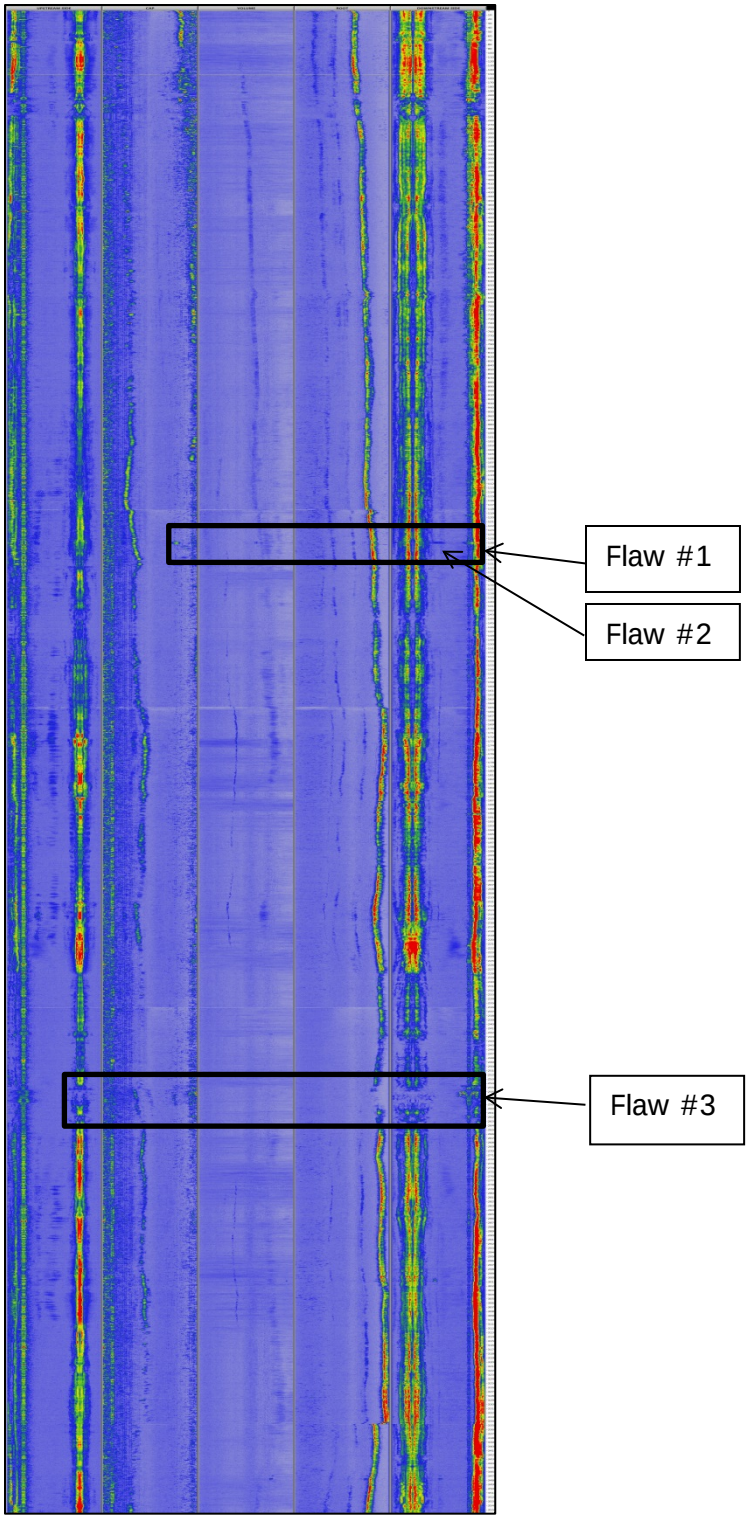

Figure 62. Pipe Sample 156320 22in AVG Wall Thickness .299in/ 7.6mm Scan direction with Flow Distance 2.2 meters

Part No. 115310	Diameter: 22"					Length :	(4980mm)		Measured Thickness :		.288" (7.2mm)	Date Examined :		July 25 2014	
IWEX Defect Number	Vertical Location from Start (0) mm	Type of Defect	Length (mm)	Depth (mm)	Height (mm)	Vertical Location from Start (0) mm	Type of Defect	Length (mm)	Depth (mm)	Height (mm)	Vertical Location from Start (0) mm	Type of Defect	Length (mm)	Depth (mm)	Height (mm)
1	3335	LOF/OD Surface	6	1.8	1.8	3276	LOF/OD Surface	8	1.9	1.9	3276	LOF/OD Surface	7	1.3	1.3

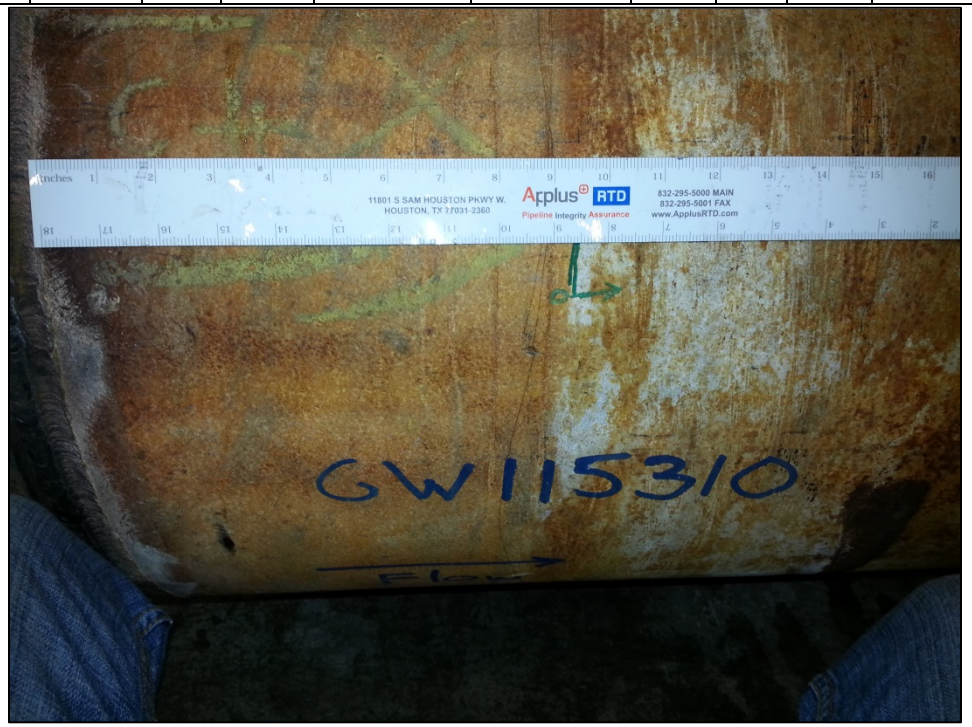

Figure 63. A picture of the fourth joint of 22-in pipe

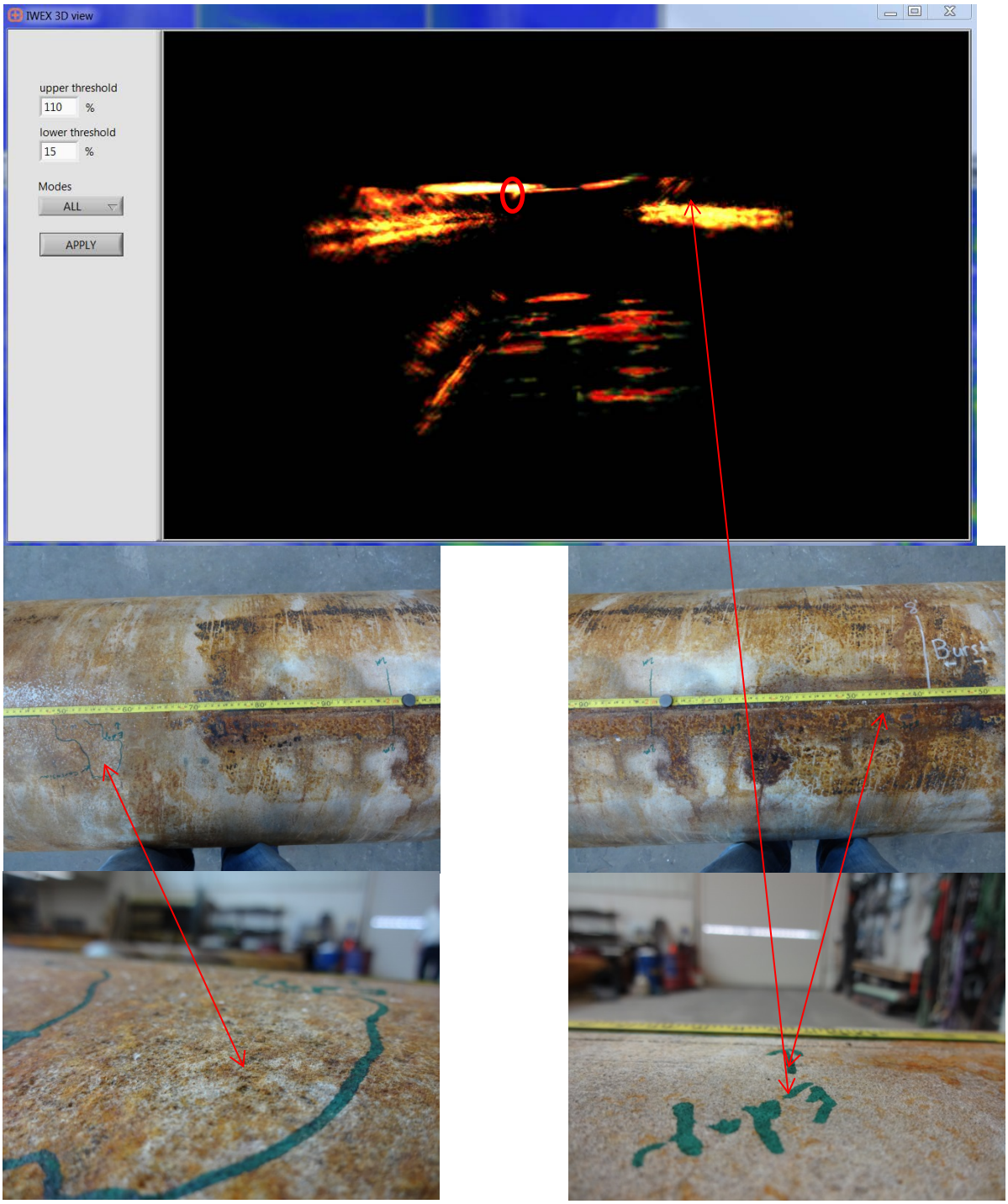

Figure 64. Pipe Sample 115310, 3335 +6, D 0 – 1.8mm, H 1.8mm, US 270 side with flow LOF OD Surface

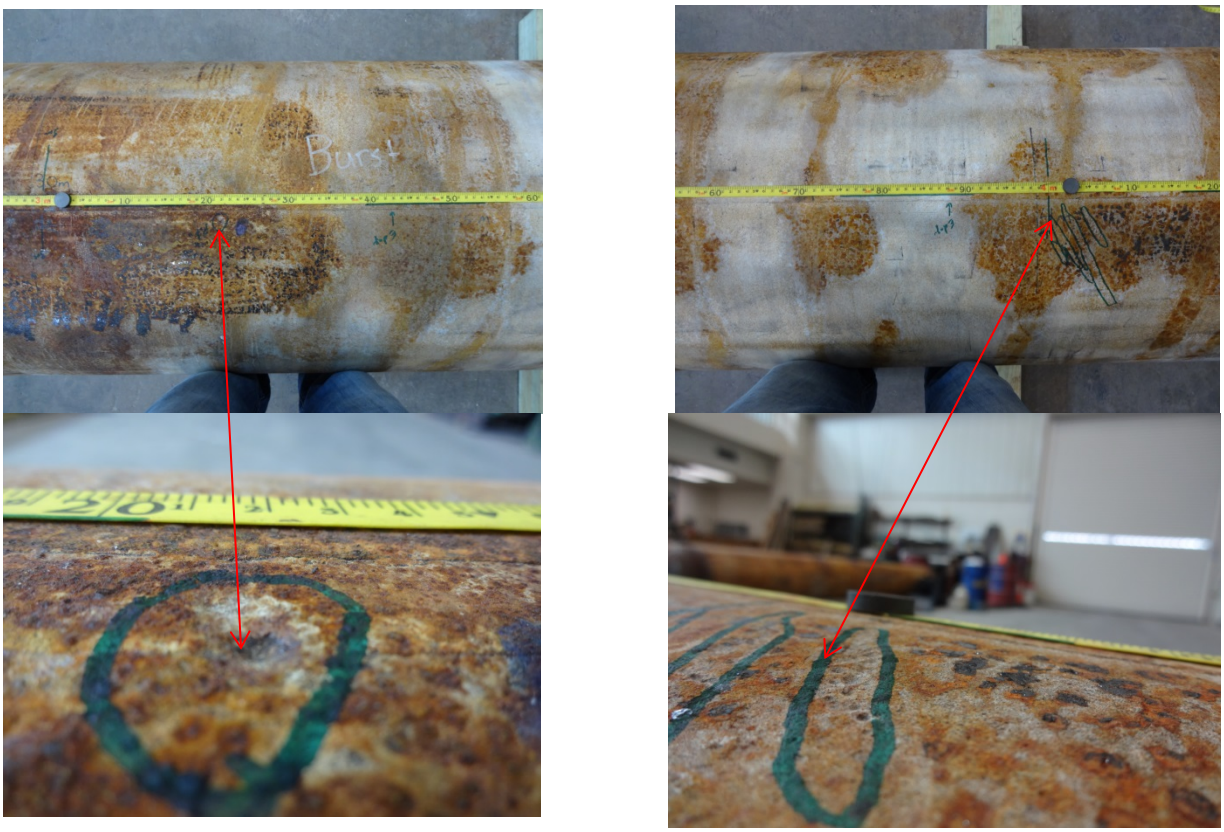

Figure 65. The images above show some of the surface conditions that made it difficult to get good images with UT

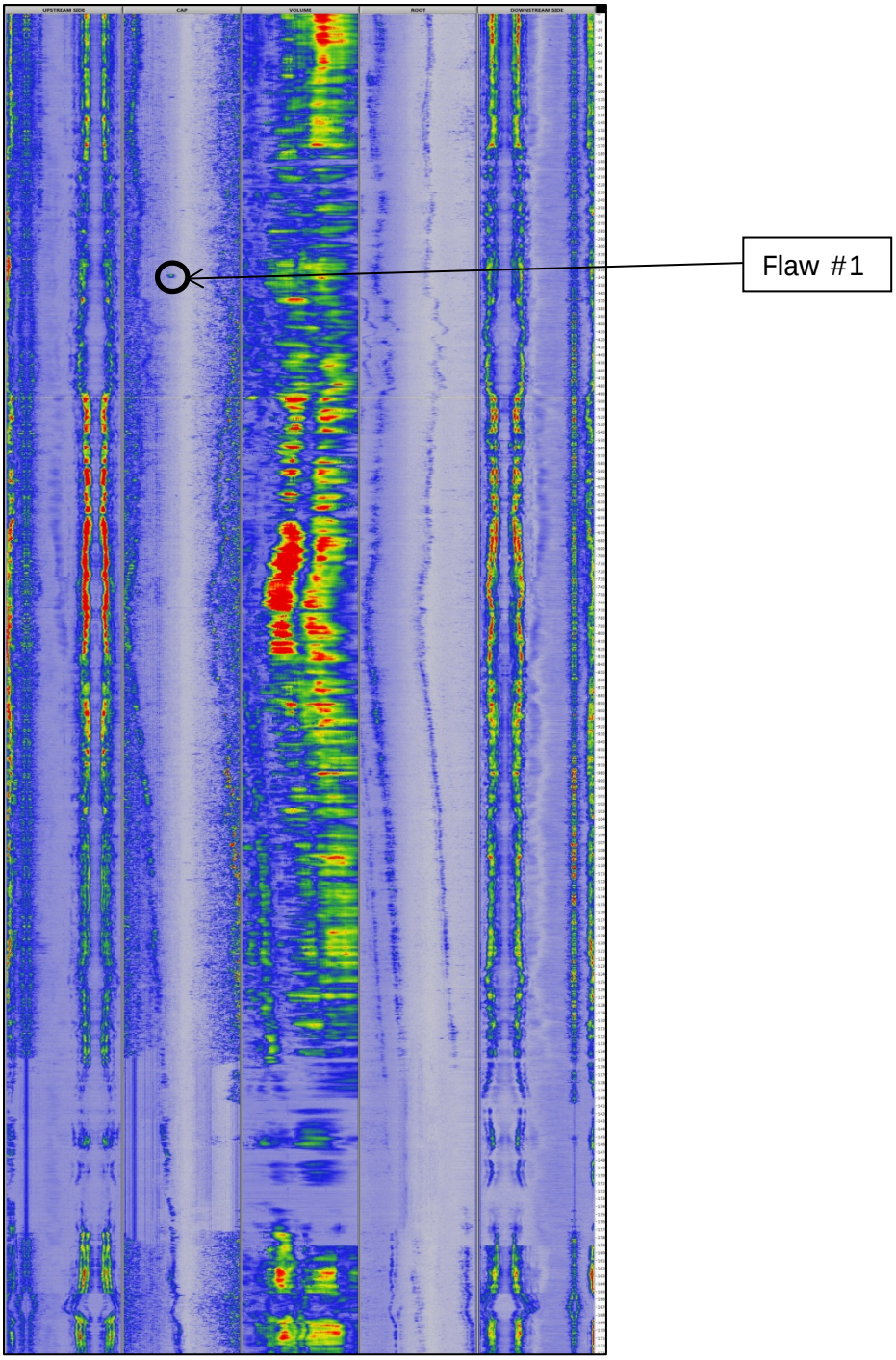

Figure 66. Pipe Sample 115310, Scan #2 starting at 3 meters

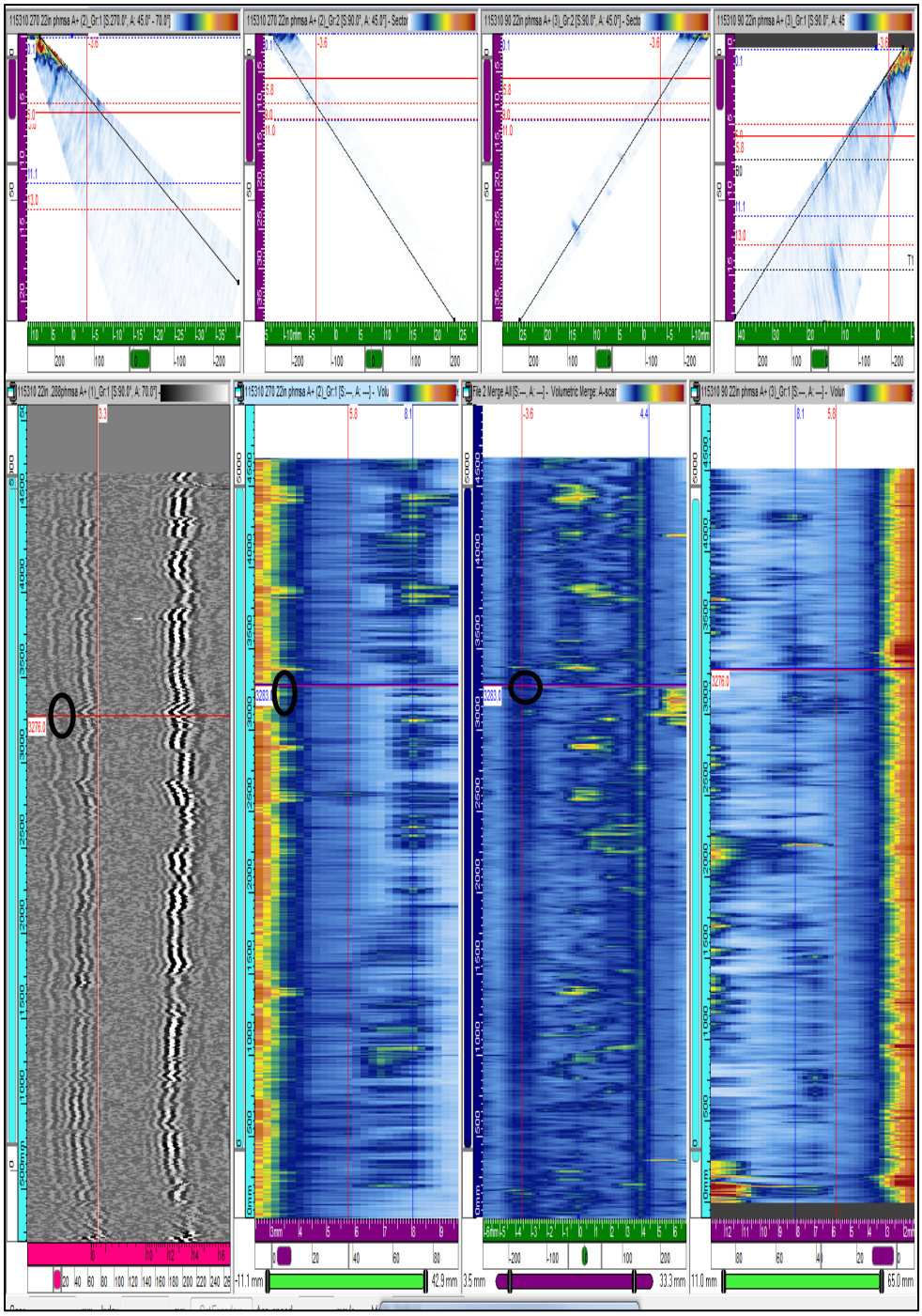

Figure 67. Pipe Sample 115310, PAUT and TOFD scan

Part No. 159070		Diameter: 22"				Length : (4960mm)		Measured Thickness :			.288" (7.2mm)	Date Examined :			June 25 2014
IWEX Defect Number	Vertical Location from Start (0) mm	Type of Defect	Length (mm)	Depth (mm)	Height (mm)	Vertical Location from Start (0) mm	Type of Defect	Length (mm)	Depth (mm)	Height (mm)	Vertical Location from Start (0) mm	Type of Defect	Length (mm)	Depth (mm)	Height (mm)
1	744	LOF/ID Surface	5.5	7.4	1.3	736	LOF/ID Surface	13	7.4	1.3	NA				
2	1086	LOD/ OD Surface	7	0.8	0.8	1085	LOD/ OD Surface	15	0.8	0.8	NA				
3	1490	LOF/ ID Surface	4.5	7.4	1.4	1485	LOF/ ID Surface	10	7.4	1.4	NA				
4	2188	LOF/ OD Surface	6	1.2	1.2	2175	LOF/ OD Surface	13	1.2	1.2	NA				
5	3906	LOF/ OD Surface	180	1.5	1.5	3895	LOF/ OD Surface	189	1.5	1.5	NA				

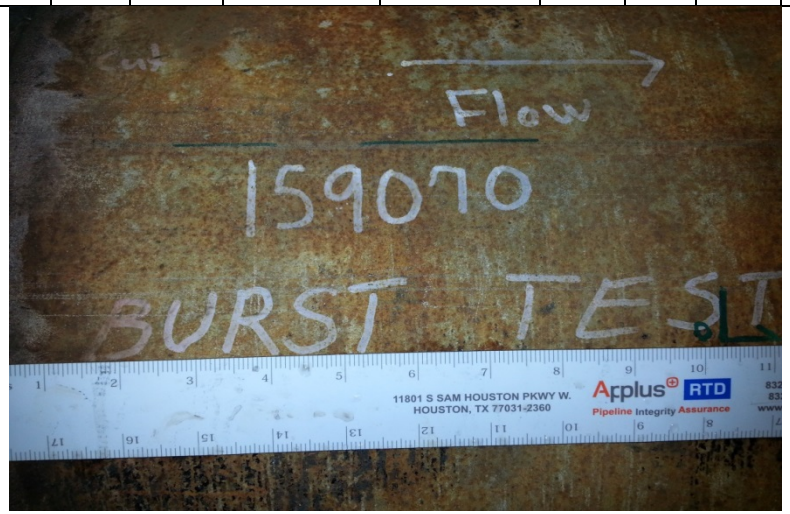

Figure 68. Picture of the fifth joing of 22-inch pipe

Figure 69. Pipe Sample 159070, 744 + 5.5mm, D 6.1 – 7.4, H 1.3mm, US 270° with flow ID surface LOF

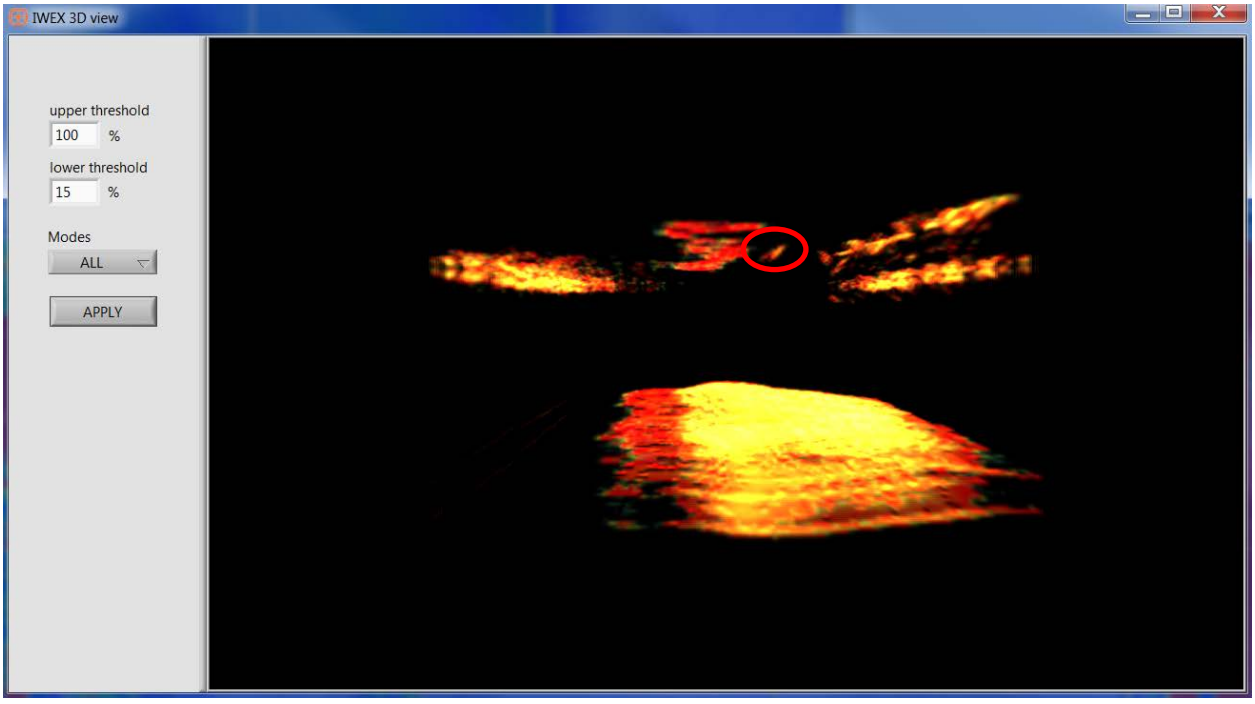

Figure 70. Pipe Sample 159070, 1086 + 7.0mm, D 0.0 – 0.8mm, H 0.8mm, DS 90° Side with flow OD LOF

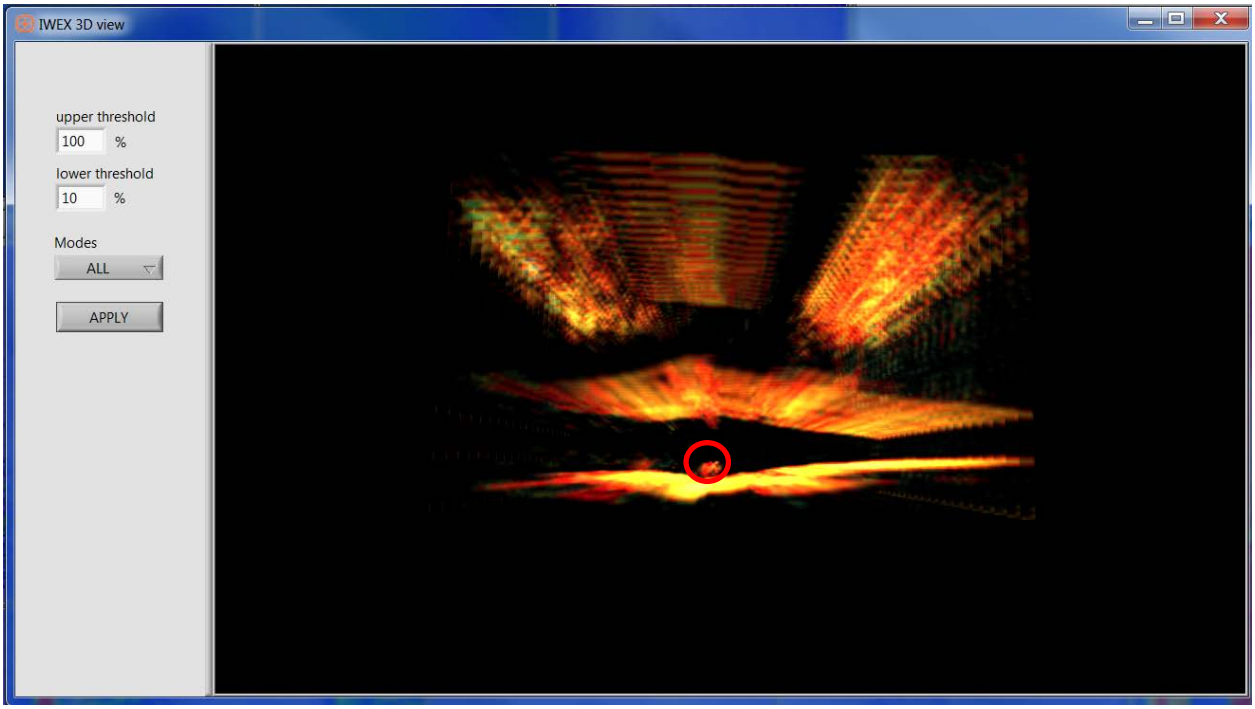

Figure 71. Pipe Sample 159070, 1490 + 4.5, D 5.0 – 7.4mm, H 1.4mm, US 270 side with flow LOF ID Surface

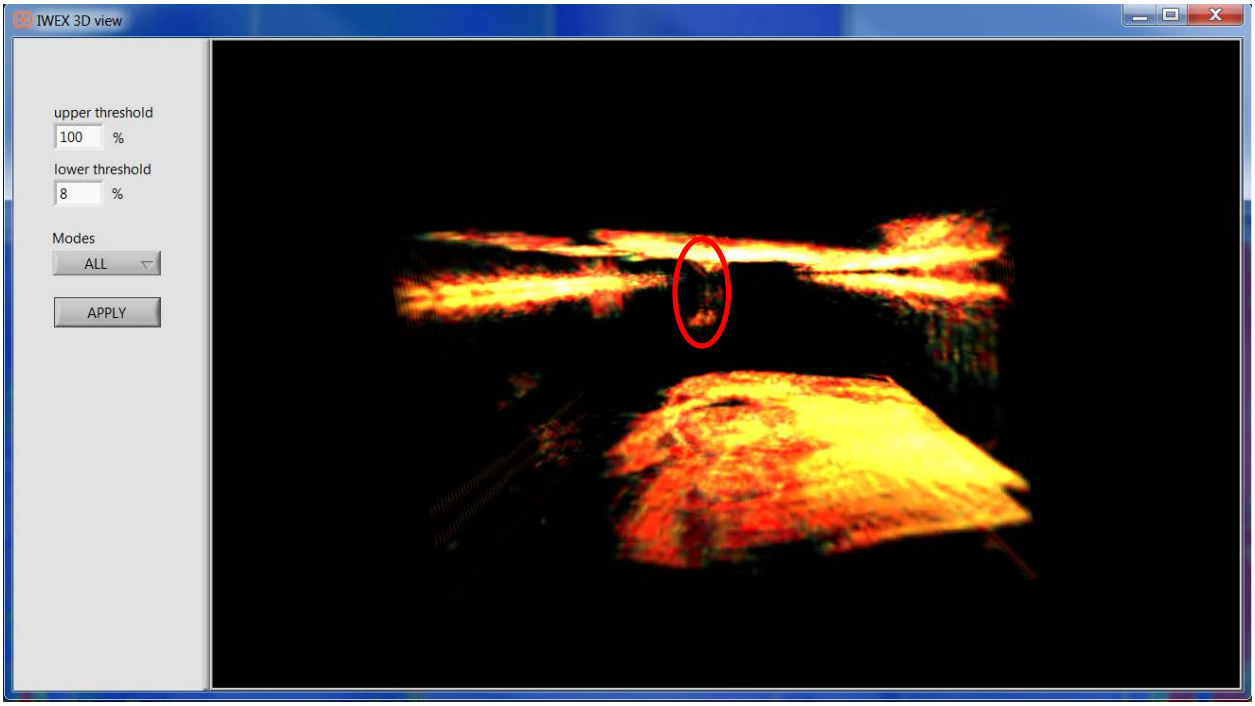

Figure 72. Pipe Sample 159070, 2188 + 6mm, D 0.0 – 1.2mm, H 1.2mm, US 270 side with flow

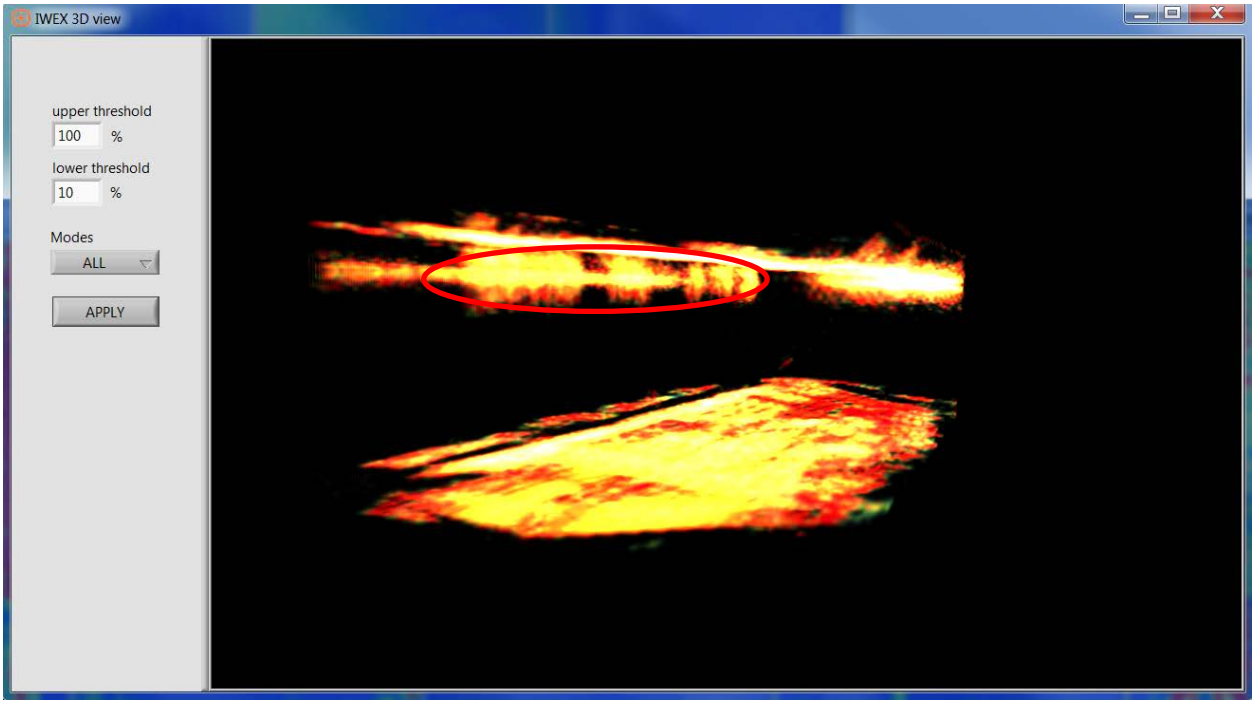

Figure 73. Pipe Sample 159070, 3906 + 180mm, D 0.0 – 1.5mm, H 1.5mm, US 270° with flow OD surface LOF

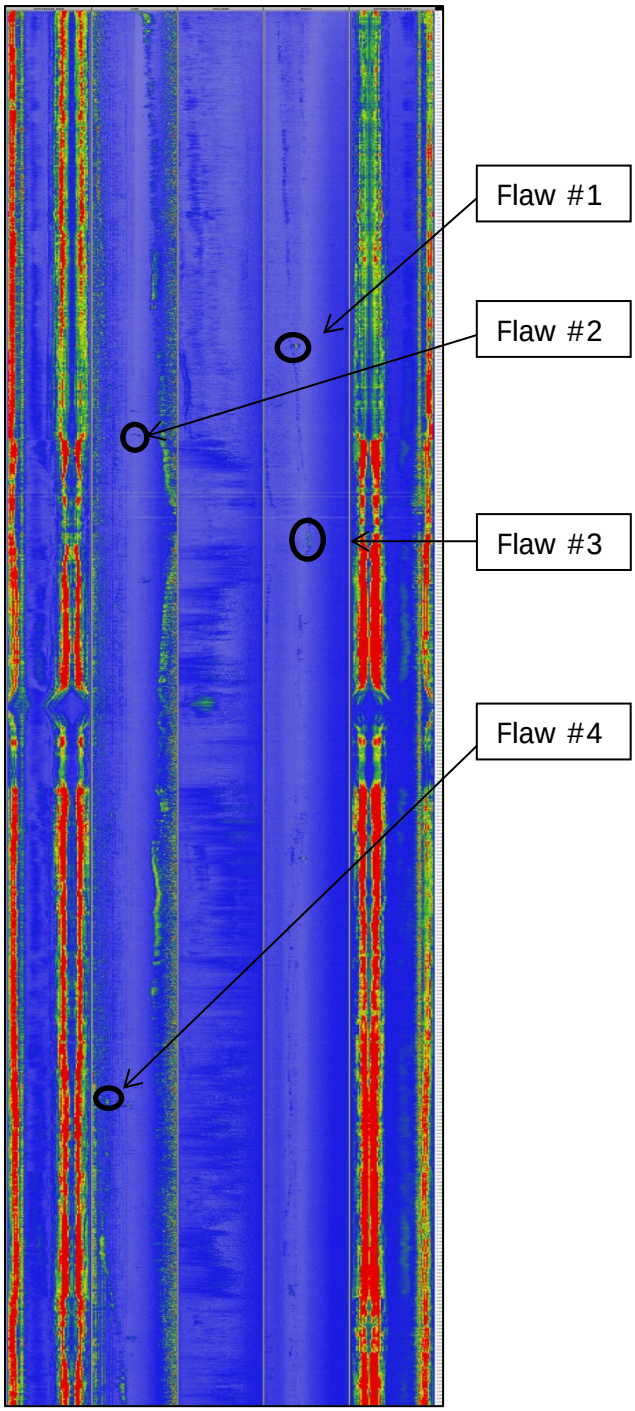

Figure 74. Pipe Sample 159070, Scan#1 0 to +3000

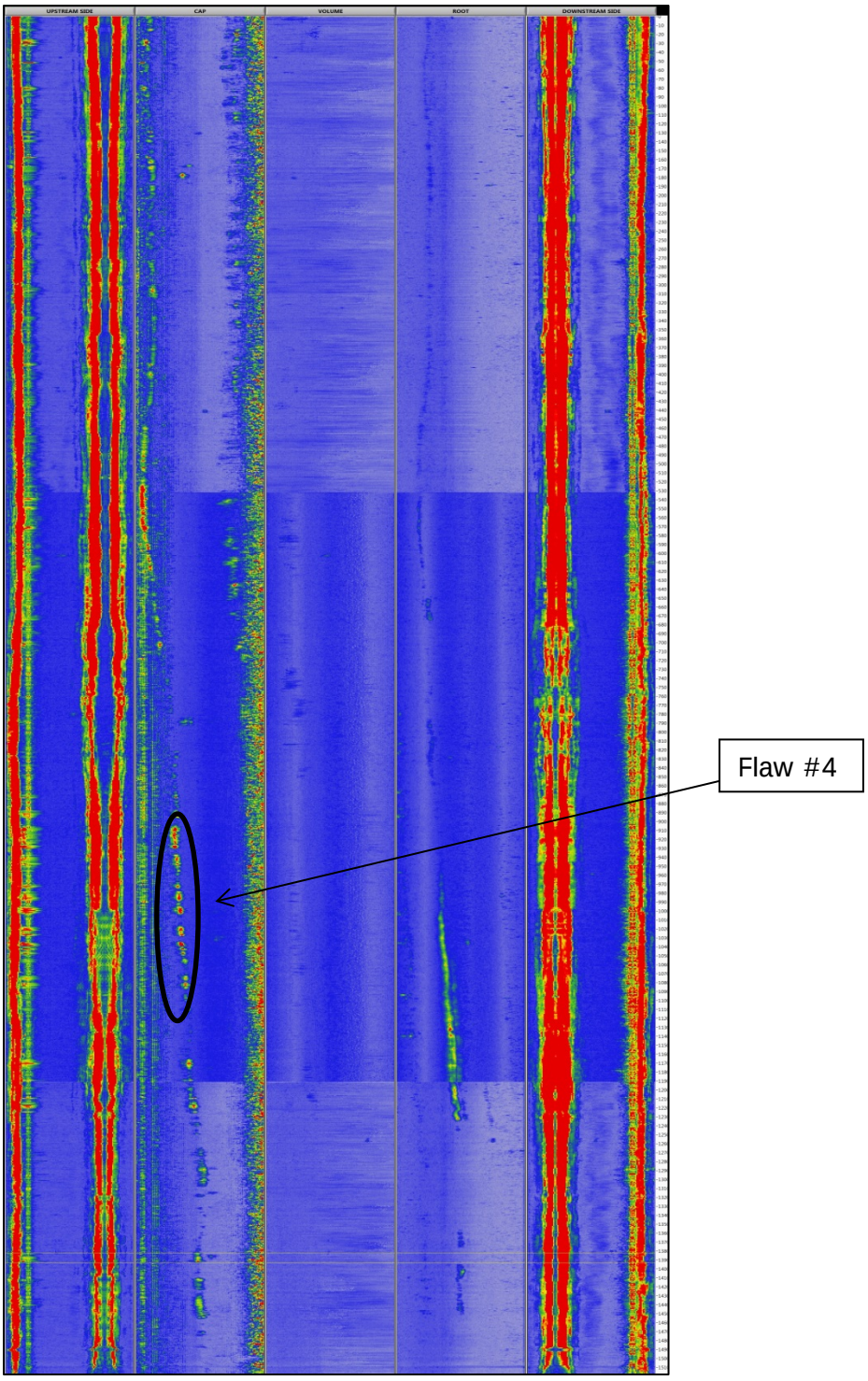

Figure 75. Pipe Sample 159070, Scan#2 3000 to 4250mm

PRCI SCC samples

SCC samples at PRCI's repository in Houston were available for testing as part of the PRCI NDE-2-2(g) project.

Results of first round of testing show a sizing error of ±1mm. There were a few different causes. The interpretation software made amplitude attenuation size easy to perform; this sizing uses the reflection signal off of a defect and looks for a 50% reduction in amplitude on the ends of the defect to pick the end of the crack-like feature. The other source of error was from lack of axial focusing of the UT energy. The transducers produce a cylindrical pulse that spreads in all directions and has an axial width of about 1cm. Many of the features imaged in the first round of testing were shorter than 1cm. Axial focusing was added to reduce the axial beam width by use of a lens in the plastic wedge between the transducer and pipe wall. These two additions produced a significant improvement in sizing error during the second round of testing.

The PRCI SCC samples were not affected by either of these errors as tip diffraction had started to become the defacto sizing method when the tests were performed; however most of the samples in the test were 16-in diameter. This is the diameter of the first set of wedges, which did not contain a lens for axial focusing.

FIRST ROUND OF SCANNER DEVELOPMENT

Scanner development has taken a rather tortuous development path. In the first part of the development effort focused on using an existing LNG tank scanner. Second efforts moved to a steerable magnetic wheeled scanner. Neither of these efforts proved satisfactory and eventually the team moved to a third design which involved a rigidly mounted screw driven linear scanner. The first two of these efforts were covered in the first round of testing and are described below.

Modified LNG tank Scanner

Jeff Vinyard of the AC in Houston designed a scanner for the IWEX system for automated scanning axially down the pipe. The scanner is a modification of a tank scanner used for other UT techniques at Applus RTD and uses suction cups and a vacuum system to hold the scanner in place. The scanner was tested in Houston and on the 16-in samples at the Kiefner lab in Columbus, Ohio. It appeared to work successfully. Diagrams of the scanner are shown in Figure 76 below.

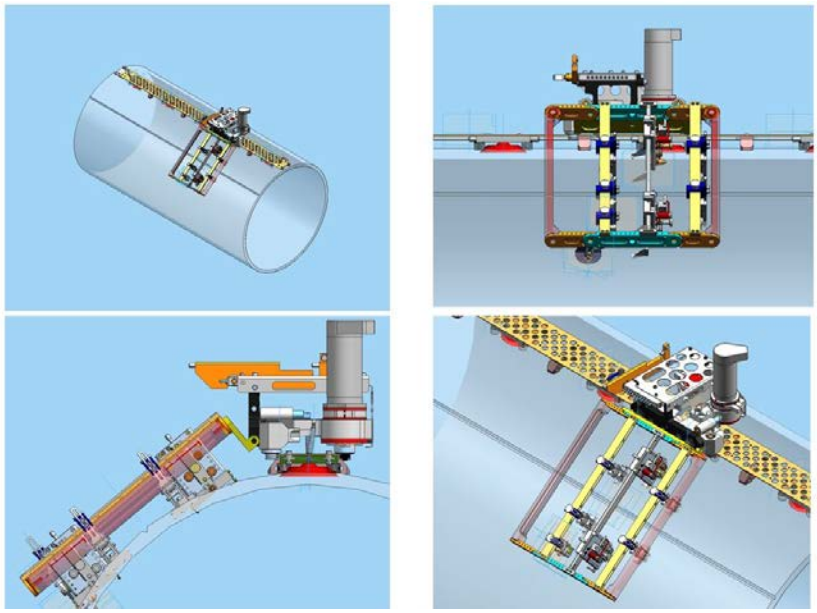

Figure 76. Diagram of tank scanner modified for automated IWEX axial scanning

Magnetic Wheel Long seam weld scanner development

Initially a modified LNG tank scanner was used for data acquisition. This scanner uses the same motor software as the current Rotoscan system meant to scan girth welds. During the process of data collection a guide band is used to keep the scanner in a very straight line. This is needed due to the sensitivity to movement that affects the IWEX data.

Figure 77. Initial scanning system: modified LNG tank scanner

The system works well but is limited to only larger diameter pipe sizes of 16-in and up to flat. In order to use this solution on smaller diameter pipes, a different solution is needed to offer the same stability as the current system.

One idea is to incorporate an ark Y-module to the Navic system. Seen below is the Navic scanner with two Phased Array probes and two TOFD probes. The second photo is with the current 24-in Straight Y-module. This scanner has the ability to turn during data accusation. We will ask Jireh to develop a Y-module in the shape of an arc that will be motorized for probe positioning while the scanner itself remains on top of the pipe. The main problem with this currently is that it will not track/drive in a perfectly straight line. Once the magnetic wheels start to gather small bits of metal the wheels begin to skip or bounce up and down causing the data to not be collected as well as it should.

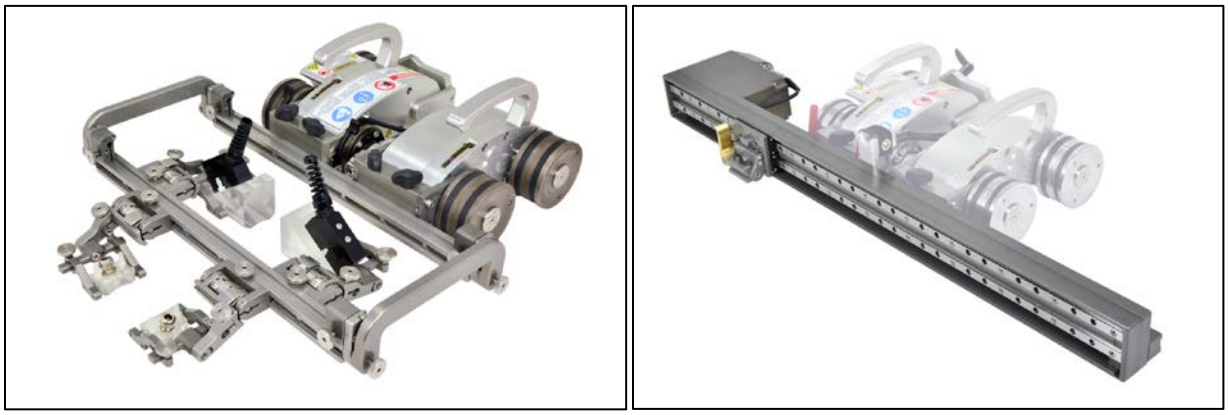

Figure 78. The magnetic wheeled scanner with attachable scanning bar

A possible solution envisioned to overcome the magnetic wheel portion of the problem to achieve scanning in a straight line was to incorporate a laser guidance system as shown in Figure 79 below.

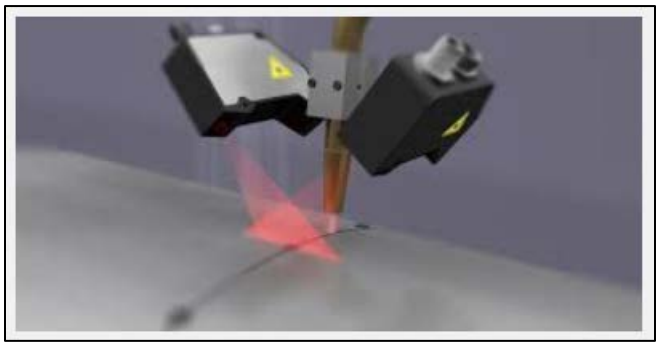

Figure 79. An example of a laser guidance system

These lasers are currently used for precision cutting and are guided by mapping a line that has been placed on the part. If these can be incorporated into the scanner and simply mark the long seam with a visible line then we should then be able to track/scan the long seam.

Another option for tracking in a straight line could be to incorporate an eddy current array probe to find and track the weld. On occasion it can be very difficult to find the long seam. This option could also offer conformation of near or surface breaking indication.

Below, in Figure 80, the left image is an array probe and data from a weld with no defects showing that we can find the weld and the other images showing a few EDM notches and round bottom holes. On the right side is another version of software showing EDM notches and a long seam that has been ground flush.

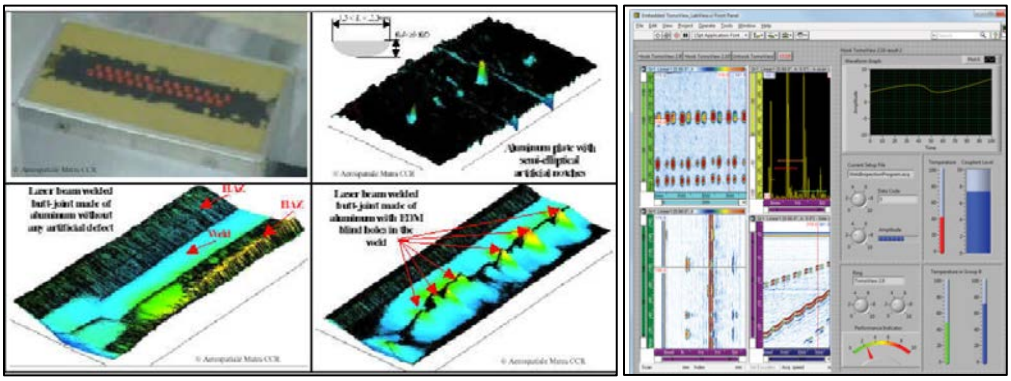

Figure 80. Diagrams showing how an eddy-current system for tracking the seam might work

With this option there would be a considerable amount of time to develop the software that could take the data and communicate with the scanner to make it track straight. This would also mean that now the operator also needs to have eddy current knowledge.

For simplicity and current accessibility there is a magnetic track available. These tracks come in 20-in lengths and there is an encoded scanner that is attached and then manually pushed/pulled along the pipe. This gives us a small amount of equipment to do a lot of scanning. The operator would need perhaps three of these tracks and as the scanner moves from one track to the next the last track can be placed in front of the rest in the direction of the scan and the inspection continues.

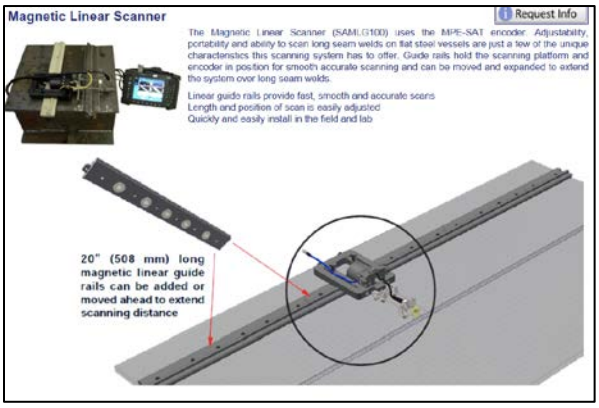

Ultimately we would like to develop our own scanner with a scanner developer such as Jireh and perhaps upgrade other scanners such as L-Pit laser scanning system to work with the same scanner giving us two tools in one box. All of these solutions would require the ability to mount the IWEX scanner on the set up or perhaps make the probe cables much longer.

PROPOSED PROCESSING IMPROVEMENTS BASED ON THE FIRST ROUND OF TESTING

The following improvements to the system have been recommended by the team:

1. Individual gain settings per mode;
2. Development of tools for the calibration of the (geometrical) setup parameters;
3. Suppression of double indications in post-processing;
4. Improved alignment for the different mode images (by measurement and/or post-processing);
5. Improved C & D scan visualization; and
6. Improvement of the signal-to-noise ratio by adaptations of filters in the hardware.

Of these identified improvements, the first two were completed in the 3rd quarter and the others have planned completion dates in the 4th and 5th quarters of the project. A write-up in Q3 Appendix C discusses how some of these improvements may be implemented.

Keeping the IWEX system cool has been a challenge. Various additional cooling has been added to keep the system from overheating. Rotterdam reports this as a known issue and has addressed cooling in future IWEX units.

There were four planned improvements for the IWEX system:

a. improved C & D scan visualization,
b. suppression of double indication in post-processing,
c. improved alignment for the different mode images (by measurement and/or post processing), and

d. improved signal-to-noise ratio by adaptations of filters in the hardware.

Of the above improvements a, b, and d were completed while item c was dropped. An improved alignment will eventually be needed to optimize the depth-sizing capability of the IWEX system, but the solution proposed for this task will not provide the ultimate solution and was dropped. Four tasks to improve alignment of the different modes were proposed in the project modification document submitted in January and it is these improvements that will eventually make the most difference in sizing accuracy and use of the system in complex geometries.

> There are currently four modes being used for inspecting axial cracking with a 5th mode being used intermittently. Mode-0 is the direct reflection from the transmitting element back to the multi-element array where the pulse originated, or as a cross mode transmitted to the multi- element array at the other transducer. Because there are no reflections off the ID, wall thickness is not used to produce the Mode-0 image, however Mode-0 produces an image of the ID which could be used to measure the wall thickness to the resolution of the ultrasonic wavelength, such as poor trim. Modes- 1, 2, 3, (and Mode-4 when used) all require knowledge of the pipe wall thickness to produce an image. A fixed wall thickness is determined during setup, but the input fixed wall thickness does not accommodate variations. A 0.1 mm error in wall thickness will result in the miss-alignment of twice the size in Mode-2, even four times that amount in Mode-4 and a lack of focusing and alignment in Modes- 1 and 3. Currently the setup is where the pipe wall thickness is determined for proper focusing and alignment of the images. The current set up consists of entering all of the nominal values for the probe separation wedge parameters and wall thickness of the pipe. The wall thickness is then slightly adjusted for weld reinforcement if present and optimal focusing is achieved at the location where the probes are placed during setup.

The ability to handle small variations in wall thickness could improve image overlay from the various modes and also could improve the focusing of some of the modes.

2ND ROUND OF TESTING AND IMPROVEMENTS

Robust ray tracing for seam welds

The calculation of travel times requires the calculation of the ray paths from an array element to an image point. Figure 81 shows the three basic paths used by IWEX.

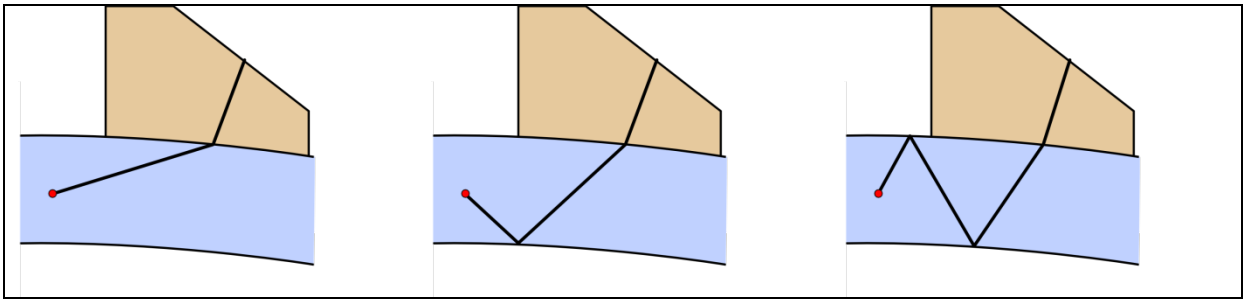

Figure 81. Three basic ray tracing paths from an array element to an image point; from left to right: 0, 1, and 2 reflections at the pipe interfaces.

In order to ensure the robustness of the calculation and facilitate the application of the algorithm in IWEX, two main issues had to be resolved:

- For imaging areas including not only the pipe body but also adjacent regions, travel times that are consistent with the overall image have to be determined. This is described in more detail in the following section.
- The determination of the ray path between two known points has to be carried out in a numerical robust way. The approach chosen is described later in this document.

Treatment of imaging points outside the pipe material

In an ideal imaging situation, the assumed geometry and the exact geometry of the pipe coincide, ensuring that all features are imaged by using only the assumed reflections at the pipe surfaces. For real measurements, deviations can occur which may lead to features ending up at different positions in the images. This may even be outside the pipe material. Therefore, it is required to extend the imaging regions outside the pipe material in order to capture these indications, even if there is no theoretical (physical) path to this region.

It is important to ensure that the travel times outside the pipe material are filled in in such a way that a continuous transition from the pipe body to the outside region is obtained. To this end, the following choices are made:

- For paths reflecting at the inner diameter of the pipe (used in IWEX-1, IWEX-2, and IWEX-3), points below the inner diameter are mirrored back into the pipe material, and the direct paths towards these points are calculated.
- Figure 82 presents the choices made for the path reflecting at the inner diameter in a graphical way. For points inside the material, the virtual path can be compared to a path for which the points are mirrored at the inner diameter as shown in Figure 82(a). Analogously, for image points outside the material, the direct path to the mirror point is calculated as shown in Figure 82(b). This ensures a continuous transition of the travel times at the inner diameter.

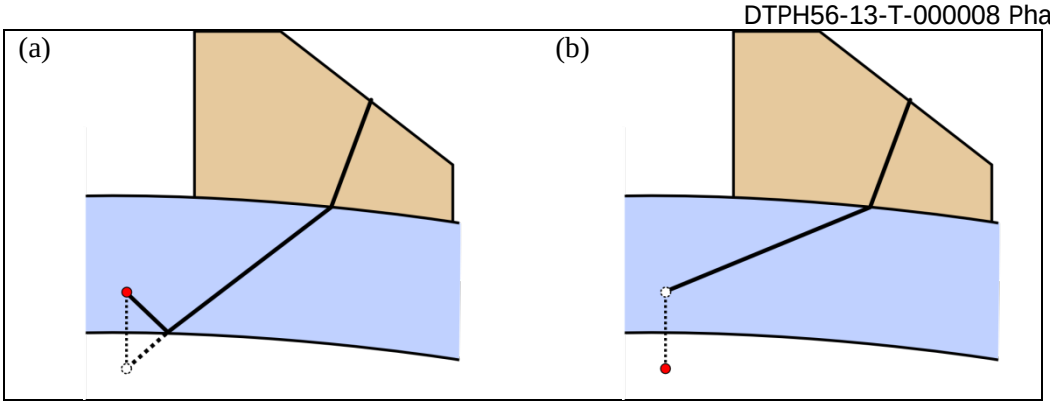

Figure 82. Path with single reflection at the inner diameter for an image point inside the material (a);image points outside the pipe material are mirrored at the inner pipe wall, the virtual path for these points is shown in (b).

- For paths reflecting at the inner and outer diameter of the pipe (used in IWEX-3), points above the outer diameter are mirrored back into the pipe material, and the paths with reflection only at the inner diameter towards these points are calculated. Figure 83 illustrates this principle. For points inside the material, the virtual path can be compared to a path for which the points are mirrored at the outer diameter as shown in Figure 83(a). Analogously, for image points outside the material, the path to the mirror point with a single reflection at the inner diameter is calculated as shown in Figure 83(b).

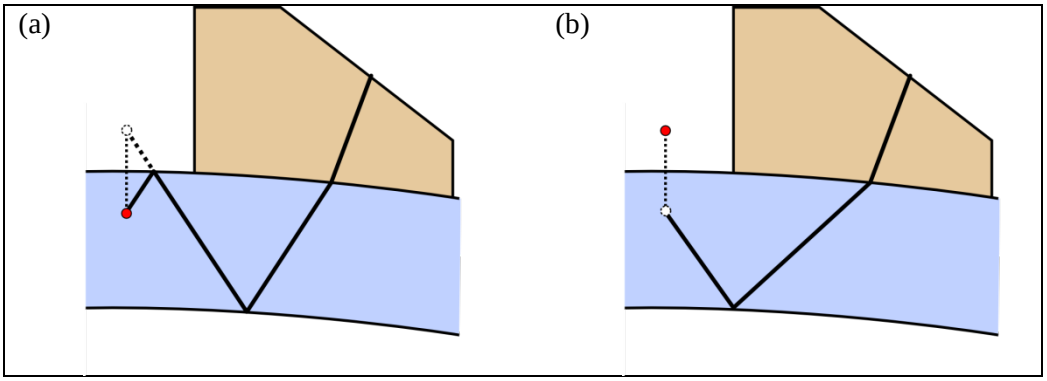

Figure 83. Path with reflections at the inner and outer diameter for an image point inside the material (a);image points outside the pipe material are mirrored at the outer pipe wall, the virtual path for these points is shown in (b).

Robust ray tracing algorithm for the seam weld geometry

In order to calculate the travel times from all array elements to the points in the image, the ray paths have to be determined. The ray path between a start point and a target point can be calculated as the path with the minimum travel time according to Fermat's principle. This problem can be solved by numerical minimization of the travel time. A choice has to be made in the unknown variables. Furthermore, the algorithm has to be set up in a robust way such that the minimum is found.

For the seam weld ray tracing problem, the intersection points at the pipe surfaces are chosen to be the unknown variables. Hence, for the three basic paths, there are up to three unknown variables: a point of refraction at the outer diameter, a point of reflection at the inner diameter, and a point or reflection at the outer diameter as shown in Fig. 83(a).

The travel time exhibits only one global minimum with respect to these three variables, corresponding to the ray path taken in the materials. Due to the well-behaved nature of this minimum, the minimization algorithm can be devised in such a way that only one variable is varied at a time. The variable that is adapted is the one leading to the biggest improvement, i.e., the lowest travel time.

The following description provides an overview of the algorithm. The coordinate system is chosen in such a way that x is the horizontal coordinate, x=0 being the weld centerline. The vertical coordinate z has its origin at the outer diameter and is positive into the pipe body.

1) Initially all intersection points to x=0, and z=0 for intersection points at the outer diameter, z equal to the wall thickness for the intersection point at the inner diameter. If the algorithm is repeated for a number of image points positioned closely together, significant speedup can be achieved by using the already determined intersection points associated with a path to a nearby image points as starting guess for the current image point.
2) Calculate the travel time of the paths formed by the current intersection points.
3) Vary all intersection points separately by adding and subtracting a defined step size in x-direction.
    a) For the direct path, two variations of the intersection point at the outer diameter are calculated.
    b) For the path with a single reflection, in addition, two variations of the intersection point at the inner diameter are calculated.
    c) For the path with two reflections, in addition, two variations of the intersection point at the outer diameter are calculated.
4) Calculate the z-positions of the intersection points according to the varied x-positions.
5) Calculate the travel times for all variations. There is one travel time for the current estimate and up to six variations, depending on the number of reflections in the path.
6) Compare the travel times and apply the variation that leads to the smallest travel time for the path taken. This way, only one intersection point is updated during a single iteration of the algorithm. If all variations lead to a larger travel time, return the current intersections points as result of the travel time minimization.

The optimal step size can be determined empirically and be set to a fixed value. When using the intersection points from a nearby image point as a starting guess, only a few iterations per image point are required to determine the ray path.

The algorithm has been verified by tests for typical setup geometries between 4-in and 30-in pipe diameter.

IMPROVED VISUALIZATION OF IWEX VOLUME SCAN DATA BY MEANS OF C- AND D-SCAN PROJECTIONS

Surface-breaking cracks tend to cause different types of indications in the IWEX image. On the one hand, a vertical indication picked up by an IWEX-3 tandem mode is present at the horizontal position of the crack. On the other hand, corner reflections cause also diagonal indications in the IWEX-2 skip mode as shown in the figure below.

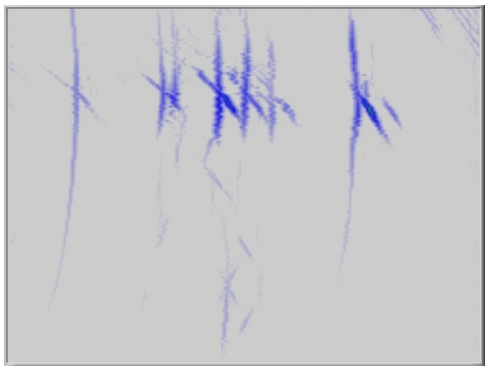

Figure 84. Cross-sectional IWEX image of cracks in the pipe body linked to the OD surface

When generating C-scan top views from the IWEX volume data, combination of all modes can lead to projections that are blurred and less clear in showing the positions of the cracks. Therefore, additional features have been implemented in the IWEX viewer software to select the modes contributing to a C- and D-scan representation. In addition, amplitude thresholds can be set to exclude indications below the noise level. Both measures lead to projections that are a cleaner and easier to interpret.

In addition, the aspect ratio for these C- and D-scans has been set to 1:1 in order to simplify comparison of IWEX data to breaks and photographs. An example of a D-scan view of a toe crack is shown in Figure 85.

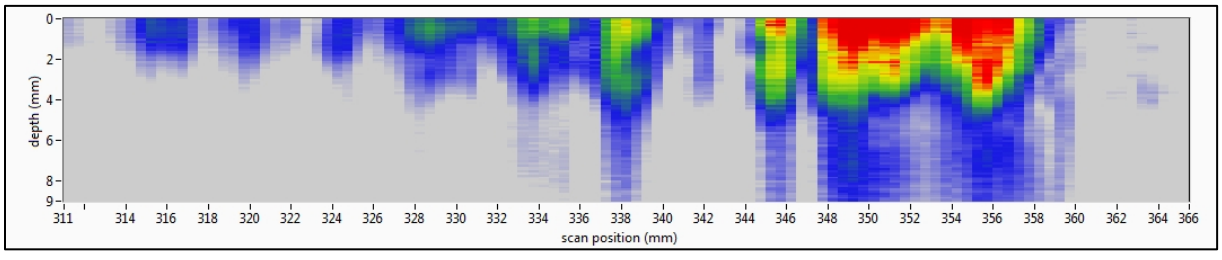

Figure 85. D-scan (side view) image of a toe crack at the OD, showing the extent into the pipe

Especially for the analysis of SCC colonies, the selection of modes for the C-scan representation has significant advantage in comparison to visualizations used previously. An example has already been given in the previous Appendix. Figure 86 shows the improvement obtained by removing irrelevant modes and adapting the color thresholds.

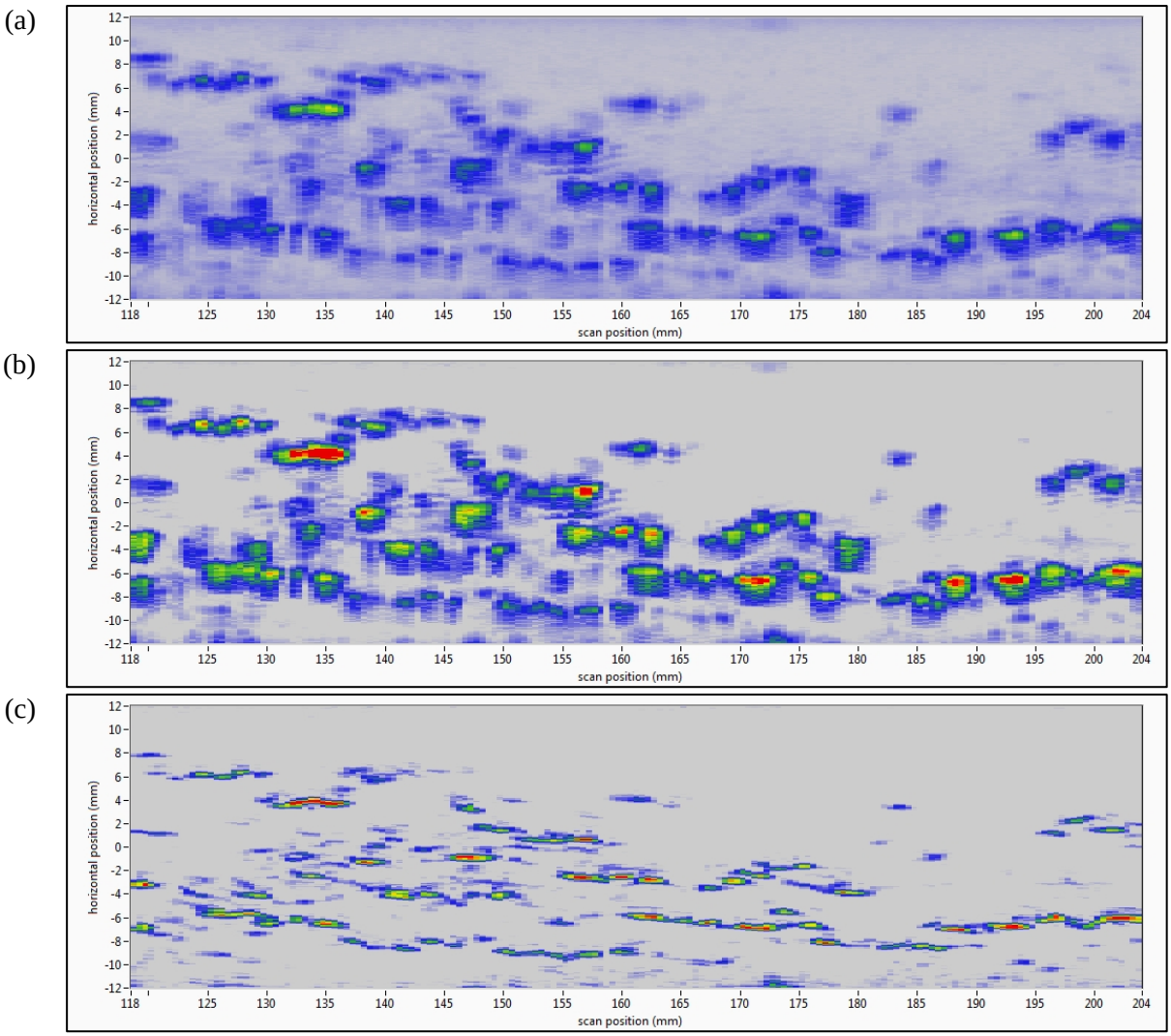

Figure 86. C-scan top view projection obtained from the scan data of pipe body cracks (a); improvement by adding a noise level threshold and increasing contrast (b); removal of diagonal indications visible in the IWEX-2 skip mode caused by corner reflections (c)

Optimization of hardware settings for increased signal-to-noise ratio

In order to increase the signal-to-noise ratio (SNR) in the IWEX images, optimized hardware settings have been determined both from a theoretical point of view and experimentally.

One of the causes for noise in the IWEX images is the selection of amplifier and filter settings in the analog part of the IWEX processing hardware. There is actually a cascade of amplifiers present:

- Low-noise amplifier (LNA); three possible settings: 15.6, 17.9, or 21.3 dB
- Post gain amplifier (PGA); four possible settings: 21, 24, 27, or 30 dB
- Variable gain amplifier (VGA): variable attenuation in the range of -42 to 0 dB

As the name suggests, the LNA has the best SNR, but limited amplification. The PGA provides the highest amplification, but has a higher noise level. The VGA is actually an attenuator with variable settings.

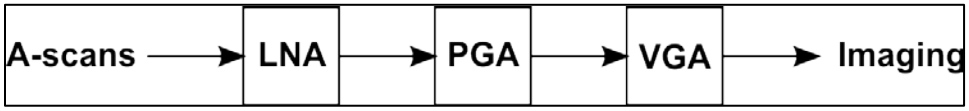

Figure 87. Amplifier chain in the analog part of the IWEX processing hardware: low-noise amplifier (LNA), post gain amplifier (PGA), variable gain amplifier (VGA).

Ideally, the amplifiers are combined in such a way that the PGA is used at its lowest amplification, the VGA is not used (no attenuation), and the LNA is set as low as possible for the application. For standard IWEX applications, the ideal setting has been determined to be a main gain of 36.6 dB, from which the settings for the different amplifiers are automatically derived by the software: LNA at 15.6 dB, PGA at 21 dB, VGA at 0 dB.

Other hardware parameters were varied experimentally in the context of girth weld inspection, leading to the following list of settings to be used if increased SNR is required:

- main gain 36.6 dB (sufficient for most applications)
- increased setting for the high-pass filter (at least 2.5 MHz for 10 MHz arrays)
- use three adjacent transmitters simultaneously (source boost = 2)
- enable bipolar pulsing

It should be noted that the last option can have an adverse effect on the image resolution and should be tested on a case-by-case basis. The combination of one or more of the above settings has been found to result in an improvement in SNR of 6 dB or more in comparison to settings recommended previously.

These results are not conclusive, but represent intermediate recommendations. A re-design of the electronics of the IWEX system is ongoing in the context of girth weld inspection. Waiting for this adaptation before pursuing further experiments is recommended.

SAMPLES FOR THE SECOND ROUND OF TESTING

12-in and 20-in ERW samples

These samples were tested at the Kiefner Metallurgical Lab in Ohio. It took some time to remove the coating from some of these samples because they contained asbestos requiring special precautions. IWEX, PA and ToFD scans were made of all the samples including several joints of 12-in and 20-in samples.

Although two 22-in samples were also included with these samples they were eventually held back for later testing in part because the defects did not appear very significant and the pipe was not very cylindrical near the seam on one side making scanning difficult.

12-in ERW Samples

Large numbers of defects were reported on the selected 12-inch Pipe ID # 8 pipe sample. The selected 10 locations were chosen at locations where a similar type of indication was reported by every technology and NDE service provider to ensure comparison data is achieved after destructive analysis. Effort was also made to ensure a variety of defects was selected to compare - detection, identification and sizing capabilities of various technologies and (OD, ID, Hook Cracks, Lack of Fusion, Trim undercut etc.). Sixteen break locations were destructively tested to obtain validation data for comparison.

Length Accuracy

Figure 88 shows a cumulative frequency Length Error Plot. Although results from SGS show a large error, no conclusive inferences can be derived from the length accuracy performance results. When large numbers of defects are present resolution of defects becomes an issue. The operator analyzing the NDE scan may record some very closely located defects as one defect while the other operator may break that area into multiple smaller defects. Although we can derive conclusions about resolution accuracy, length accuracy comparison is much more difficult. Hence, due to large number of closely located defects, a length accuracy performance comparison is inconclusive. The SGS error for Defect 2 at 6 inches was so large it skewed the results and has been omitted from the plot of the data in Figure 88 below.

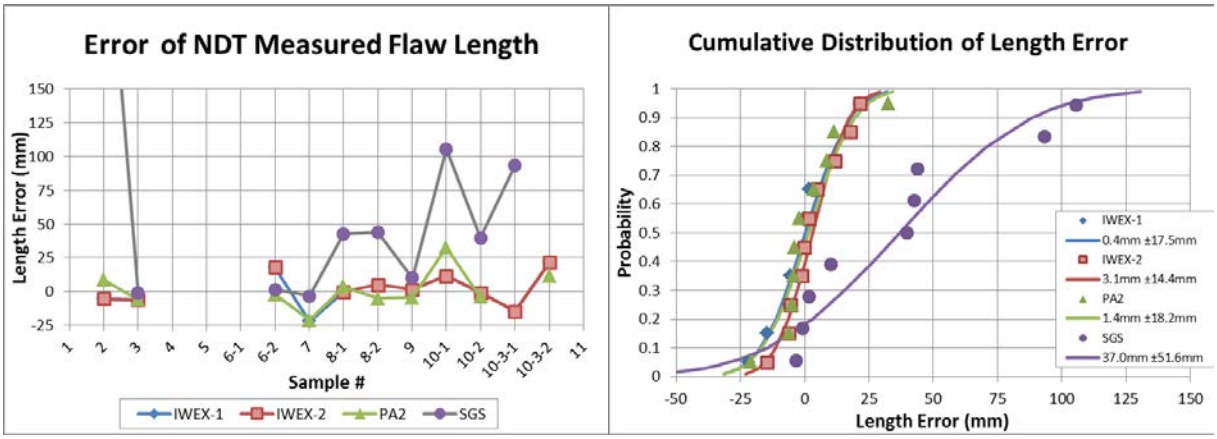

Figure 88. Length Error Plot for 12-in ERW Samples

Depth (Height in material) Accuracy

Figure 89 shows a cumulative frequency Depth Error Plot. IWEX-1 showed more conservative depth predictions. PA2 predicted conservative depth readings also. Depth predictions from PA1 varied from non-conservative to highly conservative. Also the detection capacities of PA1 were lowest among the studied data sets. With only two comparisons, the data was insufficient to include in the cumulative distribution plots in Figure 88 and Figure 89. IWEX-2 exhibited the best depth predictions among the techniques.

What is worth noting is that IWEX-1, PA2, and SGS all show different bias in the measurement of depth, they all show similar depth random measurement errors of just under ±1 mm, where IWEX-2 show a significant improvement in bias and a depth random error of under ±¼ mm. It is believed the reason for the difference that IWEX-2 used tip diffractions for detecting the crack depth where IWEX-1 was based on amplitude attenuation of the signal. The differences between IWEX-1 and IWEX-2 are explained in more detail in the next section of the report.

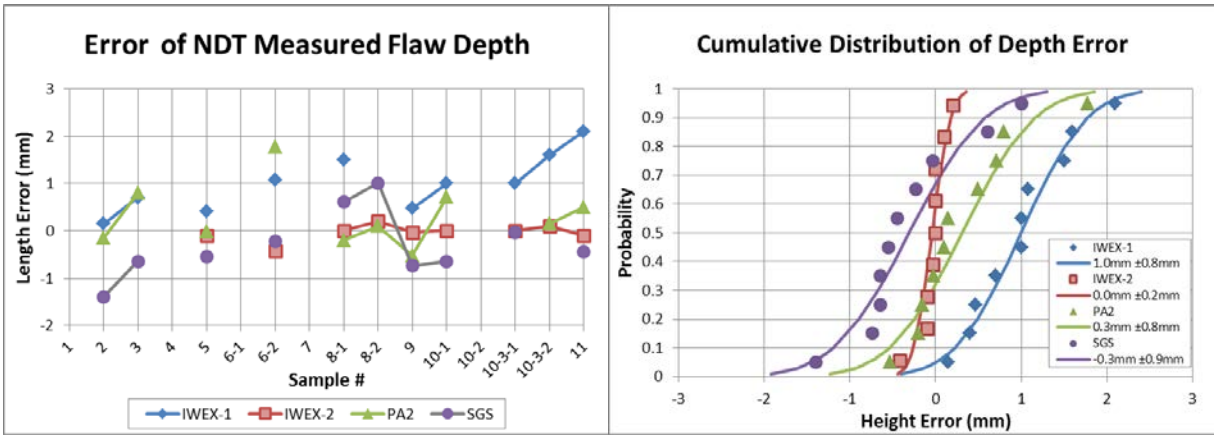

Figure 89. Depth Error Plot for 12-in ERW Samples

IWEX – Technology and recent improvements

Current ultrasonic techniques for direct assessment of defects can localize imperfections but it is very difficult to determine a flaw's orientation and exact size. Interpretation of NDE data collected relies heavily on operator skills therefore operator qualification becomes critical. Lack of experienced operators and stringent operator qualification standards make results of NDE analysis less reliable.

IWEX is a new technology, which involves full waveform capture and inversion to provide an ultrasound image of anomalies similar to existing technologies such as medical ultrasound imaging and seismic imaging. This imaging technique was originally developed for seismic exploration of oil and gas fields. This imaging technique uses inverse wave field extrapolation to make images of the interior of a medium from array measurements applied at the surface. Applying the IWEX imaging technique for ultrasonic weld inspection, enables the NDT technician to make a representative image of the interior volume of a weld, which provides a much better and easier interpretation of the position, size and orientation of the imperfections in the weld[1].

The seismic imaging technique is the most similar to IWEX in that IWEX captures the full waveform across the transducer array after each individual element of the array is fired. These signals are then processed or inverted into an image. IWEX is different from seismic images in that IWEX uses the back wall reflections in making an image. Every IWEX image is made from a combination of different IWEX Modes which are combination of different possible paths from every element to every image point. There are three possible paths from every element to every image point.

- No reflection

[1] 3D ultrasonic imaging of defects in welds by inverse wave field extrapolation, R.H. Baardman

- One reflection
- Two reflection

Figure 4 on page 4 shows an overview of all IWEX modes. One of the major improvements in the latest IWEX analysis software (Version 1.8) was the ability to turn ON/OFF various modes while analyzing an IWEX scan. High density of defects in the 12-in Pipe ID#8 made it harder to accurately resolve and size crack-like defects. The ability to select active Modes in an IWEX image provided the IWEX operator with better resolution of tip diffraction signals from crack-like defects.

Section 4, Comparison of Methods/NDE Service providers mentions data sets; IWEX-1 and IWEX-2 (i.e. both are interpreted from same IWEX scan for the 12-in Pipe ID#8 analyzed) IWEX-1 uses analysis software version 1.75 and IWEX-2 uses Version 1.8. Improvement is depth accuracy and resolution is reflected in the comparison of depth error performance between IWEX-1 and IWEX-2. Although the IWEX-1 interpretation was performed before breaking the samples and the IWEX-2 interpretation was performed after breaking the samples, the interpretation for both were obtained without looking at the metallographic images.

In earlier studies, significant improvements were obtained in analysis of Lack of Fusion (LOF) defect sizing using IWEX analysis software version 1.75. The improvements were results of improved resolution capabilities in the newer Version 1.75 (compared to Version 1.74) combined with the use of 10 MHz probes with focused wedges in place of 7.5 MHz probes with unfocused wedges. Figure 90 shows IWEX images from three LOF defects (2, 3 and 4) with the “ALL” modes picture focused on Defect 2 (Yellow cursor can be seen in the lower half of the image). Figure 91 shows these three LOF defects in the fracture surface.

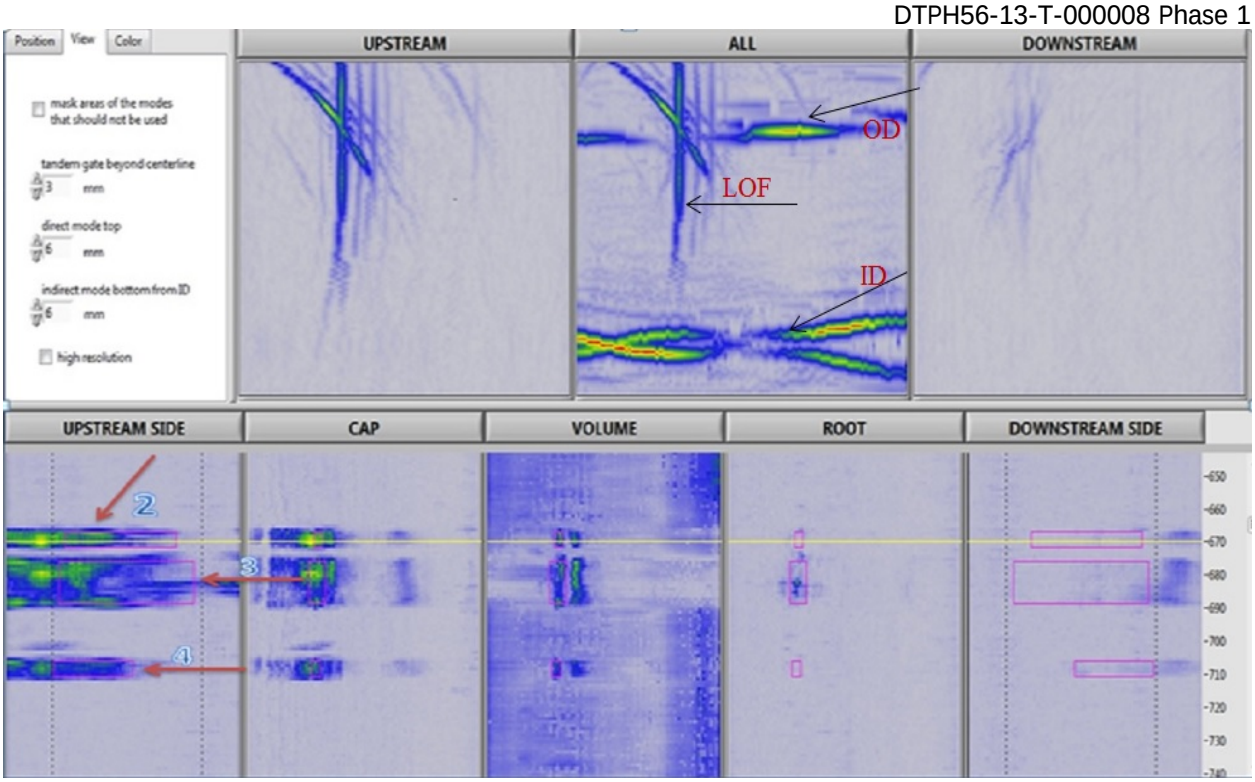

Figure 90. IWEX Image for Lack of Fusion defect (V1.75)

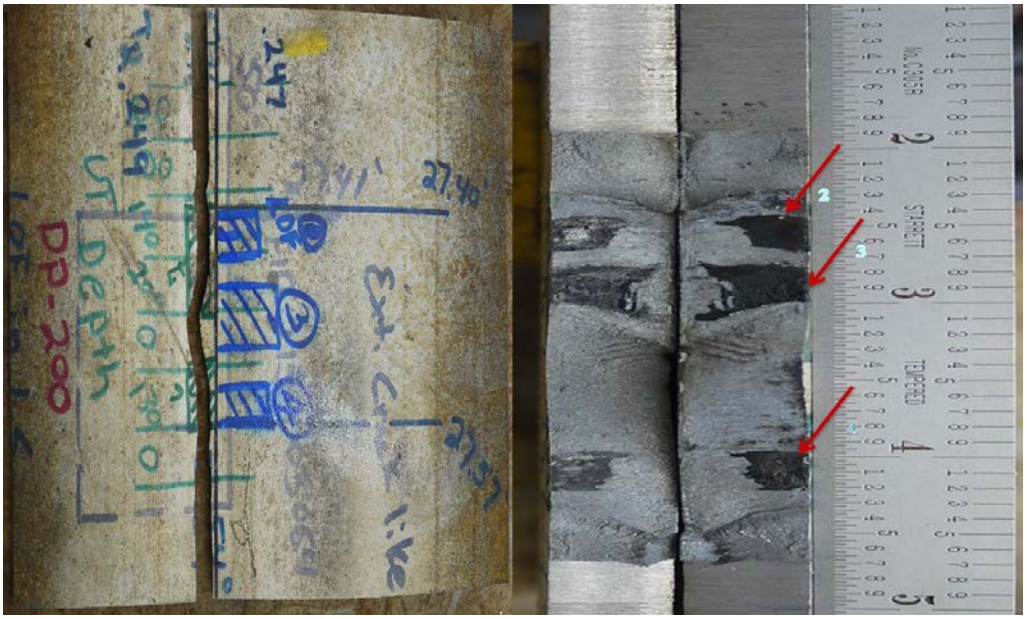

Figure 91. Lack of Fusion defects on Fracture Surface

As can be seen in Figure 90, IWEX images from LOF defects are very upright because of the shape of an LOF defect. It was observed from various destructive analyses results that sizing LOF defects using the amplitude of signal and selecting the complete depth of the defect in the IWEX image provided improved results. This analysis procedure was tested in a second set of destructive testing which was covered under a DOT PHMSA project. Results from this set of

testing confirmed the hypothesis that using amplitude based signal is the most accurate way to size an LOF type of defect. In the same experiments it was found that a 6 dB drop method (function build in with the IWEX analysis software) proved to be under sizing the LOF defects. Hence 6db drop method was rejected as the preferred method for sizing LOF defects.

IWEX-1 data set was acquired by analyzing the IWEX scan for 12" Pipe ID#8 using IWEX Analysis Software Version 1.75. Analysis was performed by using the amplitude based signal/ image. Unlike the previous case, defects in this pipe sample were mostly crack like indications. Further confirmation was achieved by destructive analysis that defects in this pipe sample were mostly hook cracks. Figure 92 shows analysis of Break Location 11 by using the amplitude method signal alone. Figure 93 shows analysis of the same defect using the tip diffraction method. (Length reading is different as only depth was investigated. For this purpose the cursor was pointed at the same location where destructive analysis (metallography) was performed at Break 11).

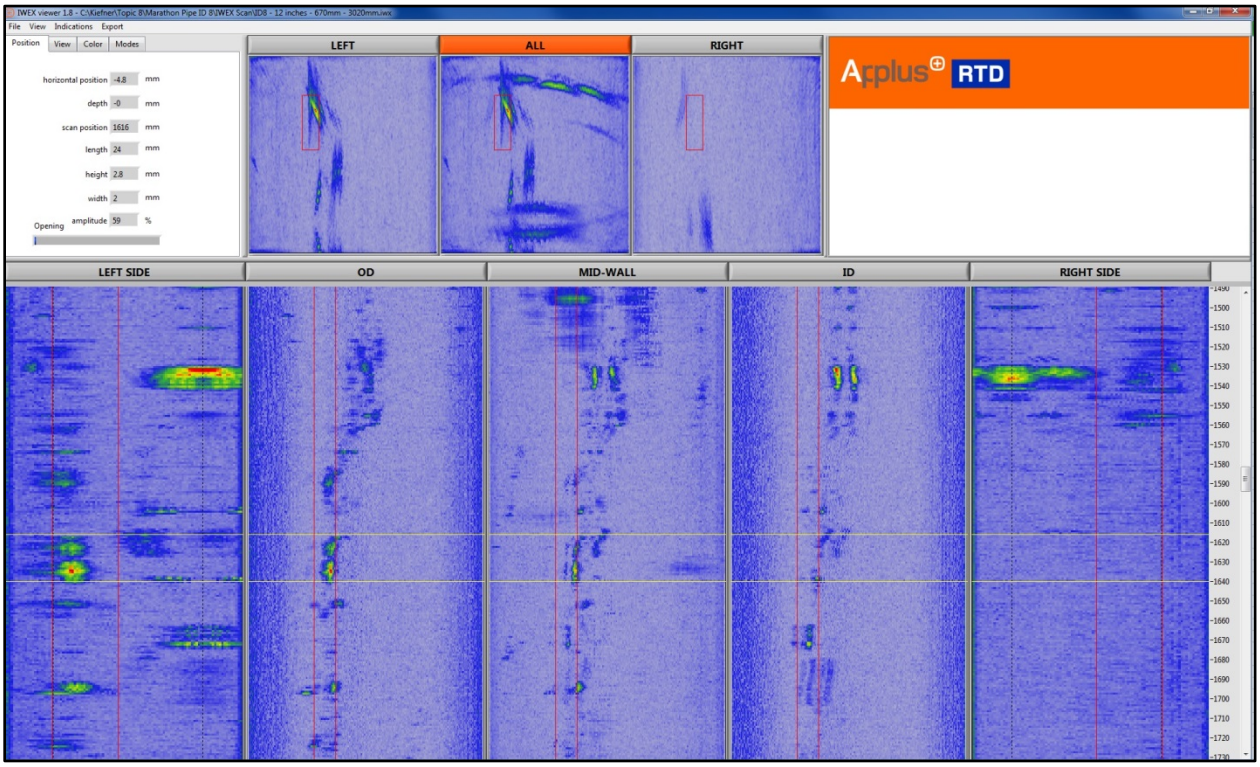

Figure 92. Break Location 11 (Sizing by amplitude method V1.8)

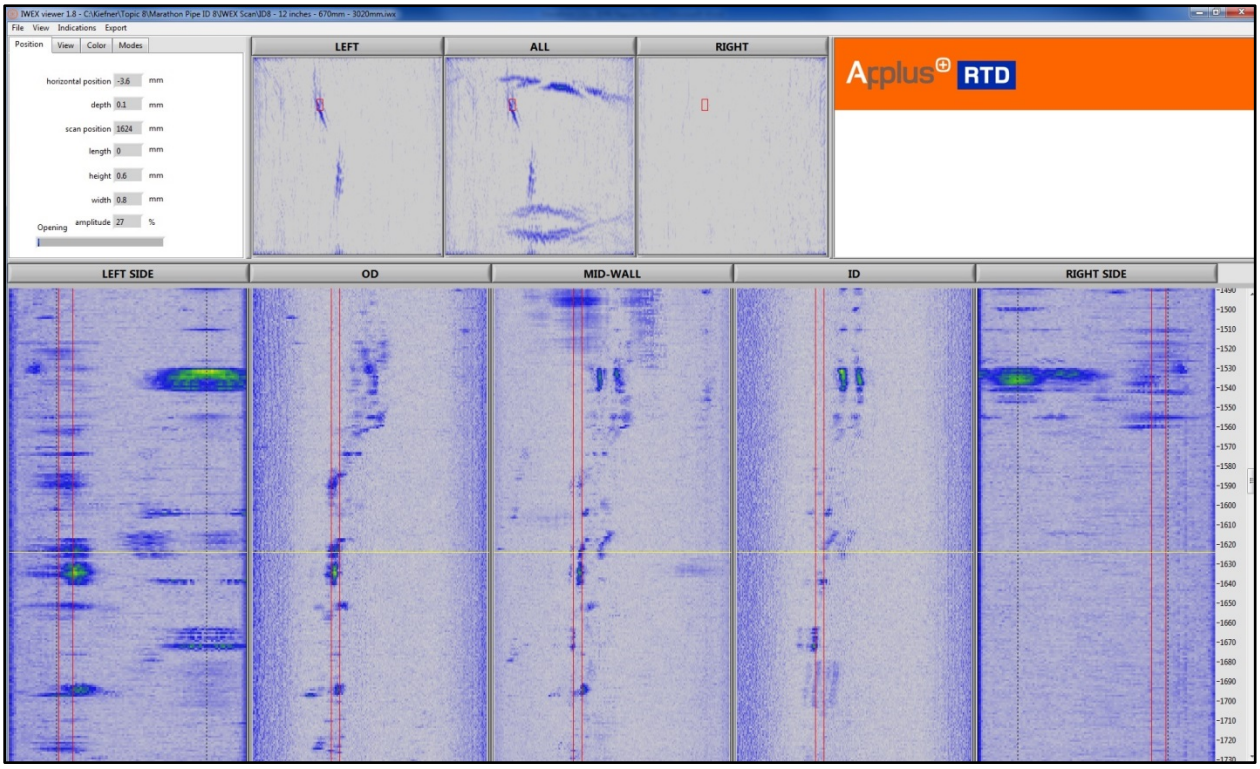

Figure 93. Break Location 11 (Sizing by Tip Diffraction Method V1.8)

Table 4 is a comparison of depths reported by IWEX-1 and IWEX-2 with results from destructive analysis. Results suggest that the amplitude method for analysis of crack like indication provided very conservative results (IWEX-1). This proved to be true for all crack like defects. IWEX-2 data set was prepared using the tip diffraction method and results showed considerable improvements.

Table 4. Depth Comparison for Break Location 11(Depths in millimeters)

Depth comparison for break Location 11		
Destructive Analysis	IWEX 1	IWEX 2
0.6	2.8	0.6

Discussions

The results of the study described in this report have shown that pipeline seam assessment capabilities for Detection, Identification and Sizing can vary, and are affected by the: technology used, pipe properties, weld geometry, experience of NDE operators, and evaluation techniques.

Time of Flight diffraction (TOFD) although very accurate in sizing was unable to provide useful information to the desired standard. This was because of the weld geometry, thin wall thickness of the pipeline and a large number of near surface defects.

Magnetic particle testing (MT) proved to call indications longer than actual length. This can be seen in the length accuracy error plot of VenA. MT though a very quick and reliable technique for finding open to surface and near surface defects can sometimes call defects longer than the actual length. Hence MT results can be conservative in cases like this 12-in Pipe ID#8 Sample. Resolution of defects poses a challenge in the case of large numbers of closely spaced or overlapping defects and MT is unable to provide the required resolution.

Phased Array provided some good results but the results varied largely with operator and thus issue of operator qualification becomes a concern. Results showed that Phased Array results varied with operator in case of detection, identification and sizing. It is acknowledged that advanced ultrasonic techniques like Phased Array and TOFD, though very reliable and effective, depend heavily on training and experience of personnel. The same concern is true for manual ultrasonic techniques. Even more so because unlike PAUT and TOFD there is no way of going back to the scan data for verification as scanning and interpretation of data is performed in real time.

The results from IWEX-2 data set proved best in comparison to all other technologies (included in this study) and NDE service providers. IWEX is a relatively new technology and there was a considerable variance between the results from IWEX-1 and IWEX-2 data sets. As the report states the reason for the difference between the two data sets was data interpretation techniques and availability of improved data interpretation software for IWEX-2, more effort is required to study the effectiveness of IWEX technology and effects of its data interpretation techniques.

Figure 92, Figure 93, and Figure 94 show the improvements in sizing capability using Version 1.8 of the IWEX viewing software. By looking at the window labeled “ALL”, the difference between amplitude sizing in Figure 92 and tip diffraction sizing in Figure 93 is apparent. Figure 94 shows how toggling on and off various modes can help with the interpretation.

12-in sample results summary

1. IWEX proved to be the most effective technique for detection, identification and sizing of seam weld defects in the studied pipe sample. IWEX-2 data set provided satisfactory results.
2. Results for advanced ultrasonic techniques (PAUT, TOFD) varied considerably with operator and therefore effectiveness of these techniques for pipeline integrity may vary largely with the operator qualification.
3. MT proved to be highly conservative in predicting lengths of defects and provided poor resolution between closely located surface defects.
4. Results from various NDE techniques and between different NDE service providers varied significantly. This variance in results can influence integrity decisions either for direct assessment or for ILI qualification/verification purposes.

20-in ERW Samples

Large numbers of defects were reported on the selected 20-in Pipe ID #1 pipe sample. The selected 12 locations were chosen at locations where a similar type of indication was reported by every technology and NDE service provider to ensure comparison data is achieved after destructive analysis. Effort was also made to ensure that a variety of defects were selected to compare - detection, identification and sizing capabilities of various technologies and (OD, ID, Hook Cracks, Lack of Fusion, Trim undercut etc.). Sixteen break locations were destructively tested to obtain validation data for comparison.

Length Accuracy

Figure 94 below shows a cumulative frequency Length Error Plot. Results from VenA were slightly conservative. No conclusive inferences can be derived from the length accuracy performance results because length information could only be achieved for six of the 16 break locations. Fractography provides the most useful information about the complete profile of the defect including total length of the defect. A large number of defects was found on the 20-inch. ID#1 pipe but fractography was not very successful on the test locations. This could be attributed to the size of the defects present on this pipe being very small. Since not enough samples produced length information, length accuracy performance comparison is inconclusive.

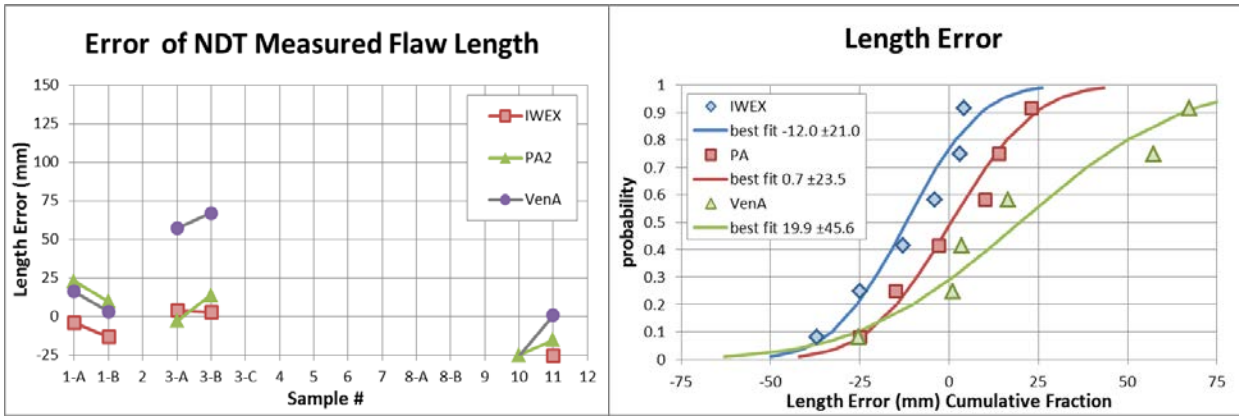

Figure 94. Length Error Plot

Depth (height in material) Accuracy

Figure 95 shows a cumulative frequency Depth Error Plot. IWEX, Phased Array and VenA all showed conservative depth predictions. Phased Array depth predictions were most conservative. Depth predictions from IWEX and VenA varied from non-conservative to being mostly conservative. Although IWEX exhibited best depth predictions among the techniques, the results from VenA were very close to IWEX.

IWEX show a slightly better random measurement error or 0.5 mm over VenA with random measurement error of 0.7 mm. Both IWEX and VenA show same bias in depth random error of ±0.6 mm.

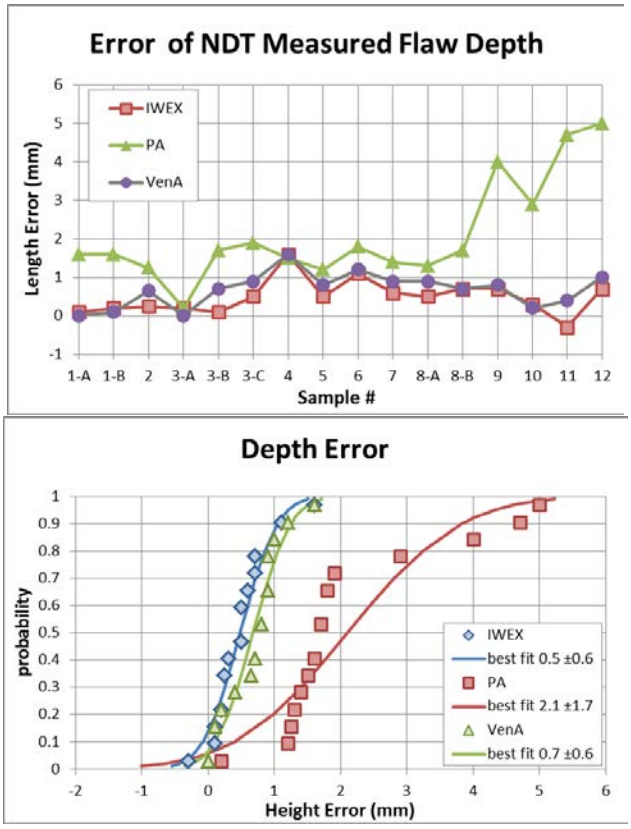

Figure 95. Depth Error Plot

Discussions

The results of the study described in this report have shown that pipeline seam assessment capabilities for detection, identification and sizing can vary, and are affected by the: technology used, pipe properties, weld geometry, experience of NDE operators, and evaluation techniques.

Time of Flight diffraction (TOFD) although very accurate in sizing was unable to provide useful information to the desired standard. This was because of the weld geometry, thin wall thickness of pipeline and large number of near surface defects.

Magnetic particle testing (MT) proved to be calling indications larger than actual length. This can be seen in the length accuracy error plot of VenA. MT though a very quick and reliable technique for finding open to surface and near surface defects can sometime call defects longer than the actual length. Hence MT results can be conservative in cases like this 20-in Pipe ID#1 sample. Resolution of defects poses a challenge in the case of large numbers of closely spaced or overlapping defects and MT is unable to provide the required resolution.

Phased array results showed highly conservative error. Metallurgical sections taken from all 10 locations provide evidence of multiple small inclusions/stringers in the seam weld area. Presence of multiple small reflectors in close proximity could be responsible for the defect being oversized by Phased Array.

IWEX, Phased Array and VenA, all provided very conservative results for the depth of defects. In some instances multiple small reflectors were found along the same flow lines in the weld area. The results from this study raise two very important concerns regarding all available NDT technologies:

1. Minimum Sizing capabilities: All technologies provided very conservative results for the defects found in this study. With more experiments we may be able to quantify the minimum sizing capabilities of NDT technologies.
2. Resolution Capabilities: When defects are in close proximity, multiple times it has been observed that the NDT technologies provide highly conservative results.

Recent improvements in IWEX technology showed considerable improvement in sizing of curved, crack like features. IWEX results in this study were best among the compared technologies but not considerable better. Future work in IWEX technology may help provide solutions to the above two problems of Minimum Sizing capabilities and Resolution Capabilities.

20-in sample results summary

1. IWEX proved to be the most effective techniques for detection, identification and sizing of seam weld defects in the studied pipe sample. IWEX data set provided satisfactory results.
2. PAUT provided very conservative results. TOFD was not very effective in the 20" pipe sample studied in this Phase.
3. MT proved to be highly conservative in predicting lengths of defects and provided poor resolution between closely located surface defects.
4. In this study, all technologies provided conservative results due to poor weld material quality. Multiple small reflectors caused every technology to call defects more severe.
5. Results from various NDE techniques and between different NDE service providers varied significantly. This variance in results can influence integrity decisions either for direct assessment or for ILI qualification/verification purposes.

36-in SCC sample

A sample of 36-in double submerged arc welded pipe with a wall thickness of 9.3 mm was inspected with IWEX as an extent to earlier experiments described in the 3rd Quarterly Report in May 2014. The pipe coupon exhibited stress corrosion cracking with associated external corrosion. In addition to this, toe cracks could be detected at the OD surface at the weld reinforcement.

36-in measurement setup

Figure 96. Cross-sectional view of the weld (left); measurement setup (right)

The experiments were carried out using a water tank and a manipulator to move the probes. The sample was submerged in water to simplify coupling of the wedges to the pipe coupon. Two separate scans were carried out to inspect the weld and the pipe body next to the weld. The setup for weld inspection is shown in Figure 97.

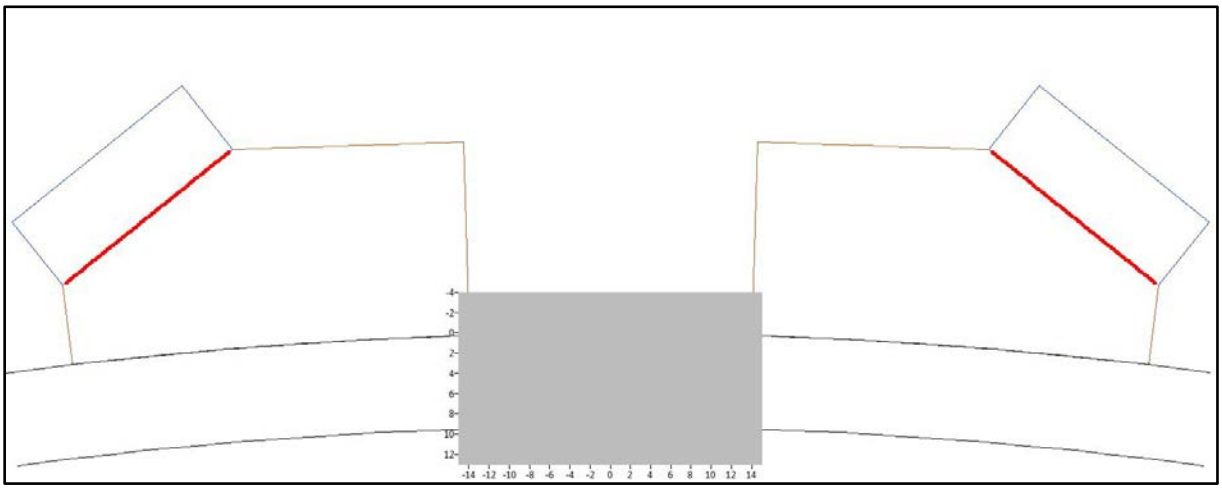

Figure 97. Measurement setup for weld inspection showing the position of the probes with respect to the weld and the selected region of interest (gray rectangle)

36-in weld inspection

A sample of 36” double submerged arc welded pipe with a wall thickness of 9.3 mm was inspected with IWEX as an extent to earlier experiments described in the 3rd quarterly report in May 2014. The pipe coupon exhibited stress corrosion cracking with associated external corrosion. In addition to this, toe cracks could be detected at the OD surface at the weld reinforcement.

Figure 98. Cross-sectional view of the weld (left); measurement setup (right)

Because of the wide weld reinforcement (20 mm, see Figure 98), the IWEX images of the double submerged arc weld are more difficult to interpret than for ERW seam welds. The reinforcement itself is visible in the image.

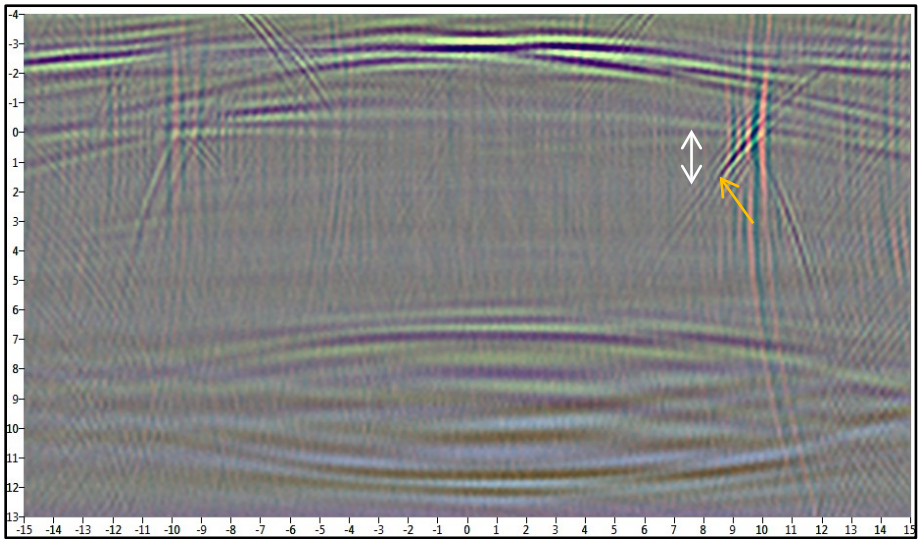

Figure 99. IWEX image showing a toe crack at the OD surface to the right of the weld with a height of 1.1 mm (white arrow indicates vertical extent; yellow arrow indicates lower tip diffraction)

In the image, the position of the interfaces to the sides of the weld deviates in a vertical direction. The OD surfaces are imaged higher than there actual position. Due to the

reinforcement, the ultrasonic paths are longer than expected from the nominal wall thickness, leading to this shift. Toe cracks at the reinforcement are visible at several scan positions at both sides of the weld. They are detected using the IWEX-3 tandem extra skip mode (indication in red). Sizing can be carried out more accurately using the lower tip diffractions shown by the IWEX-2 skip mode (diagonal indication in green).

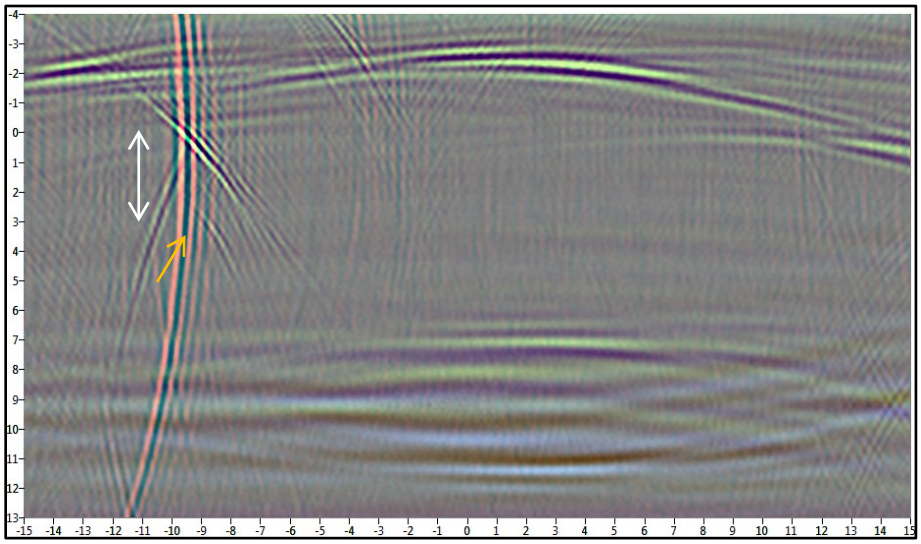

Figure 100. IWEX image showing a toe crack at the OD surface to the left of the weld with a height of 3.0 mm (white arrow indicates vertical extent; yellow arrow indicates lower tip diffraction).

Inspection of the 36-in pipe body

For the inspection of the stress corrosion cracks in the pipe body, the wedges are pulled away by about one inch from the weld. It is no longer possible to use a combination of two arrays. Therefore, the OD and ID surfaces are no longer present in the images.

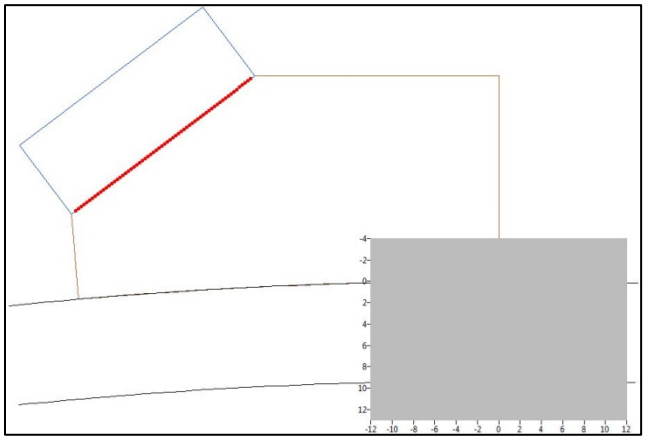

Figure 101. Measurement setup with a single array for the inspection of the pipe body showing the selected region of interest (gray rectangle)

The cracks are indicated by vertical indications in the IWEX-3 tandem extra skip mode (red) and the corner reflection at the OD surface visible in the IWEX-2 skip mode (green). As in the case of weld inspection, tip diffractions visible in the IWEX-2 mode enable accurate sizing of the flaw height (see Figure 102).

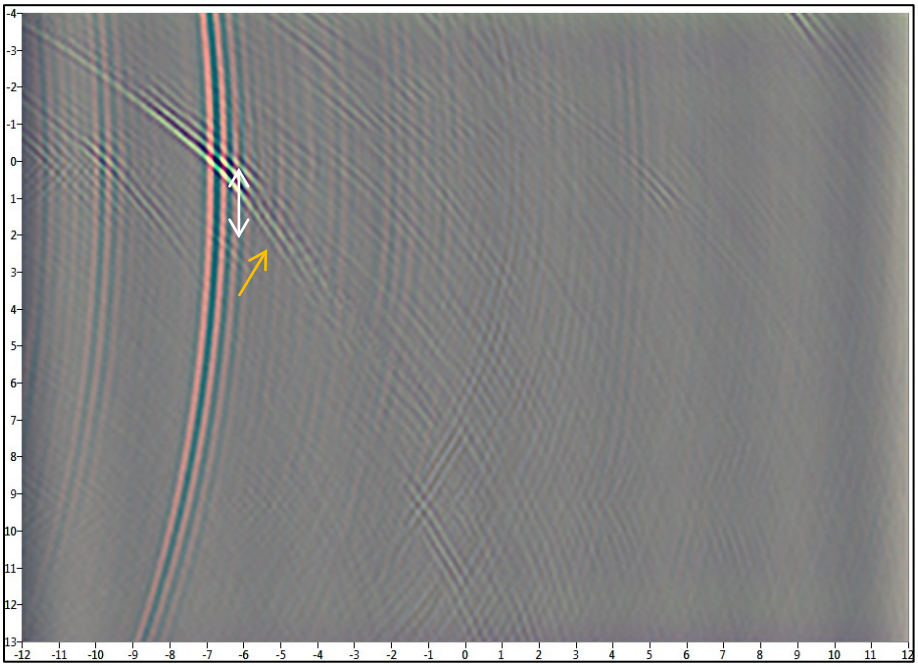

Figure 102. IWEX image obtained with one array showing a crack at the OD surface in the pipe body with a height of 2.3 mm (white arrow indicates vertical extent; yellow arrow indicates lower tip diffraction).

It should be noted that the cracks cannot be sized equally well at all scan positions. For a high number of scan positions, the tip diffractions are significantly weaker and difficult to detect. This can also be caused by the presence of several cracks next to each other at the same scan position, with one crack shadowing the other.

At many scan positions, the indications present in IWEX-3 are smeared out vertically as can be seen in Figure 97. This is caused by a limited number of array elements picking up reflections from this flaw, reducing the vertical resolution for this mode. This is related to the geometrical setup for this particular application. It has not been possible to overcome this limitation by changing the distance of the probes to the weld. Therefore, sizing using this mode alone is not accurate enough, and additional indications of tip diffractions are required.

The IWEX data volume obtained from one scan can also be represented as a C-scan top view showing the detected cracks. In Figure 103, a C-scan visualization generated from a part of an

IWEX scan is shown. It is also superimposed on a photograph of the same pipe section. It can be seen that the indications detected by IWEX coincide nicely with the visible surface cracks.

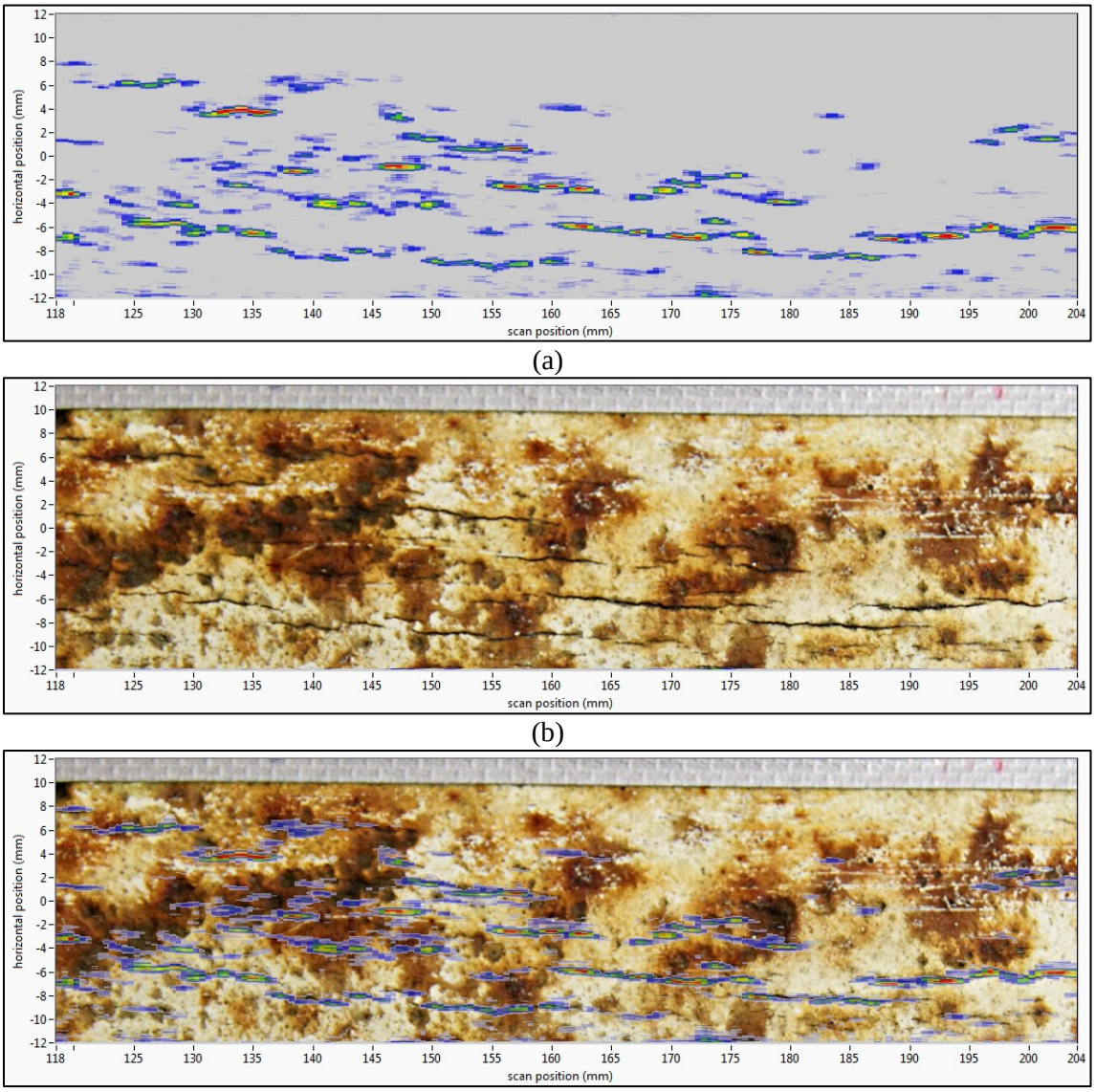

(a)

(b)

(c)

Figure 103. C-scan top view of the pipe body next to the weld obtained by IWEX inspection (a); photograph of the cracks in the pipe body for the same region (b); IWEX indications superimposed on the photograph (c)

2 SCC coupons

Two SCC coupons found at the Kiefner Metallurgical Lab that have been labeled SCC 1 & SCC 2 as shown in Figure 104. Testing on these samples was performed.

Figure 104. SCC1 and SCC 2 samples at Kiefner

The scanner was set up to do multiple line scans with 10 mm separation from the center of one scan to the next to allow for overlap. Figure 105 is an area where IWEX was used to map an SCC colony. After each of four scans a screen shot was taken, and the four screen shots were placed together creating a mosaic showing a C-scan representation on the area. The left mosaic is from cap scans or the OD 2 mm of the scans and to the right the same location is a mosaic of the volume or the mid 4 mm of the scans.

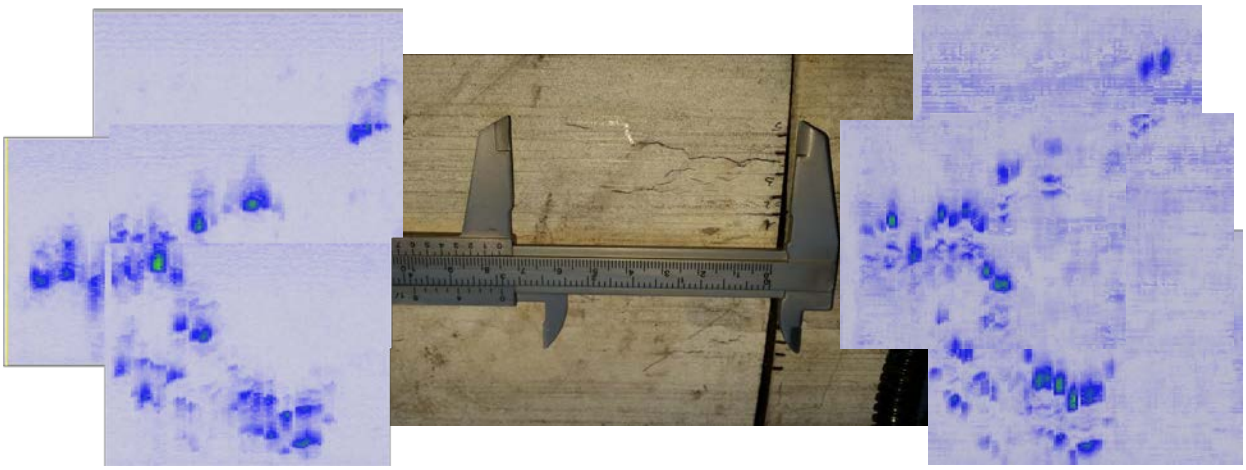

Figure 105. SCC1 and SCC 2 samples at Kiefner

Below is the same set of cracks with a top view of the 3D imaging.

Figure 106. Mosaic image of C-scan representation over pipe sample photos

In this view we have several cracks in the image and it appears we can see a crack that is deeper than the rest. Once we display this in 3D it is easier to see the location of the deepest flaw.

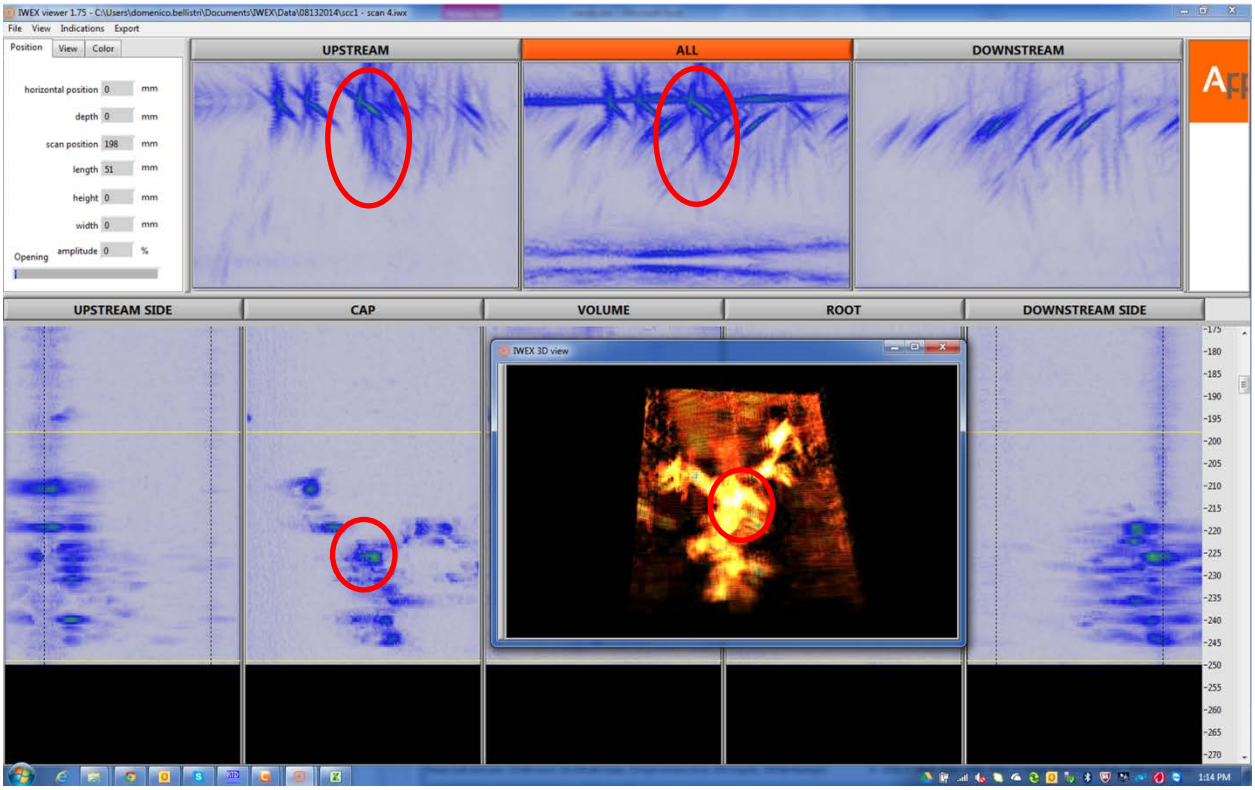

Figure 107. IWEX display

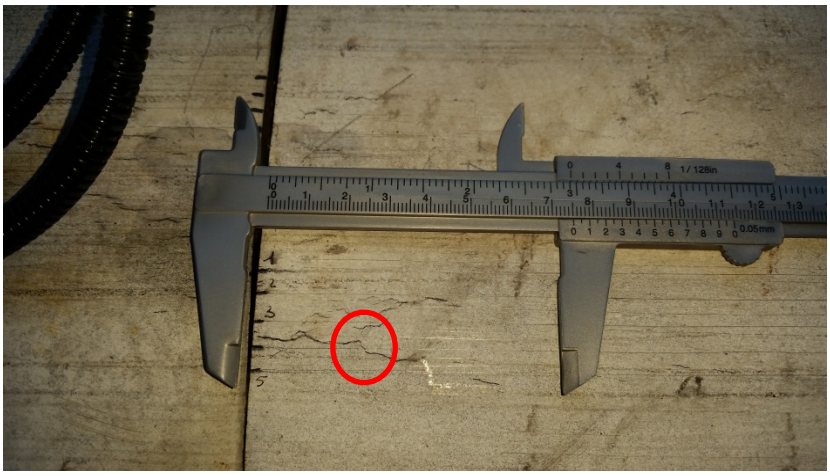

Figure 108. Image of cracking in sample

26-in FW coupon

The coupon was given to Applus RTD Canada and shipped to Houston, and subsequently Columbus for inspection. One 120 mm long anomaly was visible on the ID surface. The initial IWEX inspection performed showed four anomalies. A picture of the coupon is shown in Figure 109 below. A raised seam showing a trim was present on the ID and OD typical of A.O. Smith flash welded pipe.

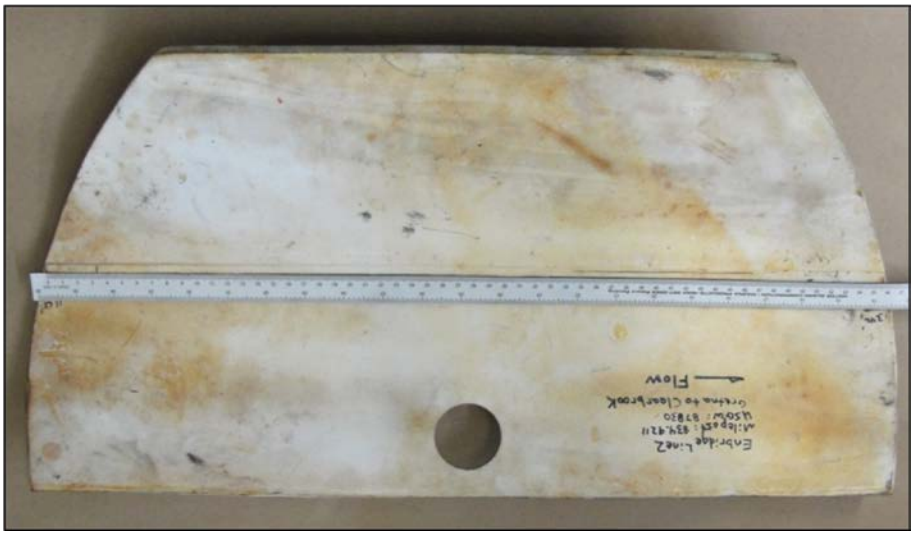

Figure 109. A 26-in diameter coupon with visible flow on the ID seam weld

Figure 110. The 26-in diameter coupon with markings showing locations of the flaws

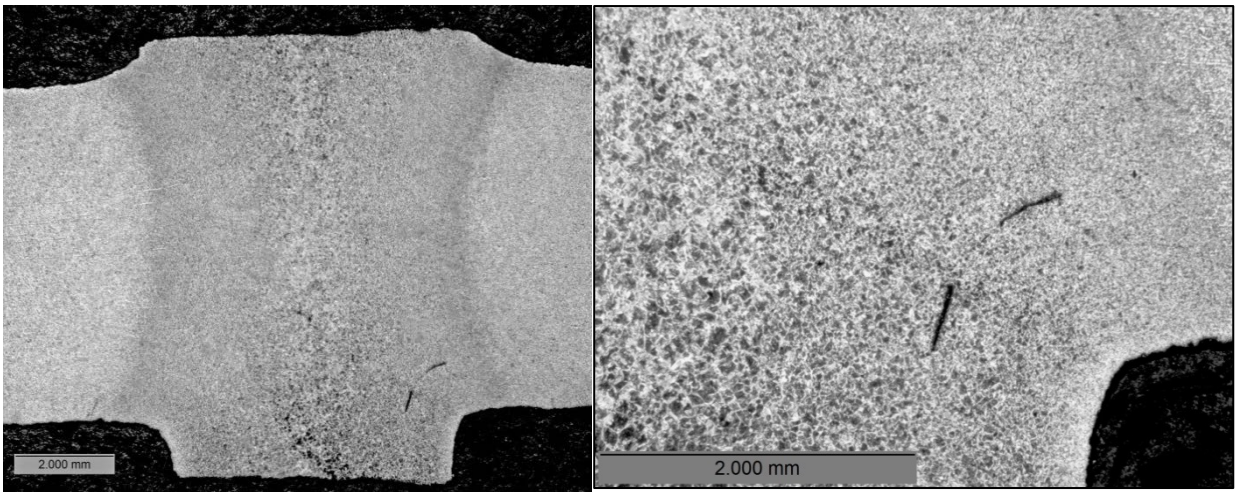

Figure 111. A section of Defect #1. The defect did not break in the desired plane, so the defect was sectioned circumferentially perpendicular to the plane of the defect. The defect height appears to be about 1.0 mm and 0.35 mm from the flash weld trim on the IDs

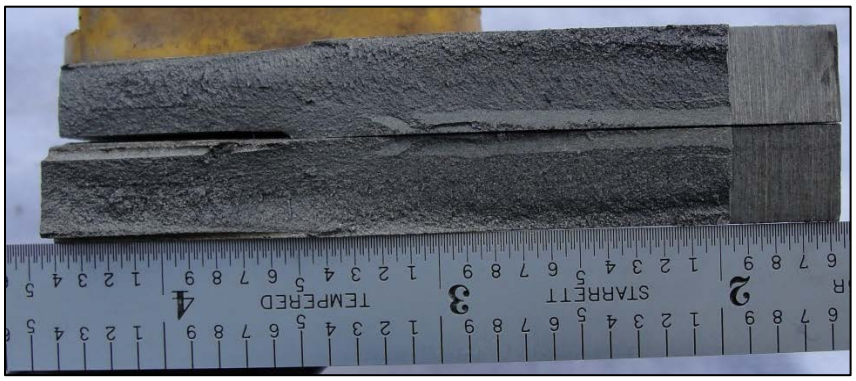

Figure 112. Fracture surface of Defect #2, the fracture broke in the intended plane for about half the fracture surface.

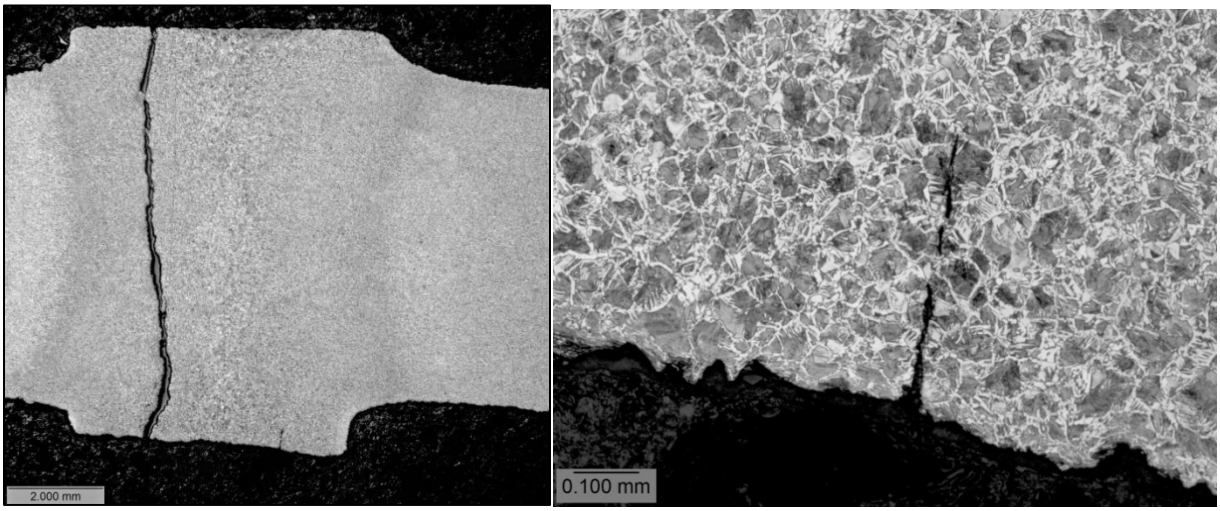

Figure 113. Section of Defect #2, showing a defect depth of 0.4 mm from the ID

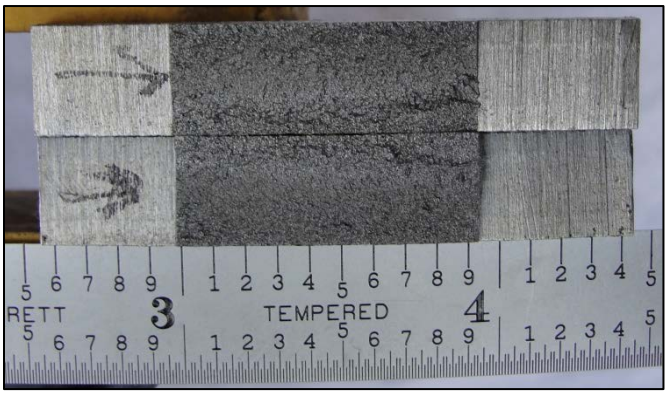

Figure 114. Fracture surface of Defect #3. The defect appears to be 0.1-in (2.5 mm) deep from the ID surface

Figure 115. Fracture surface of Defect #4, the largest defect with the internal surface breaking defect. The defect appears to be about 0.15-in (3.8 mm) deep from the ID surface.

Table 5. Results from the 26-in Flash Welded coupon

IWEX Defect Number	Vertical Location from Start (0) (mm)	Length (mm)	Type of Defect	Depth from the OD (mm)	Height (mm)	FS Length (mm)	FS Height (mm)
1	2	128	LOF	3.6	2.6		1
2	227	3	LOF	4.4	1.4		0.4
3	232	5	LOF	4.3	1.6		2.5
4	292	144	LOF	4	3.3	149	3.8

Battelle Samples

Extensive samples are available at Battelle for the PHMSA ERW project. Measurements on 12, 16, 18, 20, 22, & 24 inch pipe are still available, but have not been performed because the request to perform the inspections has languished. These samples will not be available for metallurgical breaking for some time after inspection. We will investigate inspecting the 1000+ feet in a pipe yard in the next quarter assuming an additional IWEX system becomes available in this quarter.

SCANNER IMPROVEMENTS DURING THE SECOND ROUND OF TESTING

The re-design work of the so called “Navic” scanner has run into issues which appear to be beyond the operation capabilities (and design) of this unit. This largely has to do with the weight of the IWEX- Imager at 17-lbs and its intended operational use in the field, at or near the 3:00 and 9:00 clock positions. The scanner is not able to maintain its position in longitudinal direction and droops down.

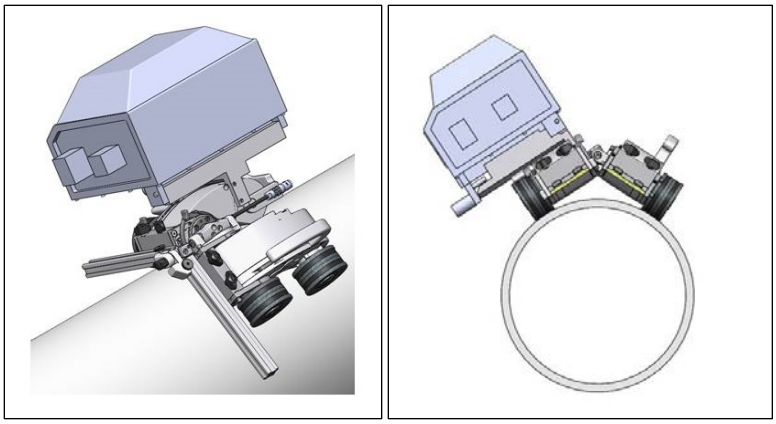

Figure 116. Magnetic wheeled scanner

As shown in the above images, the Imager sits on one half of the scanner with two magnetic wheels. The hinge takes care of keeping the magnetic wheels in contact with the pipe surface and it also allows it to operate at different pipe diameters. The magnetic force/contact area cannot be further increased.

Efforts are now being focused in the direction of using a scan system based on a rail, very similar to that being used on the larger pipe diameters. The rail system seems to be a better fit also because of the requirements of keeping the drift tolerance to a minimum of the transducer position in relation to the long seam.

Linear Scanner

The linear scanner goes back to putting the measurement on a rail capable of holding in a fixed position with respect to the long seam and capable of carrying the weight of the IWEX processor box.

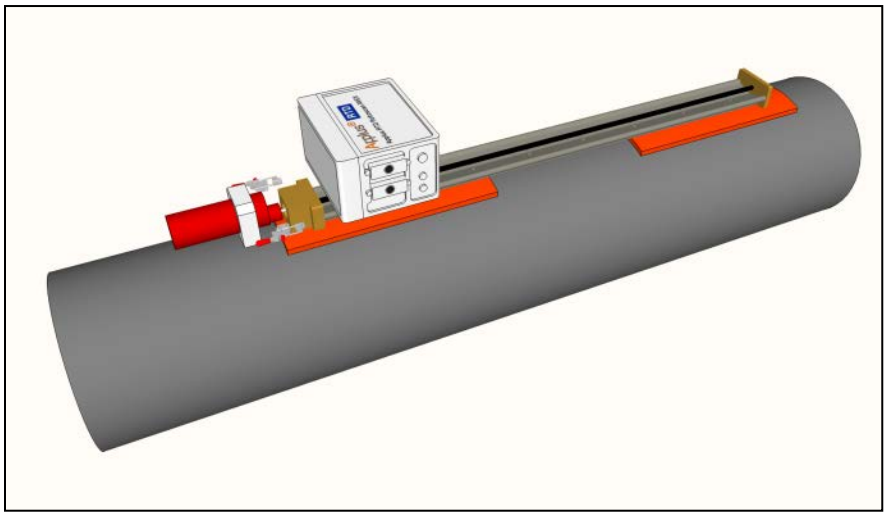

Figure 117. Linear scanner with the motor assembly on the left and the IWEX processor mounted on top

The linear scanner consists of the following parts:

- IWEX processor box
- Linear actuator
- Mounting wedges for the linear actuator
- DC drive motor
- Motor-linear actuator attachment
- Motor-linear actuator coupling
- Probes holder
- Probes frame
- Probes – transducers and wedges
- Encoder

The linear actuator has a 48-inch overall rail length without motor and can scan about 3-feet or 1-meter. This is a convenient length because it scans a sufficiently large amount of the pipe seam, produces a manageable image scan size of about 1 gigabyte and is short enough to ship to various locations for field use. The advantage of this part is it is off the shelf as it is used in other non-NDE applications and is therefore not expensive.

Figure 118. Linear actuator with a 48-inch overall rail length and a 3-ft scan length

The Applus RTD CAN Bus DC motor shown below is a standard item used in other Applus RTD equipment and interfaces easily with various software for controlling the position of the scanner.

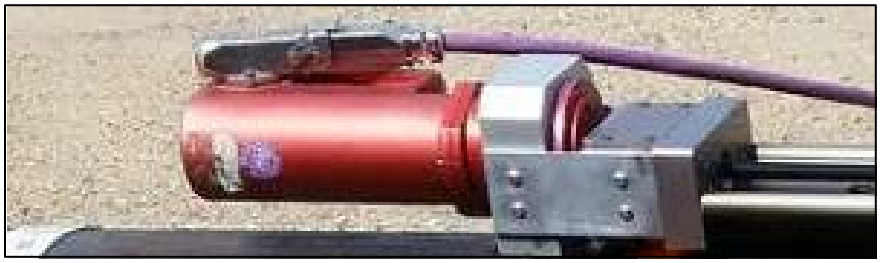

Figure 119. Applus RTD CAN bus DC motor

The interface between the DC motor and the linear actuator had to be developed and consisted of a motor-linear actuator attachment, motor-linear actuator latch toggle clamps system for ease of assembling, and a coupling.

The mounting wedge or interface between the linear actuator and the pipe is a fairly simple U-shaped design and has consisted of two mounts on each end as illustrated in the figure above or a single piece which has been used in a second implementation.

Final modifications added LED lights and a Wi-Fi enabled camera to allow the operator to see the scan in progress making sure the probes are in the center of the weld.

FIELD TRIALS

In-Field Trials, Refinement, and Demonstration

The first field trial started with a seam inspection in Texas that had 12 planned excavations. Some of the locations needed SCC inspection while others needed seam inspection. The scanner was successful in collecting data at different clock positions. During this field trial,

improvements were realized. The scanner would not support its weight on coating, therefore stronger magnetic wheels were recommended to overcome this. The probe holders and stabilization to the frame also needed improvements as the technicians found it difficult to position the probes on the pipe and keep them in contact with the pipe. An image of the scanner in the ditch is shown in Figure 120. Scanner set up time is minimal. The process of setting up the scanner is shown in Figure 121. The process of scanning the pipe is shown in Figure 122.

The results from these scans showed that only IWEX was used to find the Seam A-01 and Seam A-02 as shown in Figure 123, Phased Array (PA) and TOFD were not scanned at their location. Seam A-03 and Seam A-04 were found with IWEX, PA, and TOFD, and are shown in Figure 124 and Figure 125. The target anomaly for the project was found and correlated to Seam A-03. Pressure containing sleeves were used to repair the pipe.

Figure 120. Scanner in the ditch

Figure 121. Scanner set up

Figure 122. Scanning the pipe

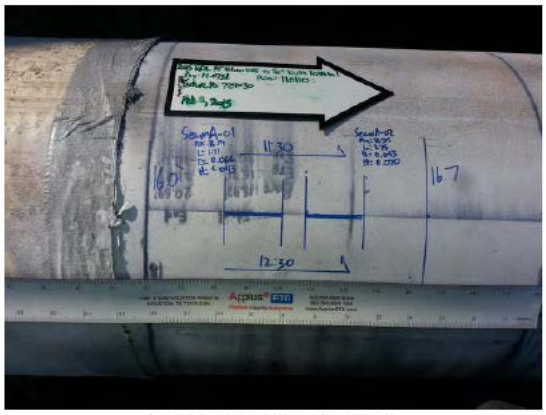

Seam A-01 and 02 Locations

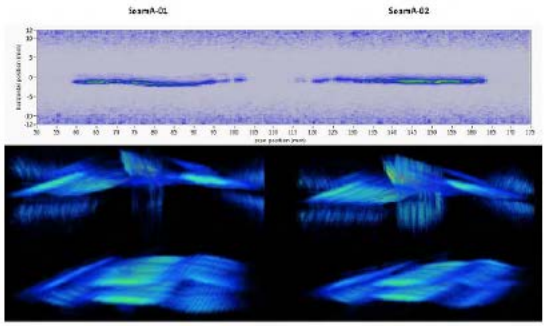

IWEX Imaging of Seam A-01 and 02

Figure 123. Pipe location and IWEX imaging of SeamA-01 and 02

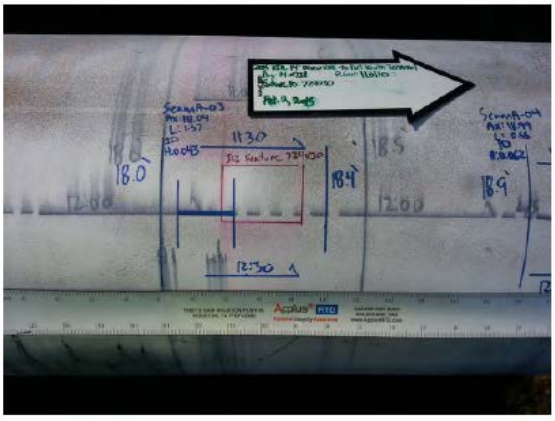

Seam A-03 Location

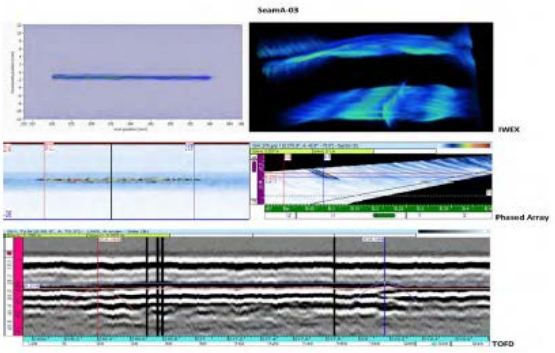

IWEX/Phased Array/TOFD Imaging of SeamA-03

Figure 124. Pipe location and IWEX/Phased Array/TOFD imaging of SeamA-03

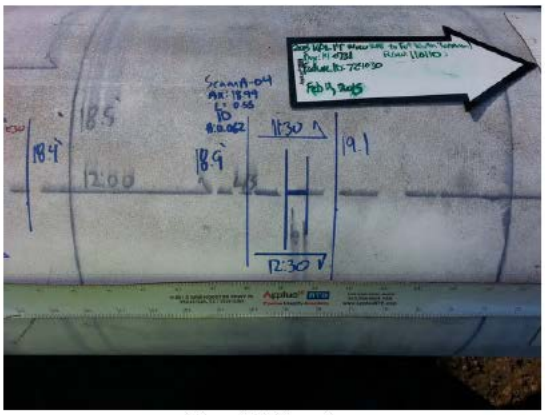

Seam A-04 Location

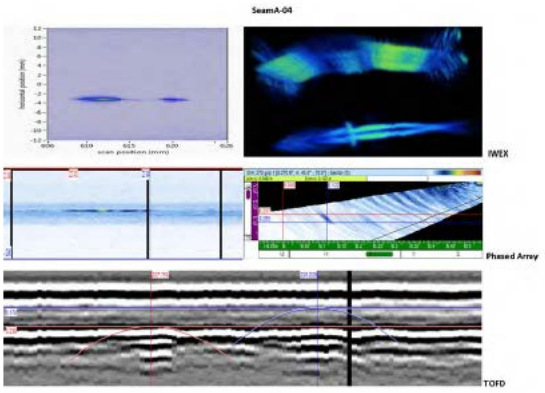

IWEX/Phased Array/TOFD Imaging of SeamA-04

Figure 125. Pipe location and IWEX/Phased Array/TOFD imaging of SeamA-04

A field trial was initiated Q7 to test the scanner during the last weeks in May on five pipe joints in West Texas.

A field trial on five joints was performed near Midland, Texas with a new participant. This pipeline operator was having trouble with cold-weld penetrators and deep microbial internal-corrosion pits, both were difficult to size using conventional UT.

One test was conducted in Canada. The field trials appeared to go well and produce good images. This was the first use of the equipment in Canada since scanning a few joints of pipe in the Applus RTD shop in the 5th Quarter.

A field trial was initiated in North Dakota on ERW pipe with multiple detected ILI anomalies in individual joints. This scanning was not completed in the 8th Quarter, but should be complete in the 1st week of the 9th Quarter.

Thirty-eight pieces of 16-in ERW pipe were set-up in a Minnesota pipe yard for scanning with IWEX ranging with pipe ranging from 3-ft to 63-ft long. The scanning was completed in 3 ½ weeks with initial interpretation of the images complete. Samples are being selected for metallurgical comparisons to the IWEX images. This field trial is one of the in-kind field trials planned for in items 99 & 100 in the recently awarded modification.

One set of field data was acquired in the 9th Quarter and was used to test the system.

A field trial was completed in North Dakota on ERW pipe with multiple detected ILI anomalies in individual joints. The ERW long seam was scanned for two joints in two separate digs, with 100+ anomalies identified in each of the two digs. Most of these anomalies are non-surface breaking upturned fiber indications, many were non-thru wall cold welds, some were hook cracks, and a few were laminations. The results have not been compared to any other information such as metallurgical freeze-breaks or ILI data.

Trials of the system continue in the 10th Quarter. These trials have been occurring in the Applus RTD office in Houston, Texas and at Kiefner's Metallurgical Lab in Columbus, Ohio. Trials in Houston have been on a 12-in ERW pipe with existing and manufactured defects in the seam. Trials in Columbus have been on 16-in EFW pipe from the DOT PHMSA Comprehensive Study to Understand Longitudinal ERW Seam Failures being conducted by Battelle. The scanner continues to work well and improvements have focused on better probe holders to eliminate some of the errors caused by unwanted probe movement during scanning.

TRAINING OF SELECT FIELD ENGINEERS

As a part of the initiative to train new field engineers to interpret IWEX images, a round robin trial, of some existing data taken to date, was put together to determine the consistency of interpretation among field technicians who are using the IWEX interpretation software and to implement procedures to improve future accuracy and consistency. Existing image datasets were selected from three sets of images captured to date: the 26-in flash weld coupon, select data from the 24-in SSAW pipe, and datasets from the 8-in ERW pipe. The test was performed in February and 4 NDT technicians with experience interpreting IWEX data participated, Pushpendra Tomar – Kiefner, Jeff Vinyard – ApplusRTD Houston, Domenico Bellistri – ApplusRTD Houston, and Peter den Boer – ApplusRTD Edmonton. Results are shown in Table 6.

Table 6. Results from an internal project round robin trial

	Push	Jeff	Domir	Peter	Push	Jeff	Domir	Peter	Push	Jeff	Domir	Peter	Push	Jeff	Domir	Peter	Pushpendra	Jeff	Dominico	Peter
26-in Flash Welded coupon																				
Iwex Defect #	Vertical location from				Length (mm)				Depth from the OD to				Height (mm)				Type			
1	2	2	2	2	127	6	5	44	4.1	6.2	6.4	7	1.4	1.3	1.2	2.3	Inclusion/Stringer	LOF		Sub-surface
2	227	227	227	227	3	5	3	3	4.5	5.7	5.5	5.4	0.8	1.5	1.7	1.7	Inclusion/Stringer	LOF		Sub-surface
3	232	232	232	232	5	6	4	61	4.5	1.6	5.5	6.1	1.1	1	1.4	2		LOF		Sub-surface
4	292	292	292	292	146	148	126	126	4.6	6.2	6.7	7.55	3	2	2.2	3.4	Lack of Penetration	Crack		ID surface breaking
24in pipe 440B SSAW																				
Iwex Defect #	Vertical location from				Length (mm)				Depth from the OD to				Height (mm)				Type			
1	4346	4346	4346	4346	37	35	15	6	0	0.7	1	0.9	0.4	0.7	0.9	0.9	Crack	TC		OD surface breaking
2	4420	4420	4420	4420	20	16	15	7	0.2	0.9	2.5	0.5	0.3	0.9	2.5	0.5	Crack	TC		OD surface breaking
3	6693	6693	6693	6693	36	15	28	11	-0.4	1.1	1.5	1.7	0.4	1.1	1.5	1	Crack	TC		Sub-surface
4	6721	6721	6721	6721	18	9	8	8	0.1	1.2	4	1.4	0.3	1.2	1	1.1	Crack	TC		Sub-surface
8in ID 8																				
Iwex Defect #	Vertical location from				Length (mm)				Depth from the OD to				Height (mm)				Type			
1	50	50	50	50	13	29	3	28	-0.7	1.1		1.5	0.7	1.1	0.2	1.5	Crack	LOF		OD surface breaking
2	106	106	106	106	6	3	3	4	4.3	6.2		5.1	1.6	0.9	6.5	1.3	LOF Called LOF because I	LOF		
3	238	238	238	238	6	6	19	8	-0.7	3.1		0.5	0.5	0.9	3	0.5	Crack	Inclusion		OD surface breaking
4	273	273	273	273	10	11	10	2	0.3	1.1		1.5	0.7	1.1	0.8	1.5	Crack	LOF		OD surface breaking
4-2						11				6.4				1.1				LOF		
5	583	583	583	583	17	18	10	14	0.2	2		0.7	0.8	1.1	1	0.7	Crack	HC		OD surface breaking
6-1	628	628	628	628	6	32	6	30	-0.1	1.3		1.5	0.5	1.3	1.2	1.5	Crack	LOF		OD surface breaking
6-2	671	671	671	671	60	38	29	23	0	1.2		0.9	1.2	1.2	2.3	0.9	Crack	LOF		OD surface breaking
7	1039	1039	1039	1039		25	21	21		2		6.4		1.5	6.5	0.6	ID Flaw I don't see any t	HC		ID surface breaking
8-1	1376	1376	1376	1376	13	17	2	15	-0.7	1.3		0.6	1	1	0.8	0.6	Crack	HC		OD surface breaking
8-2	1405	1405	1405	1405	11	7	8	2	-0.9	6.2		5.8	0.8	1.2	1	0.9	Crack	LOF		Sub-surface
9	1513	1513	1513	1510	31	12	23	10	-1	6.2		0-1.1 and 3.1 to 6.4	1.1	2.4	1.1		Crack	LOF		Near through wall
10-1	1768	1768	1768	1768	19	19	14	17	-0.2	1		0.9	1	1	1	0.9	Crack	HC		OD surface breaking
10-2	1832	1832	1832	1832	11	7	1	7	0.3	1.2		0.9	1	1.2	6.5	0.9	Crack	HC		OD surface breaking
10-3-1	1861	1861	1861	1861	13	21	8	10	0.3	1.3		6.4	1.1	1.3	1.4	1	Crack	LOF/HC		ID surface breaking
10-3-2	1883	1883	1883	1883	59	13	2	61	0.1	1.2		1.6	1.2	1.2	1.2	1.6	Crack	LOF		OD surface breaking
11	1617	1617	1617	1624	25	28	9	23	0.2	1		1.1	0.6	0.8	2	1.1	Crack	HC		OD surface breaking

Of particular surprise was the poor repeatability among the interpreters. Although not all interpreters completed all the inspections it was clear that procedures for interpretation need to be improved. As a result of the trial a detailed procedure was initiated. The current procedure is in draft form and not ready for inclusion in this quarterly report, but it should suffice as a template for repeating the round robin test in the next quarter.

One of the outcomes of the test was an awareness of the lack of consistency in identifying feature types. Through discussions with others at Kiefner involved in writing API 1176, we have decided to start with the API 5T1 for the description of Flash Weld and ERW seam inspections. Of note in the standard is the absence of the term “lack of fusion”.

Since the start of the program it has become apparent the precise sizing is paramount to the potential users of the technology for qualifying ILI runs and the calculation of burst pressures when using the technology for assessing defects in the ditch. Users would like an in-ditch measurement that is an order of magnitude better than the ILI measurement so that in-ditch measurement can be used to assess the accuracy of the more universal ILI measurement. To obtain this level of accuracy precise alignment and focusing of the various modes is needed.

Ultimately this may require a full inversion of the full waveform matrix to obtain the most uniform and accurate sizing results. IWEX results to date have varied between ±1mm and ±0.2mm and are thought to be related to mode alignment and training knowledge of the interpreters. As training of the interpreters has improved, by the use of tip diffraction signals for determining the crack tip location, future improvements will depend on the best alignment possible for the various wave modes.

Training of Select Field Engineers for In-Field Use of the System

A procedure manual for setup of the system and an additional procedure manual for interpretation of the acquired images have been started. As these procedures are tested and used by selected field engineers adjustments will be made for lessons learned.

Uniform descriptions of the types of defects found in a seam are problematic. In the writing of a new standard API 1176 Kiefner staff have started to use API 5T1 as a standard for describing ERW and FW flaws and we have started to do the same in this project.

The field setup of the system has been made much simpler though some automation of the setup parameters by Rotterdam. While setup in some cases took a day for inexperienced field technicians, the new automated setup should provide a useable setup in 15 minutes.

An interpretation training session was held in Columbus Ohio, July 16-17, 2015. Fifteen people attended including five Applus RTD field engineers from Houston, Minnesota, and Edmonton. The session was successful in moving the operation of IWEX from Application Center personnel (a.k.a. Jeff Vinyard and Peter den Boer) to the field engineers, who will be responsible for using IWEX in the field for acquiring image data of axial cracks on the seam and in the pipe body. In addition to training field engineers on interpreting IWEX images the session helped bring a consistency in interpretation. Two operators were present to bring an operators perspective to the training.

It was apparent that sizing in the seam is not as accurate as sizing in the pipe body (i.e. SCC sizing appears to be more accurate than ERW seam anomaly sizing). The consensus from the meeting is this may be caused by the manufacturing process for making an ERW seam. The pipe body is made from a rolling process, which is fairly uniform, but the seam is made from crimping the edges in an attempt to match the curvature in the pipe body. This combined with other effects such as poor trim, offset plate edges, and other effects is affecting sizing in the seam area.

The imaging is performed by determining the geometry in the seam area during a calibration step and used for subsequent imaging. This calibration determines a pipe wall thickness and

IWEX sensor separation, but also assumes a radius of curvature for the pipe. This step is taken in-part for faster processing in producing an image from the full matrix capture data. If the geometry of the seam is not perfectly consistent, then it can distort the image in the seam area for modes that use the ID and OD surfaces as mirrors such as IWEX-1, IWEX-2, IWEX-3, and more recently IWEX-4. These effects are not as critical for IWEX-0 mode data which contain no reflections of the ID or OD from producing an image. Tasks in ongoing work should help alleviate some of these imaging problems and improve sizing accuracy.

Improvements

During the IWEX interpretation and training workshop, it was apparent that the quality of the images needs improvement. Although accurate sizing and positioning of flaws is possible with the current image quality, interpreting the images can be time consuming. Excellent quality images were available that demonstrated how much easier it is to interpret images when all of the various modes are properly aligned. In addition the better focused aligned images made it possible to pick out the more subtle features needed for interpretation such as tip diffraction signals. For the first time, small (low amplitude signals) were demonstrated from the weld pipe interface (from the bevel face) for the girth weld trials that were being performed. This makes it apparent that improved calibration is the most important item to come out of the meeting. Two full matrix capture single frame scans of the raw waveforms for each pipe joint are recommended. These can provide the fundamental information that will be needed to improve the set-up for scanning IWEX images.

It was apparent that SCC appears better calibrated than seam flaws. Although uncertain, the thought behind this difference is the SCC being in the pipe body is more likely to be a constant radius, making the imaging easier. The seam weld area could have several subtle features that are making it more difficult to image properly, this could include a slightly different radius of curvature, because the edges of the weld are curved in a different manner (by crimping) than the main pipe body which is rolled (or pressed for older DSAW) into a cylinder. There could be slight bending at the weld. Both of these are effects that could be affecting the IWEX imaging but are completely compliant with tolerance needed for pipe manufacture according to API 5L. In addition there is always the possibility of offset plate edges at the weld. The full matrix capture frames will help the TCC address this issue. One frame should be taken where there are no defects and the other frame should be taken across a defect. Because these full frames are 130 Mbytes each only two are recommended to minimize acquisition time and the problems of shipping the data around on the Applus RTD network. The SCC images appeared to be more focused and aligned than ERW images from the presentations during the meeting. Because the images from ERW seams are currently more problematic for interpreting, it is recommended that efforts for automatic interpretation start with automatic sizing of SCC. Step size for SCC was discussed and generally agreed that 1mm steps are sufficient. Other items that will need to

be addressed for SCC are surface corrosion, of which significant surface corrosion has not been encountered to date. Merging of parallel scans for imaging wider colonies needs to be addressed. Depth profiles were shown, but these are currently fairly tedious to compline and there is a need for automation and to incorporate an output depth profile into an assessment equation such as the modified log-secant equation which is currently used in KAPA. The general assessment direction for ERW seams (including flash weld) was consistent. The classification of features was discussed as were the goals for flash welds, which are to make repair decisions in the ditch and to qualify the accuracy of ILI tools.

Sizing defects to an uncertainty of ±0.2mm continues to be a challenge in addition to alignment of different IWEX modes to produce a consistent picture of curving or non-planar defects. The issue of better alignment of the various modes will be addressed in the modification proposed to PHMSA and the industry.

The IWEX procedure is a living document and is being updated as software improves and new tools and functionality are aFdded. Attachments are added to establish evaluation procedures, scanner set up procedure, surface preparation procedure, and a calibration wizard procedure.

The IWEX training will consist of an 80-hour course. This course will cover theory, practical training, and data evaluation. Prerequisites for training currently require a minimum of a Level II in Ultrasonics and a Level II Certification in Phased Array and/or TOFD is recommended. Once training is complete, candidates should have knowledge to set up the equipment, setup files for scanning and trouble-shooting equipment, preliminary evaluation of data, and the ability to generate a field report.